Use of microbial fuel cells in the beneficiation of algal biomass for bioelectricity production

A thesis submitted in fulfilment of the requirements for the degree of

MASTERS IN SCIENCE

BIOTECHNOLOGY

Of

RHODES UNIVERSITY

By

Kudzai Mtambanengwe

Supervisor

Prof. J. Limson

Co-Supervisor

Mr. R. Laubscher

Co-Supervisor

Dr R. Fogel

Biotechnology innovation centre (BIC), Rhodes University, Grahamstown, 6140, South Africa.

ABSTRACT

Microbial fuel cells (MFCs) offer an alternative technology that is able to convert organic matter into electrical energy by making use of bacterial biomass as the biocatalysts. Performance of the MFCs is dependent on many factors such as substrate, biocatalyst, electrode material and optimum operational conditions including temperature and pH. Significant research has been conducted on the use of different substrates to fuel the MFC. The possibility of harvesting energy from organic waste sources in the MFC makes the technology attractive. In this study, we have investigated the use of *Chlorella*, *Arthrospira* and a mixed algal consortium obtained from the local wastewater treatment facility in Grahamstown, courtesy of the Institute for Environmental Biotechnology, Rhodes University (EBRU) as feedstock in an MFC with *Enterobacter cloacae* as the biocatalyst. Pre-treatment of the algae-based feedstock was studied as well as the influence of treatment on nutrient release and biocatalyst performance during growth studies and MFC operations. Sonication, autoclaving and a combination of the two were used as the pre-treatment methods. Pre-treatment resulted in the release of nutrients from algal cells to the media. Peak nutrient realease was observed when a combination of sonicating and autoclaving was employed. Sonicating and autoclaving the mixed consortium from EBRU resulted in an MFC peak power density of 101.2 (± 4.58) $mW.m^{-2}$. This represented more than 80% of the peak power density obtained in RCM medium. Operational conditions during MFC studies such as pH, temperature, nutrient utilisation by the biocatalyst and performance of the proton exchange membrane were measured during the course of the study. Growth kinetics and MFC operations were shown to be optimal when the substrate feedstock was acidic. However, for longer MFC operations (120 hours), total power output was greater by 3 to 5 fold when the feedstock was at acidic pH (4-6) than when the pH of the substrate feedstock was alkaline (8 and 9). Further MFC studies were performed on the effect of electrode materials including activated carbon fibre and carbon paper. The study examined also the use of live *Chlorella* and *Arthrospira* cultures as biocathodes in an MFC. We also showed that activated carbon fibre performs well as an electrode catalyst for both anode and cathode without any need of modification. Biocathode studies showed that the main limiting factor to biocathodes performance was light irradiance.

ACKNOWLEDGEMENTS

I would like to express my deepest gratitude towards the following persons:

- Prof. J. Limson, my supervisor. She knows she has been patient in trying to sculpt this rough cut into a perfect, exquisite piece. Her invaluable guidance has been a motivating factor.
- Mr R. Laubscher, my co-supervisor. He has an unimaginable in-depth knowledge of algae. His help in this project has been invaluable and words cannot quantify his contribution.
- Dr R. Fogel, the BioSENs oracle. His constant critique and guidance has helped to bring the final product out.
- My family, Mr N. Mtambanengwe and Dr F. Mtambanengwe, for the sacrifices they have made to ensure that I got the opportunity to explore and dig at my brain, and enjoy the lovely time I have had at Rhodes University, courtesy of their willing or unwilling funding.
- The BioSENs research group, Lance Ho my neighbour for the last 3 years, for the light humor that kept me sane, Shane Flanagan for his in-depth notes during presentation and the rest of the lab. This has been a lovely experience.
- Ms. T. Mutsvairo for her constant presence and support. Very much appreciated.
- Kuziwa F. Mtambanengwe, for the confusion he had when we talked about my research.
- To my friends, Julian Mavuwa, Kuda Kamuzonde, Martin Spencer, Leonard Musuwo, Boss G, Chrissy P, The Brig and Gates. You guys have been wonderful also not forgetting my day one's Chippie the man and Shumie.

For FloBoth, this is for you guys, my inspiration

CONTENTS

LIST OF ABBREVIATIONS

a	Autoclaved
BOD	Biological oxygen demand
CE	Controlled environment
COD	Chemical oxygen demand
CoTMPP	Cobalt-tetramethoxyphenylporphyrin
CV	Cyclic voltammetry
DMF	Dimethyl formamide
EBRU	Environmental Biotechnology Research Unit
FePc	Iron (II) Phthalocyanine
HRAP	High Rate Algal Ponds
IAPS	Integrated algal pond system
IEC	Ion exchange capacity
M	Molar
MFC	Microbial fuel cell
MWCNT	Multi-walled Carbon Nanotubes
OD	Optical density
ORR	Oxygen reduction reaction
P	Power
PEC	Proton exchange capacity
PEM	Proton exchange membrane
R	Resistance
RCM	Reinforced clostridial medium
RPM	Revolutions per minute
SEM	Scanning electron microscopy
V	Volts

LIST OF FIGURES

LIST OF TABLES

Chapter 1 : Introduction

1.1 Alternative energy

The increased demand for energy worldwide has resulted in faster depletion of fossil fuels reserves (Silveira, 2005). About 87% of the global consumption of energy is through fossil fuels as shown in figure 1.1. Fossil fuels were the major driving force behind global industrialisations and they still play a major role in the process of energy production in most industries (Logan, 2008). However, fossil fuels release harmful gases and other by-products upon combustion which results in pollution (Powell and Hill, 2009). A global increase in energy consumption, that stems from increasing population growth and technological advancement, coupled with the depletion of fossil fuel reserves has led to investigations into alternative energy sources (Powell and Hill, 2009). Fossil fuels are limited and non-renewable, and this has compounded the need to find alternative energy sources that are renewable (Silveira, 2005; Powell and Hill, 2009). Albeit, the low availability of reserves of oil and natural gas can be supplemented by other fuels such as coal and methane hydrates (Logan, 2008). Carbon dioxide release from the combustion of fossil fuels is a major contributor to the greenhouse effect (Farret and Simoes, 2006). This has led to the consideration of environmental needs when sourcing and investigating alternative energy sources (Logan, 2008). The investigation into possible alternative energy sources is highly desirable if the alternative energy sources and systems are environmentally friendly and are also able to provide sufficient energy for the demands available (Farret and Simoes, 2006). Energy production from renewable resources which do not result in a net carbon dioxide emission is considered to be very desirable due to the rising problem of global warming (Du *et al.*, 2007; Logan, 2008). Renewable resources that do not have harmful by-products are also highly desirable (Logan, 2008).

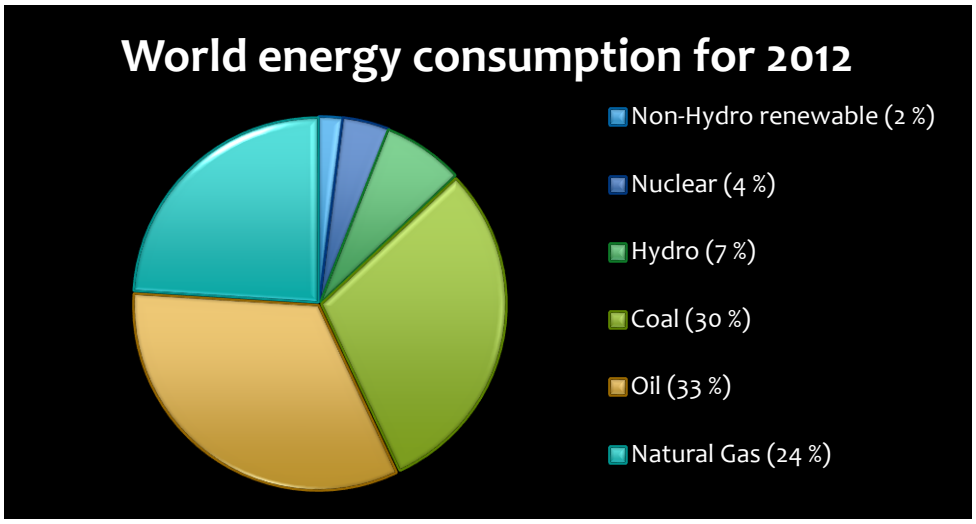

Figure 1.1:Global energy consumption data from 2012 (adapted from Internet Reference 1)

1.2 Biomass energy and utilisation

Solar, wind, biomass, geothermal, fuel cells and hydroelectric energy are forms of alternative and renewable sources of energy (Farret and Simoes, 2006). These alternative energy sources are considered to be "environmentally friendly" and readily available as the energy can be harnessed from the sun, wind, water, plants and waste (Farret and Simoes, 2006). There are various sources of biomass energy as is shown in figure 1.2. The use of biomass energy in the form of plant matter and organic waste is particularly attractive (Farret and Simoes, 2006). This is because unlike solar, wind and hydro energy which are heavily dependent on environmental conditions and climate, biomass can be harvested in most conditions (Silveira, 2005). The combustion of biomass and its processing results in the evolution of energy as heat, electricity or transport fuels (Silveira, 2005). Harvesting the energy from biomass sources, especially organic waste, has the benefit of both waste degradation and energy harvesting. Most organic waste streams contain a complex biomass matrix (Silveira, 2005). The use of bacteria to degrade biomass sources and in turn harvest the energy is possible through the use of a microbial fuel cell (MFC) (Logan, 2008). This can lead to the harvesting of many sources of biomass including biodegradable organic waste and treating it for energy acquisition (Logan, 2008). This could potentially decrease the energy invested into waste treatment or even possibly make the systems energy neutral (Logan, 2008). The use of algal

organic matter as a biomass source is advantageous because algae require less space for growth compared to land based plant biomass and have high growth rates (Velasquez-Orta *et al.*, 2009).

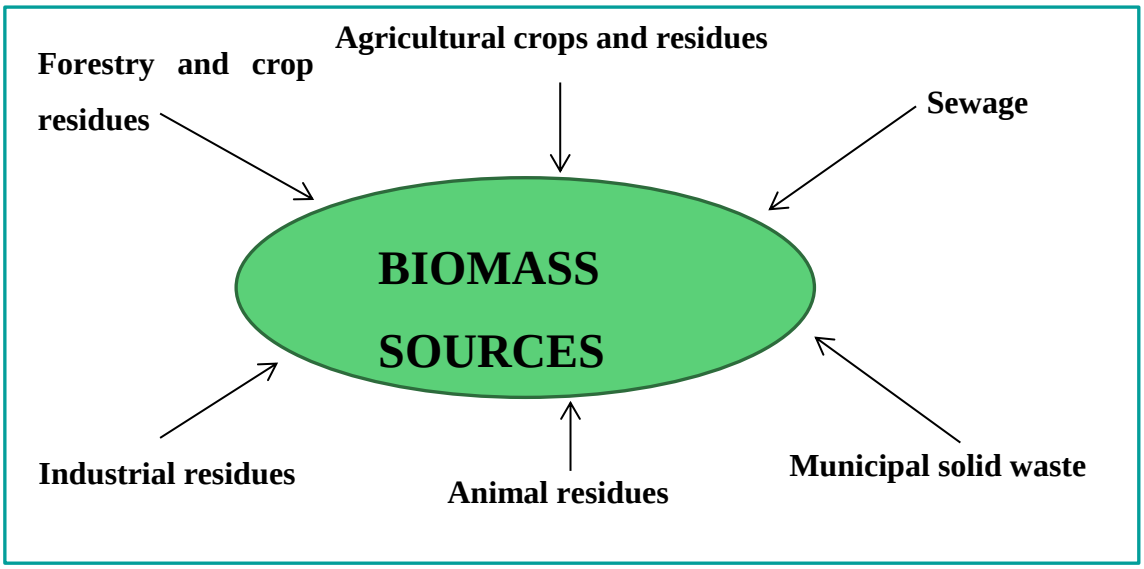

Figure 1.2: Common sources of biomass (adapted from internet reference 2)

1.3 The microbial fuel cell

1.3.1 Basic overview and mechanism of action

Microbial fuel cells (MFC) have the ability of electricity generation from biomass waste by exoelectrogenic bacteria (Logan, 2008; Peighambardoust *et al*., 2010) with the process shown schematically in figure 1.3. Electricity generation occurs through the conversion of chemical energy to electrical energy without the need of combustion (Peighambardoust *et al*., 2010). This occurs through the oxidation of substrate at an anode by the exoelectrogenic bacteria (Peighambardoust *et al*., 2010). The degradation of organic matter and biomass waste by the microorganisms results in the production of electrons that travel through the cell (Logan, 2008). The electrons are then released to an acceptor, the anode electrode, which then transports the electrons through the circuit to the cathode, where a terminal electron acceptor such as oxygen is reduced (Logan, 2008). The reduced oxygen accepts the protons that travel through the proton exchange membrane and becomes water (Logan, 2008).

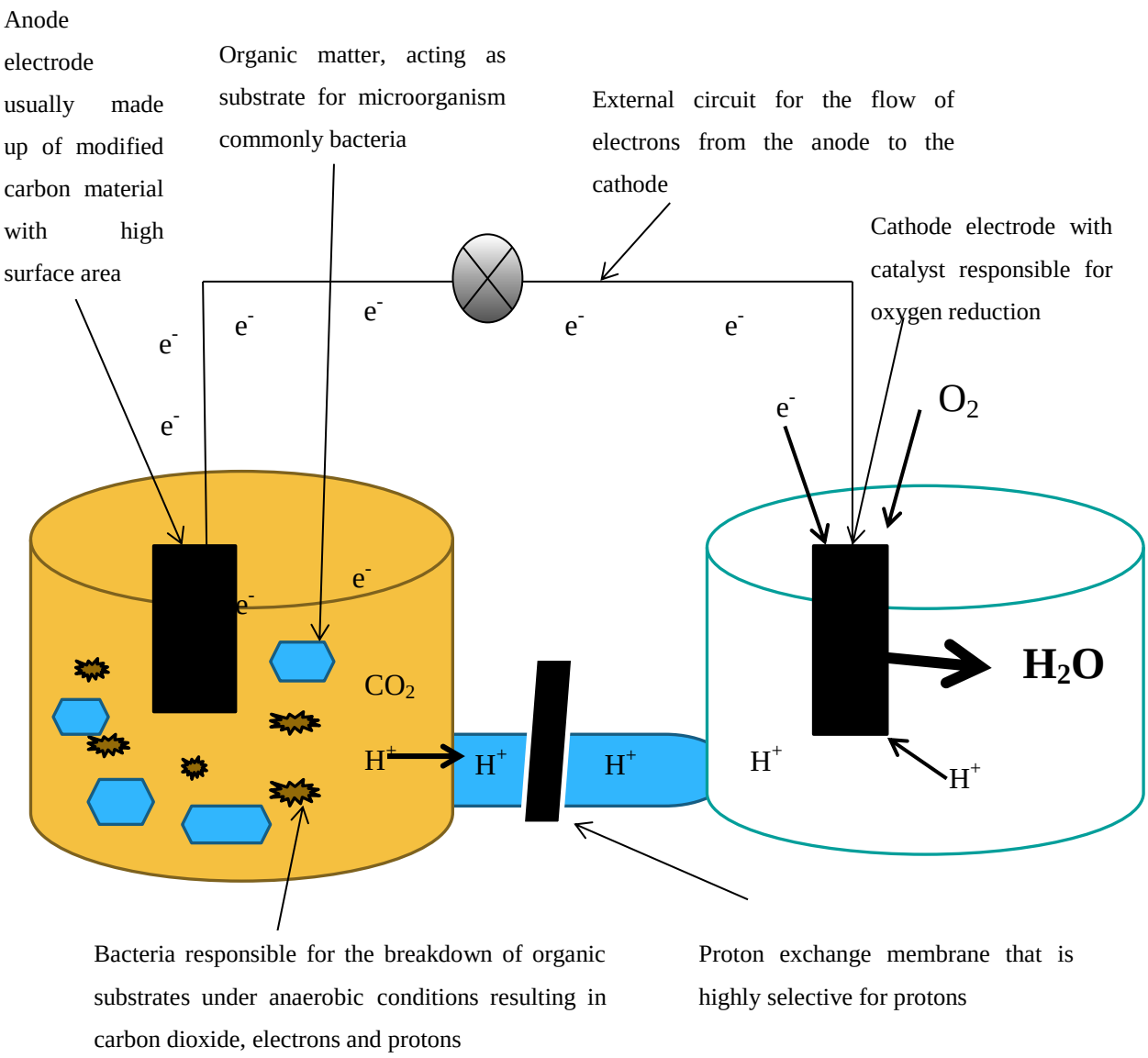

Figure 1.3: General schematic diagram of a two chambered H-type microbial fuel cell. Anaerobic anode shown on the left and aerobic cathode on the right.

Logan (2008) stated that the use of MFC technologies to generate electricity from bacterial biomass represented at the time, the newest approach for generating electricity. The advantage of MFC over traditionally used chemical fuel cells is that an MFC can be operated under mild reaction conditions such as room temperature and neutral pH and it can also

utilise biomass waste as a source of energy (Rodrigo *et al.,* 2007). Rodrigo *et al.,* (2007) noted that MFCs generally consist of three main categories, namely:

i. Cells that use a primary fuel as the substrate of choice to generate hydrogen or ethanol which can be used as a secondary fuel in a conventional fuel cell. The primary fuel used can be organic waste, glucose and acetate.

ii. Cells which generate electricity directly from an organic fuel source such as glucose and acetate.

iii. Cells which combine the utilisation of photochemically active system and biological moieties to harvest the energy from sunlight and convert it into electrical energy.

1.3.2 MFC architecture

Power production in the MFC is dependent on many important factors, including the reactor configuration, electrode material, performance of the proton exchange membrane, substrate type used in the MFC and the optimum conditions of operations (temperature and pH) (Behera *et al.,* 2010). The use of H-type MFCs (as shown in figure 1.3) in research, results in low power density productions because of the high internal resistances and electrode based losses (Logan *et al.,* 2006). The power density is also dependent on the surface area of the cathode relative to the anode, the distance between the cathode and anode, and the surface area of the proton exchange membrane (Logan *et al*., 2006). However, the use of H-type MFCs is suitable for the examination of basic research parameters that include substrate, electrode material and microbial catalyst (Logan *et al*., 2006). The rate of fuel oxidation, electron transfer to the electrode by the biocatalyst, resistive load of the circuit, proton transport through the membrane and the oxygen supply and rate of reduction in the cathode (Gil *et al.,* 2003) are the factors that directly affect the MFC performance. Most microbial fuel cells use oxygen at the cathode as the electron acceptor, however the diffusion of oxygen into the anode chamber can affect the power generation because of the anaerobic nature of the bacteria used in the anodic chamber (Kiely *et al*., 2011a). MFC technology has seen considerable advances in terms of understanding of the bio-reactions and improvements on

the engineering side, such as in cell architecture, material used in the cell system and the solution chemistry (Logan *et al*., 2006; Logan, 2008; Huang *et al*., 2011).

1.3.3 Anode chamber

In the anode chamber of an MFC, microorganisms act as biocatalysts for the oxidation of a substrate (Valkiainen *et al*., 2010). The catalysis of substrates in MFCs by fermentative hydrogen-producing bacteria increases the flexibility of substrate utilisation (Peighambardoust *et al*., 2010). The substrate utilisation in the anode chamber occurs under anaerobic conditions (Du et al., 2007). The breakdown of the substrate results in the conversion of the chemical energy stored in organic bonds to electrical energy (Du *et al*; 2007, Behera *et al*., 2010, Gil *et al*., 2003). The bacteria do not act as catalysts for direct electricity generation so there is a requirement for an additional catalyst for the electricity generation (Zhuang *et al*., 2011). Electrons liberated from the cells are transferred from the anode chamber to the cathode chamber through an external circuit whilst the protons move from the anode chamber to the cathode chamber through the proton exchange membrane (PEM) which separates the two chambers (Gil *et al*., 2003; Rabaey *et al*., 2005).

i. Anode fuel sources

Some of the energy present in most organic matter can be utilised in an MFC (Kiely *et al*., 2011a). MFC fuel sources include biodegradable organics such as volatile acids, carbohydrates, proteins, alcohols and cellulose in some cases (Logan, 2008). The full utilisation of complex carbohydrates such as cellulose and sugars is limited as they can only be partially oxidised (Kiely *et al.,* 2011b) resulting in the production of other bio-products such as hydrogen and acetate along with other organic substrates as by-products (Behera *et al*., 2010). For MFCs to be competitive with other forms of renewable energy production, liquid organic waste is considered to be a good substrate as an electron donor because it is free and a waste product (Behera *et al.,* 2010). Velasquez-Orta *et al*., (2011) used bakery wastewater, brewery wastewater, paper wastewater and dairy industries wastewater in MFCs as feedstock successfully.

The main limiting factor with the use of wastewater as a feedstock is that it sometimes contains xenobiotic compounds which cause it to be recalcitrant as a feedstock (Pant *et al*., 2009). Some complex organic fractions are resistant to microbial degradation or may be

degraded into other organic fractions without the release of electrons (Reimers, 2007). Acetate feedstock is a common feedstock in MFC studies because it is easily used by microorganisms and therefore serves as a model for research purposes (Pant *et al.,* 2009).

Studies utilising microalgae as a feedstock for MFCs have emerged (Velasquez-Orta *et al.,* 2009). The use of *Arthrospira* as feedstock has been studied in MFC (Celecki and Yavuzatmaca, 2008) with success. Velasquez-Orta *et al*., (2009) successfully used algal biomass (*Ulva luctula* and *Chlorella vulgaris*) as feedstock to minimise cost in MFC operation. In a different study, Rashid *et al*., (2013) used a mixture of *Scenedesmus* (pretreated) and activated sludge as MFC feedstock. However, the use of some algae in MFCs results in limited nutrient liberation because cell walls make the algae recalcitrant.

Cell disruption pre-treatment methods are necessary as upstream processes before use as a feedstock in MFCs to improve nutrient liberation for microbial use. Various methods have been used for algae cell disruption including microwaves, sonication, bead beating, osmotic pressure and autoclaving, to aid in nutrient release (Lee *et al.,* 2010). These methods are more suitable for a laboratory setup but are not as feasible in industrial and field applications. However, the study of these methods allows for information gathering for future algal disruption methods that may be applicable in the field on a larger scale. Microwaves shatter cells using the shock of high frequency waves, sonication disrupts cell walls and membranes due to a cavitation effect and bead beating causes direct mechanical damage to the cells because of the high-speed spinning with fine beads (Lee *et al*., 2010). The use of concentrated NaCl solution results in osmotic shock of the cells however longer periods of treatment (48 hours) are required (Lee *et al*., 2010). Autoclaving results in cell disruption due to the high temperature and high pressure during the process (Lee *et al*., 2010). Shi *et al*., (2007) demonstrated the use of high temperatures to improve polysaccharide yields from *Chlorella*. The study of the cell disruption methods of microalgae allows for the comparison of energy input against output.

ii. Anode electrode materials

The nature of the electrode material used in microbial fuel cells affects power density as well as coulombic efficiency (Kim *et al*., 2008). Coulombic efficiency is defined as the ratio of total electrons recovered as current to maximum possible electrons, if all substrate removal

produced current (Kim *et al*., 2008). The anode material and its structure directly affect bacteria attachment, electron transfer and substrate oxidation (Tsai *et al*., 2009) with research showing surface area, surface potential and surface roughness significantly affect the anodic reaction (Liang *et al*., 2011). Ideal anodic material must be conductive, biocompatible (not toxic to the microbes) and chemically stable (Zhu *et al*., 2011; Lee *et al*., 2008). The choice of biocatalyst (microbe) and the choice of the electrode catalyst all affect the performance of the fuel cell.

a. Types of carbon electrode material

Carbon materials such as carbon paper and carbon cloth are used in many microbial fuel cell applications due to their good stability in the inoculum mixture, high conductivity and high specific surface area (Zou *et al.*, 2008; Zhu *et al*., 2011). They are also low cost (Liang *et al*., 2011). Carbon felt is inexpensive, has a high surface area, is highly conducting but quite fragile (Kim *et al.*, 2008). Graphite electrodes have a high surface area, are stable in media however they have low current generations when unmodified (Kim *et al*., 2008). The use of carbon based electrodes in the anode has the main limitation of having low catalytic efficiency (Zou *et al*., 2008). The use of carbon based electrodes therefore results in low power densities experienced for fuel cells due to the limited electron transfer rate from exoelectrogenic bacteria to the anode (Peng *et al*., 2010). The current challenge with MFCs utilising carbon electrode materials is to link microbial catabolism with electrode reduction (Peng *et al*., 2010). Attempts to increase anode performance by adapting chemical and physical modifications of electrode materials have been studied and adapted (Kim *et al*., 2008).

b. Anode electrode modifications and catalyst supports

Modification of the carbon electrode materials surfaces through physical and/or chemical processes improves efficiency (Zou *et al*., 2008; Zhu *et al.*, 2011). Modification and optimisation of the anode, facilitates the electron transfer (Liang *et al*., 2011) through the improvement of the biofilm-electrode interaction (He *et al.*, 2011). Anode materials modified with organic or inorganic charge transfer mediators have been shown to result in a more rapid transfer of electrons (Kim *et al*., 2008). The use of carbon nanotubes to modify the carbon electrode surface improves power density due to the properties of carbon nanotubes, that

include a high conductivity and a high surface to volume ratio as a result of their small sizes (Zou *et al.,* 2008; Liang *et al*., 2011). Carbon nanotubes can act as catalyst supports and they offer enhanced catalyst activity in microbial fuel cells (Tsai *et al*., 2009). Mshoperi *et al*., (2013), demonstrated modification of the anode electrode with different grades of carbon black. Carbon black modifications of the anode by Mshoperi *et al*., (2013) resulted in comparable results to MFCs with MWCNTs modified anode electrodes. The use of novel anode modifications such as polyaniline-modified platinum, carbon nanotubes/polyaniline composite, polypyrrole coated carbon nanotubes composite and composite graphite have been shown to increase MFC and electrode performance (Wei *et al*., 2012). Increasing surface area results in an increase in the reactivity area which in turn increases electrode efficiency such as the carbon fibre (He *et al*., 2011).

iii. Anode microorganisms

The catalysis of reactions by microbes in the anodic chamber results in the oxidation of the substrates and subsequently production of electrons and protons (Du *et al*., 2007). While CO_2 is produced as an oxidation product, there is no net CO_2 emission because the CO_2 in the renewable biomass recently came from the atmosphere by way of photosynthesis, unlike a direct combustion process of fossil fuels (Du *et al.,* 2007). Electric current generation is made possible by keeping microbes separated from oxygen (O_2) and this requires an anaerobic anode chamber (Du *et al.,* 2007).

Various microorganisms have been studied in MFCs as catalysts for current generation. Wei *et al*. (2012) describe the use of *Shewanella oneidensis*, *Geobacteraceae*, *Clostridium butyricum*, *Rhodoferax ferrireducens* and mixed cultures from natural environments such as wastewater, in MFCs as commonly utilised biocatalysts. In their review, Du *et al*. (2007) detail the use of microorganisms in MFCs. Many microorganisms are able to transfer electrons from organic substrate metabolism to the anode (Du *et al*., 2007). Electrons produced during this process are transferred to a final electron acceptor through direct contact (Du *et al*., 2007). In MFCs that do not utilise mediators, metal reducing bacteria under anaerobic conditions that belong primarily to the families of *Shewanella*, *Rhodoferax* and *Geobacter* release electrons to the anode, with the anode acting as the final electron acceptor (Du *et al*., 2007). Most mediator-less MFCs utilise dissimilator metal reducing

microorganisms (Du *et al*., 2007). Mediators can be utilised for electron transfer to the anode for microbes that are unable to transport the electrons to the anode (Du et al., 2007). The mediators act as electron shuttles between the anode and the microbe, transporting the electrons to the anode. *Actinobacillus succinogenes, Desulfavibria desulfuricans, Escherichia coli, Pseudomonas fluorescen, Proteus mirabilis* and *Proteus vulgaris* to name but a few are microbes that require extraneous mediators (Du *et al.,* 2007). Some microbes for example *Pseudomonas aeruginosa* can provide their own mediators in MFC operations. The use of fermentative hydrogen-producing bacteria in an MFC increases the flexibility of substrate utilisation (Zhuang *et al.,* 2011). Cellulose degradation by *Enterobacter cloacae,* a facultative anaerobic bacterium, in an MFC is possible for the generation of electricity (Catal *et al.,* 2010).

iv. Enterobacter cloacae

E. cloacae is a motile, ornithine decarboxylase positive bacteria that belongs in the genus *Aerobacter* (Cooney *et al*., 2014). The *E. cloacae* complex is mainly distinguished from other *Aerobacter* species based on the DNA-DNA hybridisation of the whole genome (Cooney *et al*., 2014). Its natural habitats include soil, water (fresh, brackish, waste and marine), vertebrate and invertebrate hosts. It is a common species in clinical specific human infection accounting for over 90% of all *Aerobacter* clinical infections (Mahon et al., 2011). It is a facultative anaerobe that has been observed to grow at temperatures ranging from 20 – 37 °C at neutral pH on lab media (Cooney *et al*., 2014). It is able to produce gas from organic matter during fermentation (Cooney *et al*., 2014) and has a high rate of hydrogen production during the fermentation of carbohydrates (Kumar and Das, 2001). It is also able to produce energy from various lignocellulose biomass sources. This is very attractive because of the abundance of lignocellulose sources such as plant dry matter (Catal *et al*., 2010). Due to its facultative anaerobic nature (therefore reducing the need to strictly maintain anaerobic conditions at all times) and its hydrogen producing capabilities, *E. cloacae* was selected (Edwards *et al.,* 2012). *E. cloacae* has been studied as an MFC biocatalyst (Nimje *et al.,* 2011; Edwards *et al*., 2012; Mshoperi *et al*., 2014). The scope remains for studies to examine the role of pH, temperature and substrate utilisation in an MFC.

1.3.4 Cathode chamber

The cathodic reaction frequently involves the reduction of O_2 as the final sink for the electrons and protons liberated from the fuel sources at the anode in the oxygen reduction reaction (ORR) (Gil *et al.*, 2003).

i. Oxygen reduction reaction

The use of oxygen as the final electron acceptor in an MFC is a result of the availability and accessibility of oxygen and its high redox potential of 1.23 V (Wang *et al*., 2011). However, the diffusion of oxygen into the anode chamber can affect the power generation because of the anaerobic requirement in the anode (Kiely *et al*., 2011a). The use of a PEM can inhibit the leaking of oxygen to the anodic chamber (Logan, 2008). Cathode materials which are responsible for the ORR are the main limiting factor in scaling up the MFC (Liu *et al*., 2010). The ORR is an energetically costly reaction because of a high overpotential barrier when performed on carbon or graphite electrodes, therefore catalysts like platinum are required (Martin *et al*., 2011). Carbon materials have been used as ORR catalysts in the cathode (Zou *et al.*, 2008). However, modification of these carbon materials is necessary because by themselves the carbon electrodes have little catalytic efficiency (Zou *et al*., 2008). This is because they have poor oxygen reaction rates, and the addition of catalysts to their surfaces may accelerate the reaction rates (Uria *et al*., 2011). Platinum remains the best catalyst for the ORR (Kim *et al*., 2011). Cheaper alternatives for ORR are required if scaling up of the system is going to be economically feasible. The development of ORR catalysts for fuel cell applications is a major research field (Zhao *et al*., 2005).

ii. Platinum and issues associated with use of platinum

Platinum has many shortfalls as cathodic material, including its expensive nature, its tendency to poisoning by the formation of a platinum oxide layer on the surface therefore limiting its life span and its sensitivity to biological and chemical fouling (Uria *et al.*, 2011; Martin *et al*., 2011). However, cost remains a key limitation.

iii. Metallophthalocyanines (iron (II) phthalocyanines) as platinum alternatives

Macrocyclic complexes containing nitrogen produce active catalytic properties for the microbial fuel cell (Kim *et al.*, 2011). A variety of alternatives including compounds made up of first row transition metal, high surface area graphite-granules and activated carbon have

been suggested as platinum substitutes (Martin *et al*., 2011). Manganese oxides, polypyrolle, iron (ii) phthalocyanines (FePc) and cobalt tetramethylphenylporphyrin (CoTMPP) are low cost and they offer a good alternative to platinum although they show slightly less power generation (Martin *et al*., 2011). Cobalt in a macrocyclic complex for chelating the metal, has been known to be a very efficient catalyst. However, it catalyses only a two-electron reduction system of oxygen which generates hydrogen peroxide as an intermediate (Kim *et al*., 2011). The production of hydrogen peroxide reduces the efficiency of the system and degrades catalytic activity of the cathode (Kim *et al*., 2011). The use of iron in a macrocyclic complex uses the direct four-electron system with no harmful intermediates in between and it is very stable at neutral and alkaline pHs making it very suitable for use in an MFC (Kim *et al*., 2011). The use of FePc and CoTMPP as platinum substitutes on carbon supports showed similar activity to platinum based electrodes (Zhao *et al*., 2005; Qiao *et al.,* 2010). The use of FePc and CoTMPP demonstrated excellent durability (Zhao *et al*., 2005).

iv. Carbon supports for ORR catalysts

Materials that have a high specific area such as granular graphite, alternative inexpensive chemical electrocatalysts like noble metals and microbial biocathodes have been considered as possible replacements for platinum (Rozendal *et al*., 2008). An improved catalytic reduction by non-noble catalysts would greatly improve the efficiency of the system (Kim *et al*., 2011). Studies successfully modified carbon paper electrodes using MWCNTs and FePc as potential platinum electrode substitutions for the ORR (Edwards *et al*., 2012). Mshoperi *et al*., (2013) also successfully used FePc on a carbon black support as modification in the cathode for the ORR catalysis. Carbon paper was used which proved to be effective in MFC studies and could also be easily physically modified (Edwards *et al.,* 2012; Mshoperi *et al*., 2013). However the brittleness of carbon paper is a drawback.

v. Biocathodes

In their review, He and Angenent (2006), provide an argument for the use of biocathodes in MFCs. Microorganisms can act as catalysts to assist in electron transfer in the cathode. Algae produce oxygen through photosynthesis, therefore removing the cost of an external oxygen supply (He and Angenent, 2006). Use of biocathodes improves MFC sustainability compared to abiotic cathodes because there is no consumption and replenishment of electron mediator

(He and Angenent, 2006). Aerobic biocathodes provide oxygen for the oxygen reduction reaction, whereas anaerobic biocathodes utilise other compounds such as nitrate, sulphate, iron, manganese, selenite, arsenate, urinate, fumarate and carbon dioxide as terminal electron acceptors (He and Angenent, 2006).

1.4 Integrated algal pond system

Wastewater ponds are natural pond systems (Tadesse *et al*., 2004). An example of a wastewater pond is the integrated algal pond system (Tadesse *et al*., 2004). An integrated algal pond system consists of a facultative pond, a high rate algal pond and a sedimentation pond (Oswald and Asce, 1990). The first pond in the series is a facultative pond. The facultative pond has an aerobic surface and an anaerobic internal pit for sedimentation of sewage suspended solids and methane fermentation (Oswald and Asce, 1990). The upflow velocity in the internal pit is low resulting in the suspended solid removal through sedimentation being above 95% and the BOD removal of above 65% (Oswald and Asce, 1990).

The second pond in the series is the high rate algal pond (HRAP). The HRAP is a shallow (0.2 – 1.0 metres in depth), open raceway pond (with water velocities approximately 0.15 – 0.30 m/s) (Park *et al*., 2011b). The HRAP is used for the treatment of wastewater including municipal, industrial and agricultural wastewater from the facultative pond (Park *et al*., 2011b). In the HRAP microalgae have rapid growth resulting in the release of oxygen from photosynthesis (Oswald and Asce, 1990; Neba and Rose, 2004), which also generate algae biomass that, when recovered from the IAPS, could serve as potential feedstock in an MFC). Photosynthetic oxygenation by the algae varies with light intensities (Tadesse e*t al*., 2004). The oxygen released is used by aerobic bacteria to oxidise most of the soluble and biodegradable BOD remaining in the effluent from the facultative pond (Oswald and Asce, 1990). Biochemical and hydrodynamic processes for the HRAP are affected by meteorological factors such as wind, rain and temperature (Tadesse *et al*., 2004). The pH of the HRAP increases as a result of photosynthesis, due to the rapid consumption of carbon dioxide produced by bacterial respiration (Tadesse *et al*., 2004). The atmospheric carbon dioxide present in the pond on hot days is minimal due to elevated surface water temperatures which increases the gas escape. This results in a carbon dioxide deficit in the water (Tadesse

et al., 2004). The concentration of hydroxide ions in the water increases which results in a pH rise well over pH 10 (Tadesse *et al*., 2004). Under high light conditions, increased photosynthesis results in high rates of algal biomass being produced in the HRAP (Park *et al*., 2011a). The microalgae growing in the HRAP assimilate nutrients from the wastewater and harvesting of the algal biomass ensures nutrient recovery (Park *et al*., 2011a). In the HRAP, large volumes of microalgae are produced (Christenson and Sim, 2011). In HRAP wastewater treatment, mixed cultures consisting of *Scenedesmus spp*, *Micractinium spp, Actinastrum spp, Pediastrum spp, Coelostrum spp*, *Chlorella spp* and *Ankistrodesmus spp* are common (Park *et al*., 2011a).

1.5 Microalgae

Aquatic environments and subaerial environments are the main habitats for algae (Barsanti and Gualtieri, 2005). Algae can be defined as thallophytic (plants that lack roots, stems and leaves) photosynthetic organisms. They are highly pigmented and exist in many natural colours (Sambamurty, 2005). The diversity of algae makes them adaptable to most environments and they can be found in most aquatic environments varying in pH, temperature and salinity (Barsanti and Gualtieri, 2005). Microalgae cultures can generate significant quantities of biomass, and they generally have higher biomass productivity than plant crops in terms of land area required for cultivation (Pittman *et al*., 2011). They offer an alternative to land based organic sources of fuel and feedstock and have several advantages. The use of algae is viewed as not being in competition with food production (Velasquez-Orta *et al.,* 2009). This is because areas that may be used for algae aquacultures may be unsuitable for agricultural purposes, such as deserts and wastewater treatment plants (Gouveia, 2011).

1.5.1 Microalgae growth conditions

Algal blooms occur naturally in summer months in northern Europe (Wu *et al*., 2011). Cyanobacteria like *Arthrospira*, have an optimum growth rate at temperatures around 25° C (Wu *et al.,* 2011). However, the outdoor cultivation of algae is very complex as it requires many internal and external factors to consider (Becker, 1995). Under natural conditions most algae grow as mixed communities and those with the most favourable conditions at any particular time proliferate better which results in different community concentrations over time (Becker, 1995). For the successful culturing of a single species, growth conditions have

to be optimum for the selected species (Becker, 1995). If nutrient solution is to be developed, several factors including carbon, phosphorous, sulphur, potassium and magnesium have to be present in large amounts. Iron and manganese have to be present in smaller amounts, and other elements have to be available as trace amounts such as cobalt, zinc, copper and molybdenum (Becker, 1995). The pH of the media is also very important as well as other additional organic components and growth promoting substance such as vitamins (Becker, 1995). The growth of microalgae in open ponds is desirable in that open ponds are low cost (Becker, 1995). However, open ponds offer lower control of operating conditions, which in turn can cause low biomass productivity as well as contamination possibilities (Becker, 1995). Only highly selective species are not contaminated, and parameters such as light intensity, temperature, pH and dissolved oxygen further complicate the growth parameters of open ponds (Becker, 1995). Zheng *et al*., (2011), in their studies, yielded dry weights of about 2.5 $g.l^{-1}$. The *Chlorella* enters its log phase after 2 days and the stationary phase after 7 days at 25° C (Zheng *et al*., 2011).

1.5.2 Microalgae in wastewater

Microalgae can grow in most aquatic environments including brackish water, wastewater, seawater and freshwater (Gouveia, 2011). In wastewater cultures, microalgae utilise nitrogen and phosphorous in their metabolic processes thereby aiding in the bioremediation of the wastewater (Gouveia, 2011; Pittman *et al*., 2011). Microalgae can be cultured throughout the year and cultures in wastewater can be grown without the use of fertilisers and pesticides, thereby reducing the environmental impact (Gouveia, 2011). However, the growth of microalgae in wastewater is dependent on concentrations of essential nutrients including nitrogen, phosphorous and organic carbon, and the ratios of these nutrients is important, as well as light availability, temperature, oxygen concentrations and carbon dioxide availability (Pittman *et al*., 2011).

1.5.3 Current uses of microalgae

Microalgae like *Arthrospira spp*., *Scenedesmus spp*., *Chorella spp*. and *Pediastrum spp*. have many current uses for commercial and industrial purposes. The production of nutritional supplements, cosmetics, antioxidants, bioplastics, animal feed and natural dyes from microalgae is common (Barghbani *et al*., 2012) Purified polysaccharides from microalgae

such as agar and carrageenan have been studied and applied for their health benefits which include antitumor activity (Shi *et al.,* 2007). The rapid growth of rates of microalgae as well as the high intracellular lipid content makes them suitable candidates for biodiesel production through the transesterification of the triacylglycerol lipids (Lee *et al*., 2010; Liu *et al*., 2011; Pittman *et al*., 2011). The production of liquid fuel and gas from microalgae is done through thermochemical conversion methods which include gasification and pyrolysis (Pittman *et al*., 2011). Biochemical conversion of microalgae through fermentation and anaerobic digestion results in the production of other products such as bioethanol or methane (Pittman *et al.,* 2011). Dried algal biomass may also be combusted (Pittman *et al.,* 2011). Research has also been done on the use of microalgae as feedstock in MFCs (Lee *et al.,* 2010; Zheng *et al.,* 2011; Rashid *et al*., 2013). Microalgae has also been used as biocathode in MFC studies (Fu *et al*., 2009; Powell *et al*., 2009; Gonzalez *et al*., 2013; Wu *et al*., 2014).

Arthrospira is rich in protein content (55 – 70%), contains fatty acids, carbohydrates and vitamins (Ogbonda *et al*., 2007; Celeki and Yavuzatmaca, 2008). *Chlorella* is found in both fresh and marine water. It is a unicellular green algae that is rich in protein (50 – 65%) and also contains variable amounts of carbohydrates (10 – 20%) (Sheng *et al.,* 2007). The cell walls of *Chlorella* are composed mainly of hemicellulose and saccharides which results in minimal release of intracellular nutrients to media (Zheng *et al*., 2011). Algaenans are derived from cells walls of microalgae such as *Tetraedron minimum, Scenedesmus communis* and *Pediastrum borganum*, and these are algal material that have a high hydrogen and carbon ratio (Blokker et al., 1998). A range of processes have been suggested for cell disruption to enhance nutrient release including sonication, microwaves, enzymatic reactions, chemical reactions, grinding (Zheng *et al*., 2011). For example, lipid release by *Chlorella* cells in a study by Zheng *et al*. (2011) differed according to the pre-treatment steps. Untreated *Chlorella* cells had minimum lipid release in medium of about 3% of the total *Chlorella* dry weight, ultrasonication increased the lipid release to about 15%, cellulase enzyme use increased the lipid concentration to about 24% and grinding in liquid nitrogen increased the lipid concentration to about 29% (Zheng *et al*., 2011). Few studies have explored the use of microalgae as feedstock in MFC's and none have explored in depth species from high rate algal ponds. Substantial research yet remains in this area, for example pre-treatment of algal feedstock for MFCs or application in cathodic compartments.

1.6 Problem statement

MFCs couple the process of wastewater treatment and energy generation. In wastewater treatment plants that utilise IAPS there is an abundance of algal biomass. Utilisation of the biomass is desirable as this would improve the overall efficiency of the treatment system. Few studies have explored the application of algal biomass from an integrated algal pond system (IAPS) and the nutrient utilisation of the algae in an MFC. Pre-treatment of the algae and its effect on the MFC performance still need to be explored. MFC architecture is a key component and studies in this research group have shown that the use of FePc, MWCNTs and carbon black can improve performance of the MFC. The studies act as a valuable benchmark. However, the scope of the catalyst supports need to be explored further, including the use of carbon paper and activated carbon fibre. The effect of pH and temperature on *E. cloacae* in an MFC is not well studied. The use of algae and mixed consortia of algae as biocathodes in an MFC can be further explored.

1.7 Hypothesis

In this thesis it is proposed that microalgae harvested from the IAPS can be utilised as feedstock in a two-chambered MFC with performance enhanced when the algal cells are disrupted. Through the use of different algae as alternative substrates in a modified MFC, the economic viability of the MFC technology can be explored. There is also limited information of the performance of an MFC utilising algae as biocathodes. The study of algae as potential biocathodes would increase the scope of use of algae in MFCs not limiting them to being utilised as subtrates. The levels of dissolved oxygen in the cathode chamber can potentially be improved by using algae as bio-cathodes.

The cost of the overall MFC architecture, is a limitation as is low power output. The cost can be reduced by using substitute material including carbon fibre electrodes that are flexible and have a more defined 3D structure without affecting the power output drastically.

1.8 Aims and objectives

The main aim of the study was to explore algal based media from a high rate algal pond as a feedstock in an MFC and to examine the use of pre-treatment steps on MFC performance. The second aim of the study was to study the microenvironment analysis of the anodic chamber in terms of change in pH, change in temperature and nutrient utilisation in the MFC during operation when *E. cloacae* was the biocatalyst. The last aim of the study was to examine activated carbon fibre and algal based biocathodes and the effect on the performance of the MFC.

The aims of the study were carried out by implementing the following objectives.

In chapter 3; titled Microbial Fuel Cell studies: Examination of select algal species as substrates. Pretreatment of algae based feedstock through sonication and autoclaving and the effect on nutrient release: *E. cloacae* growth in algal-based feedstock from the HRAP and commercial nutrient media were studied. After successful metabolic growth of *E. cloacae*, MFC studies using algae based feedstock and commercial nutrient media were performed at 35° C.

In chapter 4; titled Factors affecting MFC performance: pH, temperature and proton exchange membrane: The change in pH and temperature in the anode chamber, during MFC operation for algal based feedstock and commercial nutrient media when *E. cloacae* was the biocatalyst were examined. The nutrient utilisation of the feedstock by *E. cloacae* during MFC operation was also examined. Controlled pH studies were examined, using buffered *Arthrospira* feedstock as the anode media. The fouling and performance of proton exchange membrane (Nafion®) after a 120 hour MFC operation was examined as well.

In chapter 5; titled Influence of electrode material on performance and study of microalgae as biocathodes in an MFC: Use of activated carbon fibre as electrode material in an MFC was examined and compared to carbon paper. Live algal cultures were examined as biocathodes under different light intensities.

Chapter 2 : General methodology

Several methodologies used in the thesis are described below and methodologies specific to each chapter are described in the respective chapters.

2.1 Microbial Fuel Cell

2.1.1 General setup of MFC

A two-chambered H-type MFC was assembled using 250 ml Schott bottles connected by a glass bridge clamped together with brass clamps (figure 2.2). The MFC were operated in controlled environment (CE) rooms at 35° C unless stated otherwise. The average glass bridge diameter was 1.5 cm with the proton exchange membrane (PEM) (Nafion™ N117, Johnson Matthey Technology Centre, UK) sandwiched between the bridges to separate the anode and cathode side. The average anode and cathode electrode was spaced at 20.7 cm. The anode and cathode chambers were connected externally using an insulated copper wire through a resistor circuit element, with resistance equal to 820 Ω (± 3 Ω). Potential difference measurements across the resistor were taken as mV using a TopTronic T 1300H (Hellermann Tyton) multimeter. The working volumes for both the anode and cathode were 120 ml of anolyte and catholyte respectively.

Power was calculated using the equation $P = V^2/R$ (Logan, 2008) and the power density was calculated using the equation $PD = \frac{V \, x \, V}{R \, x \, A}$. where P = power in watts (W), V = voltage from the potential in volts (V), R = resistance through the circuit in ohms (Ω) and A = electrode surface in square metres (m^2).

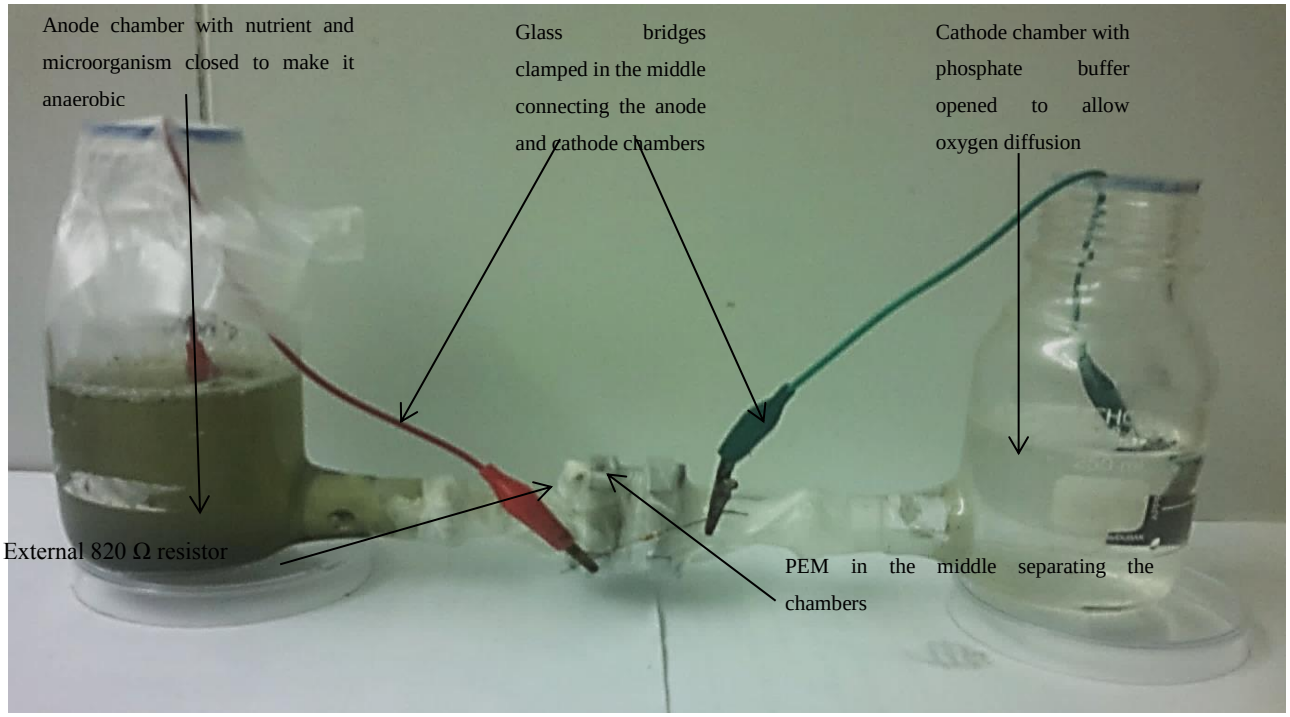

Figure 2.1: Lab set-up of an H-type two-chambered MFC

2.1.2 Proton exchange membrane

Nafion® membrane was used as the proton exchange membrane in the MFC studies because it has a high selective permeability to protons (Behera *et al*., 2010) and has been used with considerable success in similar research (Edwards *et al*., 2012; Mshoperi *et al*., 2013) which served as a benchmark in these studies. Using the method adapted from Zawadzinski *et al*., (1993), Nafion® (n117) membrane was treated as follows – Nafion® membranes were cleaned by placing them in 3% ($^{v}/_{v}$) H_2O_2 at 100° C for an hour. The step was then followed by rinsing in milliQ at 100° C water for an hour. The membranes were then further cleaned and sulphonated by placing in H_2SO_4 (0.5 M) at 100° C for an hour. This step was then followed by a final rinse step in milliQ water at 100° C for an hour. The membranes were then stored at room temperature away from direct light in sterilised milliQ water until it was required.

2.1.3 Anode feedstock

Reinforced clostridial medium (composition: Meat extract 10 $g.l^{-1}$, peptone 5 $g.l^{-1}$, yeast extract 3 $g.l^{-1}$, D (+) – glucose 5 $g.l^{-1}$, starch 1 $g.l^{-1}$, NaCl 5 $g.l^{-1}$, sodium acetate 3 $g.l^{-1}$, l-

cysteine hydrochloride 0.5 $g.l^{-1}$ and agar 0.5 $g.l^{-1}$) , *Arthrospira, Chlorella,* and a consortium of microalgae from the high rate algal ponds (HRAP) at the integrated algal pond systems (IAPS) at the institute for Environmental Biotechnology at Rhodes University (denoted EBRU consortium in the study) were examined as the feedstock for *E. cloacae* in an MFC. To the anode chamber of the MFC, 150 ml of the different feedstock (33 g dry weight in a litre of milliQ water) was placed in the anode chamber of the MFC. To the nutrient solution 200 µl of log phase *E.cloacae* (between 10 and 15 hours of growth) was inoculated. After connecting the anode electrode, the anode chamber was sealed with cotton wool and parafilm®, before lightly screwing the lid back on.

2.1.4 Cathode solution

In the cathode chamber, phosphate buffer (0.25 M) at pH 7.0 (± 0.2) was used for unless otherwise stated. Disodium hydrogen phosphate ($Na_2HPO_4.2H_2O$) and sodium dihydrogen phosphate ($NaH_2PO_4.H_2O$) were used to make up the buffer.

2.2 Electrode modifications

2.2.1 Multi-walled carbon nanotubes

Method for functionalization of the multi-walled carbon nanotubes (MWCNT) was adapted from Xu *et al*., (2007). A mixture of 10 ml 55% ($^{v}/_{v}$) nitric acid (Merck chemicals) aqueous solution and 30 ml 98% sulphuric acid (Holpro Lovasz) was prepared.

To this mixture 100 mg crude MWCNTs (diameter = 110 nm – 170 nm, length = 5-9 µm; >90% purity) (Sigma-Aldrich) was added and the mixture sonicated in a bath sonicator (Elmasonic sonicator, ELMA) for 8 hours at room temperature. To the mixture, 200 ml sodium hydroxide (Merck chemicals) (0.2 M) was added and left overnight to settle. The top acidic layer that had been formed was decanted and the settled MWCNTs were resuspended in milliQ water. Centrifugation at 23 932 g was performed for 20 min and the top acidic layer decanted and the settled MWCNTs were resuspended in milliQ water. Centrifugation was performed again at 15 317 g for 10 min with the top acidic layer decanted off and MWCNTs resuspended in milliQ water. The process was repeated at a centrifugation speed of 15 317 g until a pH of 7 for the supernatant was obtained. The MWCNTs were dried at 70° C for 72

hours and resuspended in dimethyformamide (DMF) (Merck chemicals) at a concentration of 5 $mg.ml^{-1}$ until required.

2.2.2 Iron (II) Phthalocyanines

Iron (II) phthalocyanines (FePc) (Dye content ~ 90%) (Sigma-Aldrich) were prepared by diluting 5 mg FePc in a ml of absolute ethanol and sonicating for an hour. The sonicated mixture was stored in the dark at room temperature until required.

i. FePc:MWCNT mixture

After sonication of FePc in absolute ethanol and the sonication of MWCNTs in DMF, 50 µl of MWCNT solution (5 $mg.ml^{-1}$) was added to 150 µl of FePc solution (5 $mg.ml^{-1}$) and sonicated for 5 minutes to mix the solution.

2.2.3 Anode electrode modification

Carbon paper (Toray TGP-060) (Alfa Aesar GmbH & Co. KG) electrodes were used as the electrode material (2 cm x 2 cm) unless stated otherwise. Modification (when required) for anode electrodes was performed using the drip dry method whereby 200 µl (5 $mg.ml^{-1}$) of functionalised multiwalled carbon nanotubes (MWCNTs) was dripped onto the electrode surface and was dried at 60° C in an oven for 20 minutes before use.

2.2.4 Cathode electrode modification

Carbon paper (Toray TGP-060) (Alfa Aesar GmbH & Co. KG) electrodes were used as the electrode material supports (2cm x 2cm). Modification of the cathode electrodes (when required) was performed by the drip dry method whereby a mixture of 50 µl MWCNTs (5 $mg.ml^{-1}$) : 150 µl iron (II) phthalocyanines (FePc) (5 $mg.ml^{-1}$) was dripped onto the electrode surface and then dried in an oven at 60° C for 20 minutes before use.

2.4 Microorganism

E. cloacae strain 16657 which had been obtained from DMSZ (Deutsche Sammlung von Mikroorganismen und Zellkulturen Gmbh) is a facultative anaerobe that was used as the microorganism of choice in these studies. Growth studies of the strain was undertaken in RCM, *Chlorella*, EBRU and *Arthrospira* feedstock respectively, at 35° C in a controlled environment room (CE room). Growth of *E. cloacae* in the different nutrient substrate feed

used was monitored for 24 hours using the turbidimetric method, at 600 nm using a UVmini-1240 spectrophotometer (SHIMADZU). *E. cloacae* in its logarithmic growth phase was inoculated into the studied media (figure 2.1). Microbial interference during optical density readings was minimised by autoclaving the feedstock media before inoculation with *E. cloacae*. *E. cloacae* growth in the substrate feed was monitored over a period of 24 hours and analysed using a spectrophotometer by taking absorbance readings at OD_{600}nm. Algal particulate interference during examination of alternative nutrient feedstock was minimised by pelleting down large algal particles at 1 876 g for 20 seconds (Microfuge Centrifuge, Beckman Coulter Inc., Germany) and making use of the supernatant.

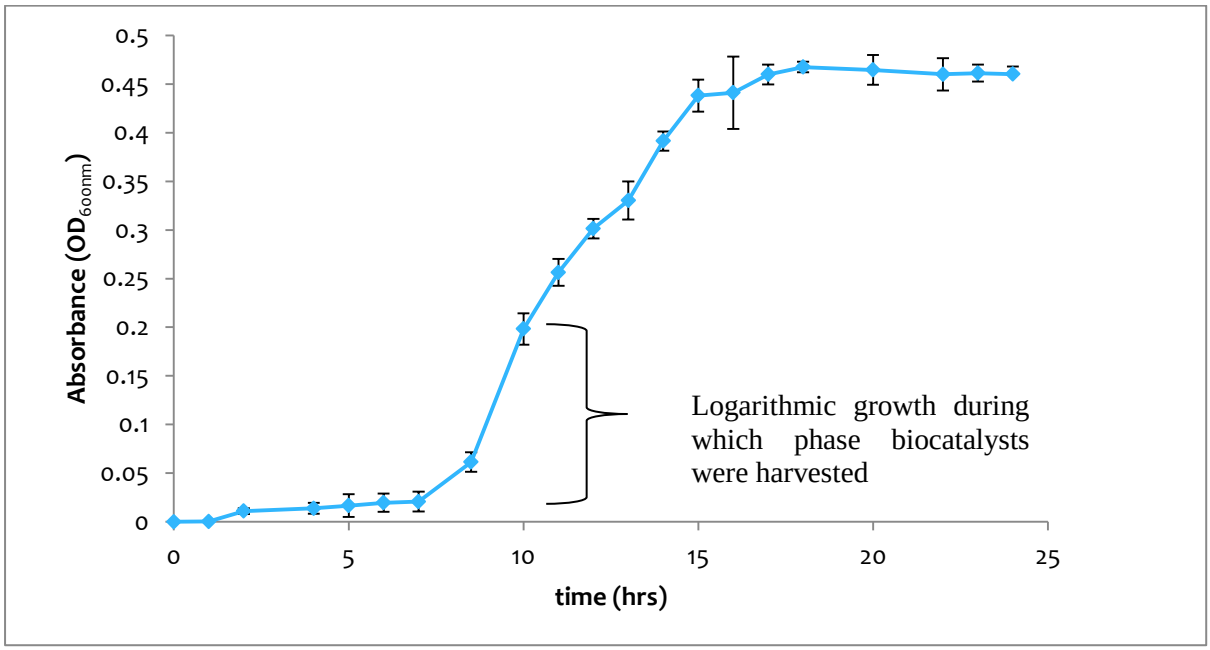

Figure 2.2: *E. cloacae* growth in RCM with logarithmic growth phase shown.

2.5 Nutrient assays

2.5.1 Carbohydrate assay

Carbohydrate concentration of the algal based feedstock and the RCM was quantified using the phenol sulphuric acid method using the method adapted from Sadasivam and Manickam (1996). Glucose (D (+), Merck chemicals) was used as the standard, using concentrations of 0.2, 0.4, 0.8, 1.0, 2.0, 3.0, 4.0 and 5.0 $mg.ml^{-1}$. The algal based feedstock was centrifuged at 1

876 g for 30 seconds to settle down large particulates. To 10 ml of the supernatant of the algae based feedstock and RCM that had been autoclaved, sonicated and autoclaved and untreated, 5 fold dilutions of the supernatants were performed before assaying. To the diluted algal based feedstock and RCM, 500 µl of 80% ($^{w}/_{v}$) phenol solution (molecular biology, ≥ 99% purity, Sigma-Aldrich, RSA) was added and the solutions were mixed vigorously using a vortex machine for 5 min and incubated at room temperature for 10 min. After the incubation, 2.0 ml concentrated sulphuric acid (98%, Holpro Lovasz) was added in a stream to each solution and the mixtures were shaken vigorously using a vortex machine for 5 min. The solutions were incubated at room temperature for 20 min. The solutions were then mixed by shaking for a minute and an absorbance reading at OD_{490nm} was taken using a UVmini-1240 spectrophotometer (SHIMADZU). A standard curve was plotted using glucose absorbance readings and carbohydrate concentrations of the nutrient solutions were deduced from the standard plot.

2.5.2 Protein Assay

Protein concentration was determined for each of the nutrients using the Bradford's assay adapted from Bradford (1976) with BSA (lyophilized powder, crystallised, ≥ 98.0% (GE), Sigma Aldrich, South Africa) serving as the standard. BSA concentration of 0.2, 0.4, 0.6, 0.8 and 1.0 $mg.ml^{-1}$ in milliQ water were used. The algal based feedstock was centrifuged at 1 876 g for 30 seconds to settle down large particulates. The supernatant of the algae based feedstock and RCM that had been autoclaved, sonicated, sonicated and autoclaved and untreated were diluted down to a final concentration of 10^{-1} (a 10-fold dilution). From the diluted algae based feedstock and RCM, 100 µl was taken and 4.9 ml Bradford's reagent (Sigma Aldrich, South Africa) was added and incubated at room temperature for 5 mins. Absorbance readings at OD_{595nm} were taken using a UVmini-1240 spectrophotometer (SHIMADZU). A standard curve was plotted using absorbances from BSA as the standard, and concentrations of the nutrients calculated from the standard curve.

2.6 Data analysis

All experiments were performed in triplicate. All data are presented as the means of triplicate measurements, and uncertainties represent standard deviations from the mean. Graphs and figures were plotted and presented using Microsoft Excel (2010) and all other calculations

and data variations were conducted using this software. Statistical analysis on raw data was performed using Statistica, ANOVA, using the Post-hoc analysis and Tukey HSD test.

Chapter 3 : Microbial Fuel Cell studies: Examination of select algal species as substrates

3.1 Introduction

Studies in to the utilisation of microalgae in terms of the generation of bioproducts like biofuels, bioethanol (Lee *et al*., 2010; Liu *et al*., 2011; Pittman *et al*., 2011), and as a feedstock for other microbes to produce bioelectricity or biomethane (Fu *et al*., 2009; Powell *et al*., 2009; Gonzalez *et al*., 2013; Wu *et al*., 2014), are desirable. A promising application for microalgae (after harvesting from wastewater) is as a feedstock in microbial fuel cells (MFC) (Huang *et al.*, 2011). Previous research has focused on the utilisation of *Chlorella* and *Arthrospira* as feedstock in an MFC (Edwards *et al*., 2012; Mshoperi *et al*., 2013).

Common freshwater microalgae include surface water algae such as *Micractinium*, *Scenedesmus*, *Pediastrum* and *Anacystis* and algae typically found in nutrient rich environments including *Chlorella* and *Chlorococcum* (Barsanti and Gualtieri, 2005). Green microalgae such as *Botyrococcus*, *Tetreaedron*, *Scenedesmus* and *Pediastrum* are known to have thick cell walls which contain algaenans (structures rich in carbon and hydrogen), this makes them potential candidates in biofuel production and potential organic feedstock in bioprocesses (Blokker *et al*., 1998).

The main limiting factor in terms of the use of algae in MFC technology is the presence of a recalcitrant cell wall that limits the access and release of nutrients to the biocatalyst (Lee *et al.*, 2010; Zheng *et al.*, 2011) resulting in limited rates and extents of biodegradation and, hence, low power densities in MFCs (Rashid *et al*., 2013). Researchers have focused on developing treatment steps to enable efficient cell disruption and nutrient recovery from the cells. Sonication, in particular, has been extensively applied to disrupt cell walls and the membranes of the cells (Lee *et al.*, 2010). Exposing cells to high temperatures and pressures such as in autoclaving can also be used as a method of cell disruption (Lee *et al.*, 2010).

Limited information is currently available on the response of the MFC system to the use of different algal-based feedstock. Integrated algal pond system ponds (IAPS) which are used in the secondary treatment of domestic wastewaters, use mixed consortia of algae to promote further aerobic bacterial decomposition of organic material leaving the primary treatment

(Neba and Rose, 2004). This results in the proliferation of algal biomass that is often harvested and thrown away, or used as animal feed or used as fertilizer.

The main aim of this study was to explore the use of microalgae (*Chlorella*, *Arthrospira* and a consortium of microalgae from an IAPS) as a feedstock in MFCs. This was done through examination of the effect of different treatment techniques for cell disruption and nutrient release from the algal cells and the study of the impact thereof on growth of *E. cloacae* and on power density generations in MFCs at 35° C. *Chlorella* and *Arthrospira* selected for these studies since they are key commercial algal isolates. A mixed consortium of microalgae (denoted as EBRU consortium) from the Institute of Evironmental Biotechnolgy, Rhodes University (EBRU) IAPS ponds, was also selected as it would give an insight into the response of the MFC to a natural unprocessed sample of algae. It also further helps to situate the study in a real world application.

3.2 Methodology and materials

3.2.1 Methods for treatment of algal samples examined as MFC feedstock

All algae feedstocks were formulated in milliQ water to a final concentration of 33 $g.l^{-1}$ and used immediately for studies.

i. Untreated algal samples

Algal feedstocks were sourced and formulated as described in chapter 2, section 2.3.2; 2.3.3 and 2.3.4. Algae suspensions which were not subjected to further pre-treatments are denoted as: "no treatment".

ii. Sonication of algal samples

Cell disruption through sonication was performed on algal based feedstock (EBRU consortium or *Arthrospira* or *Chlorella).* Sonication was performed using a Vibra cell probe sonicator (Sonics and Materials Inc., Danbury, Ct, USA) for 30 minutes at a frequency of 20 kHz and a power of 40 W in a 4° C CE room. After sonication the medium was stirred to evenly distribute the algae based feedstock in the medium. Sonication was performed to the samples prior to use and studies performed using the prepared sonicated solutions were denoted "sonicated".

iii. Heat and pressure treatment of algal samples

Heat treatment was performed on 33 g dry weight of algal based feedstock (EBRU consortium or *Arthrospira* or *Chlorella)* in a litre of milliQ water by autoclaving for 15 minutes at 121° C and a pressure of 104 kPa. This served as heat treatment for the algal based feedstock, and also served to sterilise all the feedstock. The autoclaved samples were denoted as "autoclaved".

Samples that were sonicated and autoclaved were denoted "autoclaved and sonicated".

3.2.2 Assays and characterisation studies

i. Microscopy

Cell morphology examination of algal feedstock following nutrient liberation treatments was performed using an Olympus BX50 light microscope. The algal-based feedstock was stirred to evenly distribute the particulates in the medium. From the stirred solution, a drop was taken using a drop pipette and place on a slide, before putting a cover slide and viewing at different magnifications under normal light field with no staining or preparations of the samples. Images of the algae were captured using an Olympus DP72 camera.

ii. Protein assays

Protein concentration was determined for each of the nutrients as described in chapter 2, section 2.5.2.

iii. Carbohydrate assays

Carbohydrate concentration of the algal based feedstock and of reinforced clostridial medium (RCM)(used as baseline feedstock in growth and MFC studies) was quantified as described in chapter 2, section 2.5.1.

3.2.3 Bacteria growth

Enterobacter cloacae strain 16657 (chapter 2, section 2.4) was inoculated into prepared algal based feedstock (EBRU consortium, *Chlorella* and *Arthrospira*) and RCM. Growth studies of *E. cloacae* in the different feedstock were performed in sealed 250 ml Schott bottles (anaerobic) at 35° C and absorbance was measured at OD_{600nm}.

3.2.4 MFC studies using algal-based feedstock and RCM feedstock

Two-chambered H-type MFCs were assembled and operated in CE rooms at 35° C. Nafion® membrane was used as the PEM. RCM and algal based feedstock (*Chlorella* feedstock, EBRU consortium feedstock and *Arthrospira* feedstock) were used alternately as the feedstock media in the anode. The working concentrations used are described in section 3.2.1. To minimise sedimentation of the large algal particulates, all MFCs were kept on a PSU multi-shaker (Boeco, Germany) at 100 rpm.

3.3 Results and discussion

3.3.1 Algal based feedstock cell disruption

The effect of autoclaved versus untreated *Chlorella* based feedstock and also of sonicated versuse sonicated and autoclaved *Chlorella* based feedstock was studied through the use of a light microscope and are shown in figure 3.1 and 3.2, respectively. *Chlorella* cells in the medium were observed at 400 x magnification

Untreated *Chlorella* feedstock

Autoclaved *Chlorella* feedstock

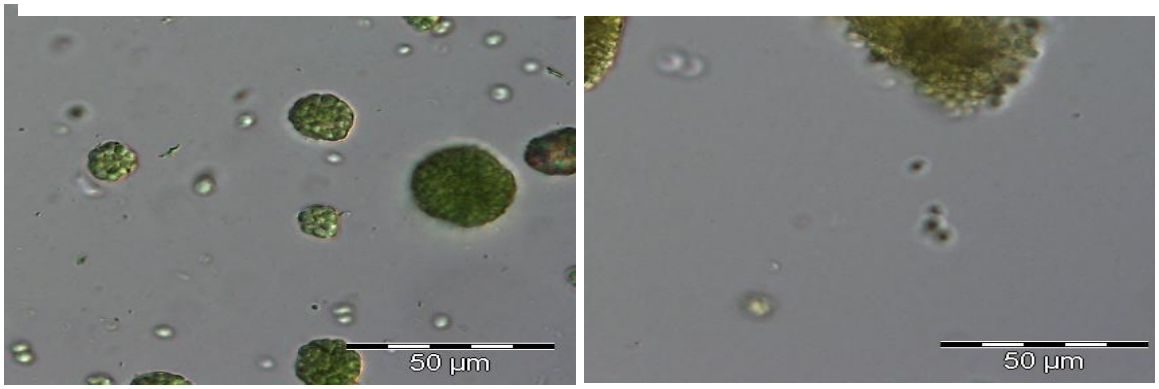

Figure 3.1: Microscopic images of *Chlorella* cells in *Chlorella* based feedstock at 400 x magnification. Left image shows untreated *Chlorella* substrate medium and the right image shows autoclaved *Chlorella* substrate medium.

Sonicated *Chlorella* feedstock

Sonicated and autoclaved *Chlorella* feedstock

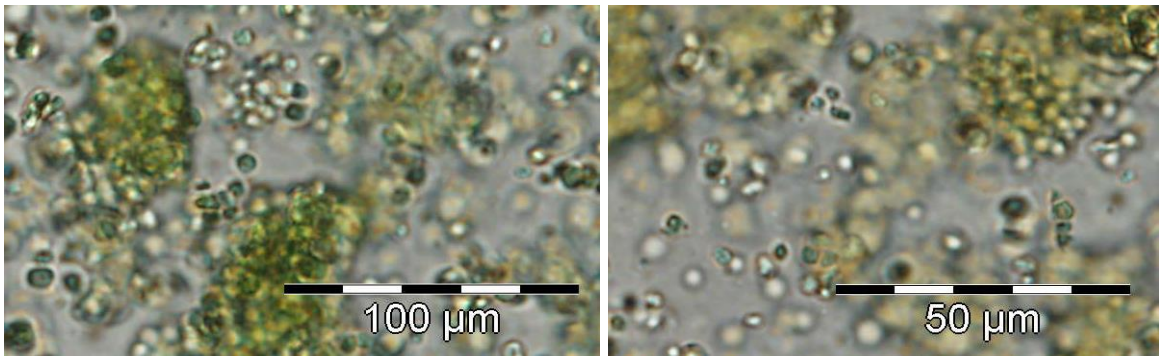

Figure 3.2: Microscopic images of the *Chlorella* cells in *Chlorella* based feedstock at 400 x magnification. Left image shows sonicated *Chlorella* substrate medium and the right image shows sonicated and autoclaved *Chlorella* substrate medium.

Chlorella cells are unicellular and circular in structure with thick cell walls (Sheng *et al*., 2007) as shown in figure 3.1. The cells are shown to be clumped together. A deep green colour is observed for the *Chlorella* untreated cells, which is a result of the cell chlorophyll and other pigments.

The autoclaved *Chlorella* cells in figure 3.1, show a loss of colour compared to the untreated cells because of the chlorophyll and other pigment degradation. Lee *et al*., (2010) observed that the process of autoclaving *Chlorella* releases lipids from the cells. This suggests that autoclaving has a role in cell disruption and the microscopy images for the autoclaved cells taken in the study also shows a visible change from untreated to cells treated by autoclaving.

Figure 3.2 shows how sonication effectively disrupts the *Chlorella* cells in solution compared to figure 3.1 which shows untreated and autoclaved *Chlorella* cells. This supports the observation by Zheng *et al*., (2011) which describes ultrasonication as a method for cell disruption in microalgae. The sonication of the medium containing *Chlorella* weakens the cell integrity and breaks the cell walls (figure 3.2). The sonicated *Chlorella* cells are more dispersed in the media with minimal clumping observed compared to autoclaved and untreated cells. From figure 3.2 it can be observed that besides breaking the cell walls, sonication also distributes the cells throughout the medium. A combination of sonication and autoclaving shows a combination of cell damage as observed in the autoclaved medium and sonicated medium. The sonicated and autoclaved step also increased the cell disruption compared to just autoclaving only. This is supported by Lee *et al*. (2010) who described also the disruption of cells after autoclaving at high temperatures and pressure.

The effect of autoclaved versus untreated *Arthrospira* based feedstock and also of sonicated versus ‘sonicated and autoclaved’ *Arthrospira* based feedstock was studied through the use of a light microscope and are shown in figure 3.3 and 3.4, respectively. *Arthrospira* cells in the medium were observed at 400 x magnification.

Untreated *Arthrospira* feedstock

Autoclaved *Arthrospira* feedstock

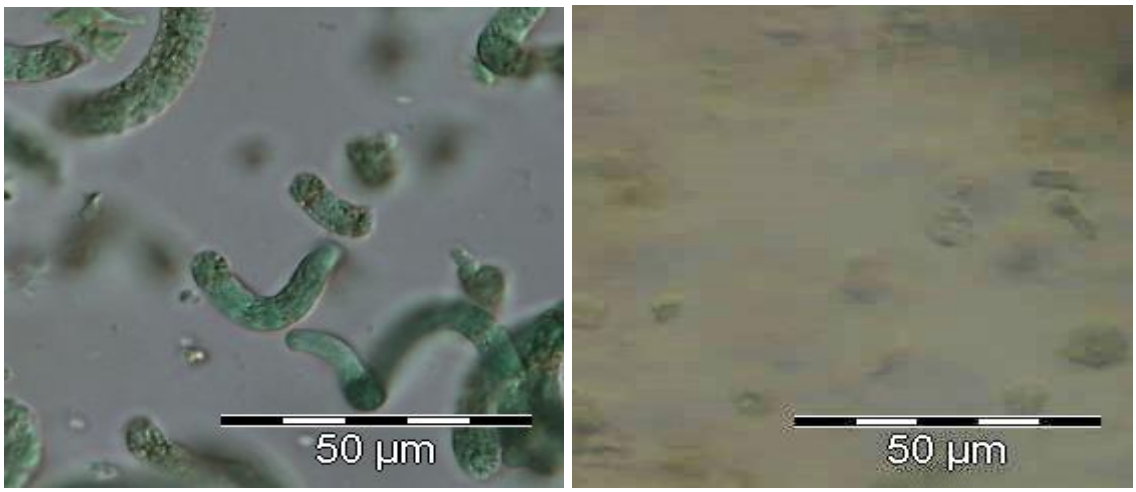

Figure 3.3: Microscopic images of *Arthrospira* cells in *Arthrospira* based feedstock at 400 x magnification. Left image shows untreated *Arthrospira* substrate medium and the right image shows autoclaved *Arthrospira* substrate medium.

Sonicated *Arthrospira* feedstock

Sonicated and autoclaved *Arthrospira* feedstock

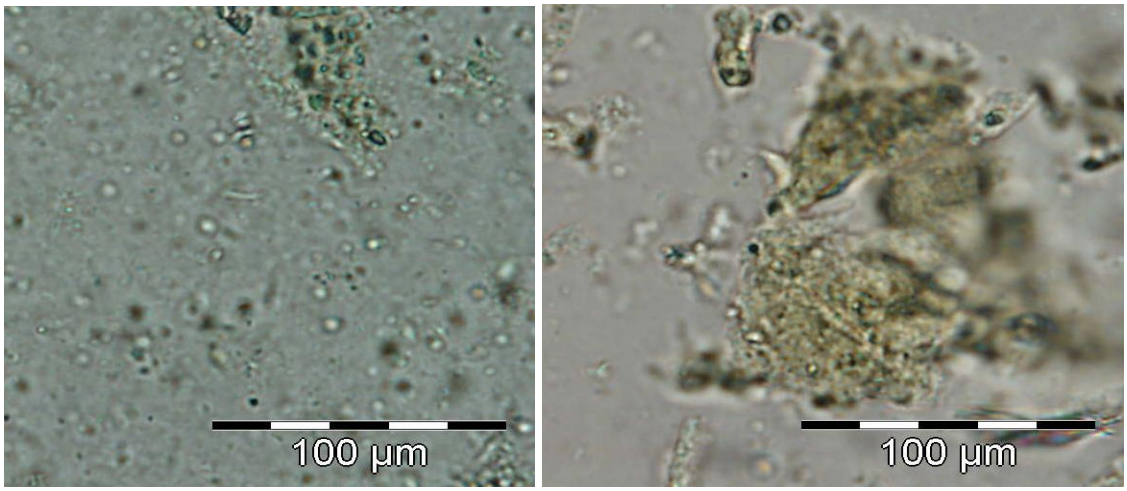

Figure 3.4: Microscopic images of the *Arthrospira* cells in *Arthrospira*-based feedstock at 400 x magnification. Left image shows sonicated *Arthrospira*-based feedstock and the right image shows sonicated and autoclaved *Arthrospira*-based feedstock

Figure 3.3 shows untreated *Arthrospira* with its filamentous structure clearly visible, as observed by Celecki and Yavuzatmaca, (2008). The helical arrangement of the trichomes (elongated terminal cells) is visible. Unlike *Chlorella*, *Arthrospira* which is a cyanobacterium does not have a cellulose cell wall, but instead has a cell wall composed mainly of proteins (60%) with the rest being made up of carbohydrates and fats (Gershwin and Belay, 2012). This provides less integrity to the cell wall and so the cells are more readily disrupted (Gershwin and Belay, 2012) compared to more recalcitrant *Chlorella* cells. This results in the need for minimal mechanical stress (heat and pressure), in order to disrupt *Arthrospira* cell walls. The observations made from images taken of autoclaved *Arthrospira* suggested that this heat (autoclaving) treatment is more effective for *Arthrospira* compared to *Chlorella*, because the former lacks a tough cellulose cell wall.

Sonication of *Arthrospira* resulted in cell breakage and the particulates being well distributed in the liquid as shown in figure 3.4. Compared to the untreated *Arthrospira*, the cells integrity is more affected by sonication. Unlike in the autoclaved step where the cells were broken into smaller particulates, sonication disrupts the cell integrity of the cell wall completely resulting in the release of small particulates into the media. Unlike the previous steps, empty vesicles are more numerous for this treatment step as indicated by the appearance of what seems to be membranes encompassing vacuoles and the release of material from the cells after this treatment step.

The effect of autoclaved versus untreated mixed algal consortium from EBRU consortium and also of sonicated versus ‘sonicated and autoclaved’ EBRU consortium feedstock was studied through the use of a light microscope and are shown in figure 3.5 and 3.6, respectively. Mixed consortium from EBRU cells in the medium were observed at 400 x magnification.

Untreated EBRU mixed consortium feedstock

Autoclaved EBRU mixed consortium feedstock

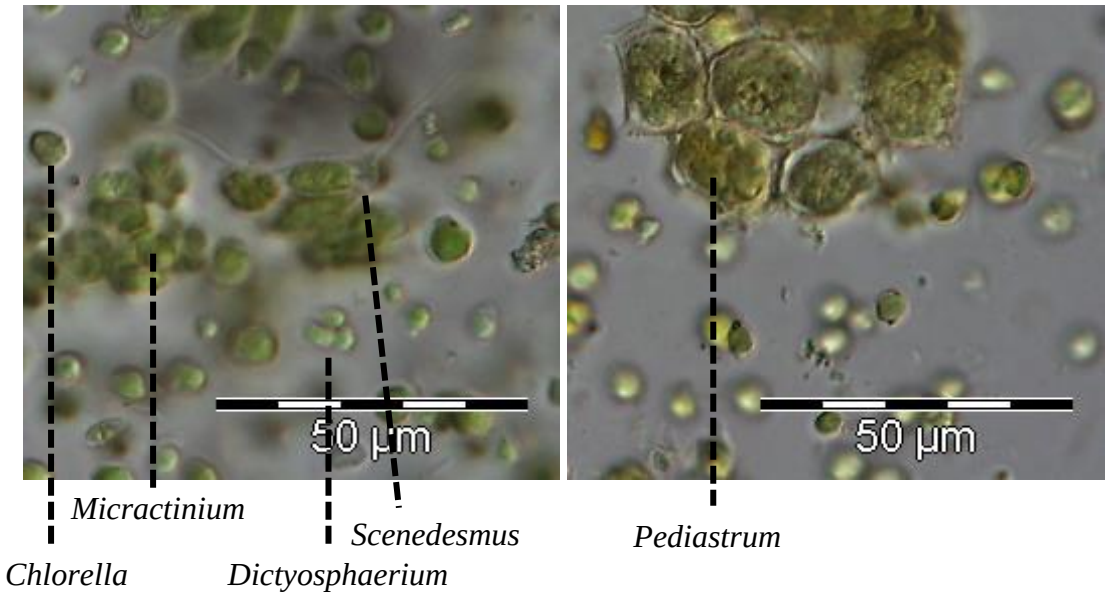

Figure 3.5: Microscopic images of the EBRU consortium algal cells at 400 x magnification. Left image shows untreated EBRU consortium and the right image shows autoclaved EBRU consortium.

Sonicated EBRU consortium feedstock

Sonicated and autoclaved EBRU consortium feedstock

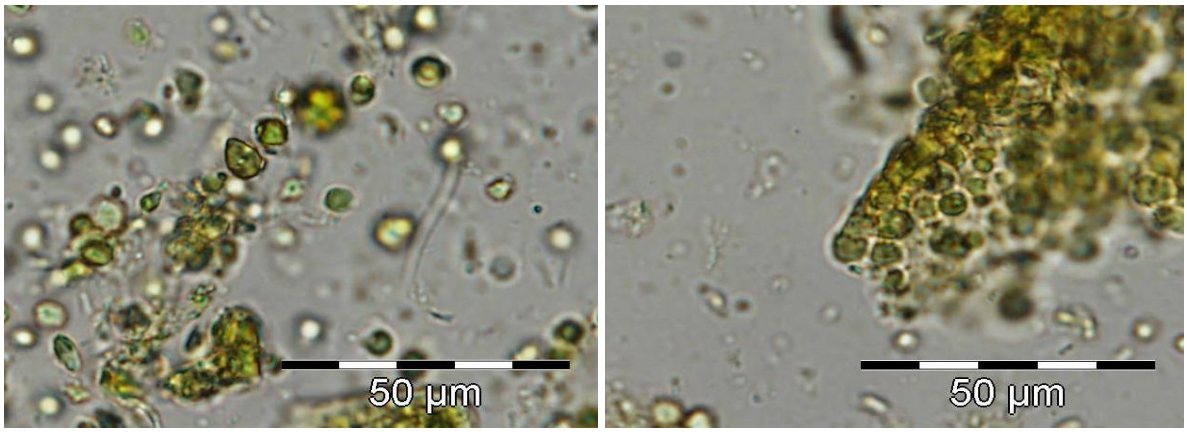

Figure 3.6: Microscopic images of the EBRU consortium algal cells at 400 x magnification. Left image shows sonicated EBRU consortium and the right image shows sonicated and autoclaved EBRU consortium.

Figure 3.5 shows the EBRU consortium which is comprised of different algae. A mixed consortium consisting of some common fresh water algae such as *Micractinium spp., Scenedesmus spp., Dictyosphaerium spp., Pediastrum spp.* and *Chlorella spp.* were identified using the image analysis from Park *et al*., (2011a) similar to reports by Becker, (1994) and Tomaseli, (2008). The environment in the IAPS from where the consortium was harvested from consists of nutrient-rich fresh wastewater which supports the consortium under different environmental conditions (Tomaseli, 2008).

After autoclaving, a loss of colour is observed for the mixed consortium. The cell density in the medium is lower compared to the untreated consortium. This results from the cell breakage that happens after autoclaving leaving the more resilient cells like *Pediastrum*, *Scenedesmus* and *Chlorella*.

Sonication of the EBRU consortium shows some visible signs of cell disruption which appear visually to be more effective than the autoclaving step for the EBRU consortium (figure 3.6) as was seen for *Chlorella*. The cells in this image appear to be clearer showing the loss of content possibly due to cell breakage. The sonicated and autoclaved EBRU images show the combined effects of the two processes, with less cell density in the media and a visible loss in cell colour being evident.

3.3.2 Nutrient characterisation of algal samples

The results of protein and carbohydrate assays in the different feedstock before and after treatment are shown in table 3.1.

Table 3-1: Carbohydrate assays and protein assays on the different feedstock.

Nutrient containing media	Carbohydrate concentration of supernatant ($g.l^{-1}$)	Protein concentration of supernatant ($g.l^{-1}$)
RCM	6.36 (± 0.39)	14.9 (± 1.23)
Chlorella untreated	2.42 (± 0.29)	4.23 (± 1.50)
Chlorella autoclaved	2.85 (± 0.28)	7.43 (± 1.67)
Chlorella autoclaved and sonicated	4.10 (± 0.30)	14.50 (± 2.46)
Arthrospira untreated	2.51 (± 0.31)	4.67 (± 0.50)
Arthrospira autoclaved	3.54 (± 0.29)	12.01 (± 1.63)
Arthrospira autoclaved and sonicated	5.01 (± 0.32)	13.45 (± 3.32)
EBRU consortium untreated	2.04 (± 0.29)	3.37 (± 2.17)
EBRU consortium autoclaved	3.81 (± 0.31)	7.34 (± 2.56)
EBRU consortium autoclaved and sonicated	5.64 (± 0.34)	15.73 (± 4.61)

Table 3.1 shows the effect of the pre-treatment of algae on the release of nutrients as seen by the increase in total carbohydrates and total proteins released into the medium with each successive treatment method. For all algal samples, a combination of autoclaving and sonication yielded the highest amount of protein and carbohydrate.

The supernatant of samples of untreated *Chlorella* feedstock had a carbohydrate concentration of 2.42 (± 0.29) $g.l^{-1}$, which is 38% (± 7.3%) of the total carbohydrate

concentration determined in RCM medium of 6.36 (± 0.39) $g.l^{-1}$. The process of autoclaving the *Chlorella* feedstock resulted in similar the total carbohydrate concentration released into the medium of 2.85 (± 0.28) $g.l^{-1}$ compared to 2.42 (± 0.29) $g.l^{-1}$ (untreated *Chlorella* feedstock). There was thus no statistically significant difference in nutrient release between untreated *Chlorella* medium and autoclaved *Chlorella* medium. Sonicating and autoclaving the *Chlorella* feedstock resulted in an increase in the total carbohydrate concentration in the supernatant to 4.10 (± 0.30) $g.l^{-1}$ which was siginificantly different to that of the untreated *Chlorella* medium, being a 69 % (± 25 %) increase in release of total carbohydrates from the cells to the medium. Untreated *Chlorella* feedstock had a protein concentration of 4.23 (± 1.50) $g.l^{-1}$ compared to the protein concentration of RCM medium which was 14.9 (± 1.23) $g.l^{-1}$. The untreated *Chlorella* feedstock resulted in a 28.4 % (± 12.9 %) release of total protein compared to RCM into the medium. Autoclaving the *Chlorella* feedstock resulted in an increase in the total protein released in the medium to 7.43 (± 1.67) $g.l^{-1}$from 4.23 (± 1.50) $g.l^{-1}$. An increase of about 1.8 times after autoclaving compared to the untreated feedstock. Sonicating and autoclaving resulted in an increase in proteins released to 14.50 (± 2.46) $g.l^{-1}$. The recalcitrant nature of the *Chlorella* cell wall results in the release of the least amount of nutrients into the medium without any pre-treatment. Zheng *et al*, (2011) described how the cell wall of *Chlorella* is comprised mainly of hemicellulose and saccharides which affect the ready release of nutrients. Zheng *et al*. (2011) observed that sonication of *Chlorella* cells resulted in an increase of lipid concentration to dry weight release from the cells to about 15 % compared to about 3 % for untreated *Chlorella* cells. Shi et al., (2007) describes how exposing *Chlorella* cells to high temperatures and sonication results in a higher release of nutrients. Many studies have focused on the release of nutrients from *Chlorella* cells as they are universally recognised as having a tough cell wall that traps the nutrients inside the cells.

Untreated *Arthrospira* feedstock had a carbohydrate content of 2.51 (± 0.31) $g.l^{-1}$ in the medium. This is 39 % (± 3 %) of the total carbohydrates in RCM medium. Autoclaving the *Arthrospira* feedstock resulted in an increase in the carbohydrate concentration in the medium to 3.54 (± 0.29) $g.l^{-1}$. This represents a 41 % (± 24 %) increase in total carbohydrate availability in the medium compared to untreated *Arthrospira* feedstock. Sonicating and autoclaving *Arthrospira* feedstock resulted in an increase of the total carbohydrate in the medium to 5.01 (± 0.32) $g.l^{-1}$. Untreated *Arthrospira* feedstock medium contained a protein

concentration of 4.67 (± 0.50) $g.l^{-1}$. Compared to RCM medium protein concentration of 14.9 (± 1.23) $g.l^{-1}$, the protein concentration in the medium was 31 % (± 7 %) of RCM medium. Autoclaving the *Arthrospira* feedstock resulted in an increase in the protein concentration in the medium to 12.01 (± 1.63) $g.l^{-1}$. Compared to the untreated *Arthrospira* feedstock, autoclaving resulted in a 157 % (± 46 %) increase in the protein in the medium. Sonicating and autoclaving resulted in the release of protein to the medium to 13.45 (± 3.32) $g.l^{-1}$. Compared to the autoclaved *Arthrospira* medium, there was no significant difference. This may be due to the lack of a resilient cell wall surrounding the *Arthrospira* cells, therefore facilitating the release of nutrients into the medium when heat and pressure are applied.

EBRU consortium feedstock when untreated had a carbohydrate concentration of 2.04 (± 0.29) $g.l^{-1}$ in the medium. Compared to RCM medium which had a carbohydrate concentration of 6.36 (± 0.39) $g.l^{-1}$, the mixed consortium medium had 68 % (± 11 %) less carbohydrates. Autoclaving the EBRU consortium feedstock resulted in an increase of the carbohydrate concentration in the medium to 3.81 (± 0.31) $g.l^{-1}$. Compared to the untreated medium this represents an 87 % (± 27 %) increase in the carbohydrates released into the medium. Sonicating and autoclaving the mixed consortium resulted in an increase of carbohydrates to 5.64 (± 0.34) $g.l^{-1}$. Compared to the untreated mixed consortium medium, this is a 170 % (± 20 %) increase. The protein concentration of the untreated mixed consortium was 3.37 (± 2.17) $g.l^{-1}$, compared to RCM medium which had a protein concentration of 14.9 (± 1.23) $g.l^{-1}$. The mixed consortium medium had 77 % (± 12 %) less protein than RCM medium. Autoclaving the EBRU consortium feedstock resulted in an increase of the protein concentration in the medium to 7.34 (± 2.56) $g.l^{-1}$. This represents about a 2 times increase in the protein concentration in the medium when the medium is autoclaved compared to untreated. Sonicating and autoclaving the EBRU consortium feedstock resulted in an increase in the protein concentration in the medium to 15.73 (± 4.61) $g.l^{-1}$. Compared to untreated mixed consortium medium, this represents about a 4.7 times increase in the protein concentration in the medium.

The process of autoclaving for all the algal-based feedstock resulted in a significant increase in carbohydrate release compared to untreated feedstock except for *Chlorella* medium. Looking at figure 3.1, there is little change in the integrity of the autoclaved *Chlorella* cells

compared to the untreated, compared to the other algal-based media. Autoclaving the algal-based feedstock, resulted in an increase in the protein released to the media. Chlorella and EBRU consortium had similar concentrations of proteins in the medium after autoclaving, unlike *Arthrospira*, which had much more proteins in the medium after autoclaving. Figure 3.3 shows how the integrity of the *Arthrospira* cells after autoclaving is more compromised compared to the other algae. This could explain the increased protein concentration compared to the other media under the same treatment. Sonicating and autoclaving for the algal-based feedstock, resulted in significant increases in carbohydrate release. The same effect was also observed for protein concentration, except for *Arthrospira* medium, where no significant difference was observed. The supplementary data for the commercially purchased *Chlorella* states that protein concentration is 50 % of the total dry weight and the carbohydrate concentration is 15 % of the total dry weight. A maximum carbohydrate concentration of 4.10 (± 0.30) $g.l^{-1}$ was observed for *Chlorella* out of a total *Chlorella* dry weight of 33 $g.l^{-1}$. This shows a 12 % total concentration of carbohydrates, which is only about 3 % lower than the theoretical maximum. A maximum protein concentration of 14.5 (2.46) $g.l^{-1}$ was observed for *Chlorella* medium after sonicating and autoclaving out of a total *Chlorella* dry weight of 33 $g.l^{-1}$. This signifies about 44 % total concentration of proteins out of a theoretical 50 %. The supplementary data for the commercially purchased *Arthrospira*, states that the nutritional composition contains about 65 % protein of total dry weight and about 15 % carbohydrates of the total dry weight. The maximum yield for carbohydrates in *Arthrospira* was about 15 % of the total dry weight and the maximum yield for proteins was about 41 % of the total dry weight after sonicating and autoclaving.

3.3.3 Growth of *E. cloacae* in treated and untreated algal based feedstock.

Figure 3.7 shows the optical density of *E. cloacae* in different feedstock media when absorbance is measured at OD_{600nm} and anaerobic growth is conducted at a controlled temperature of 35° C over a period of 24 hours.

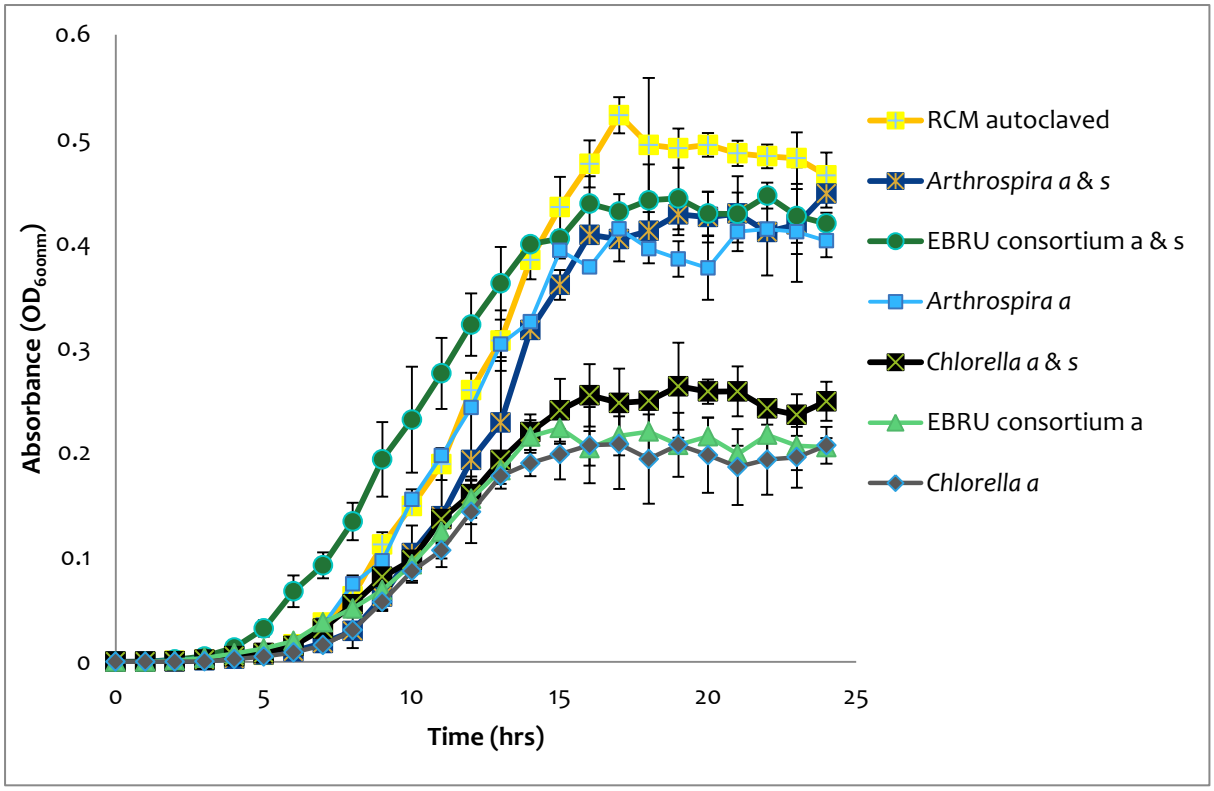

Figure 3.7: Growth of *E. cloacae* at 35° C in different feedstock media over a period of 24 hours. The nutrient media was either autoclaved (a) or sonicated and autoclaved (a & s). Turbidity was measured at an OD of 600_{nm}.

As observed in figure 3.7, the growth of *E. cloacae* in EBRU consortium feedstock that is sonicated and autoclaved enters log phase much earlier than in any of the other nutrient feedstock, with the log phase starting at 4 hours. This can be a result of the complexity offered by the mixed consortium nutrient media which would have many different available nutrients for use by the microbe. The mixed consortium may provide a medium with readily available nutrients and therefore allows *E. cloacae* culture to quickly adapt to its new environment and enter log growth phase sooner.

After 14 hours of growth, *E. cloacae* cultured in RCM recorded a higher absorbance than for the culture grown in any of the feedstocks including that derived from the EBRU consortium (figure 3.7). This could be a result of the more easily utilisable nutrients in RCM relative to that of the mixed consortium. RCM also had the highest carbohydrate and protein concentration levels. RCM is an industry processed substrate, optimised for microbial inoculation and studies. RCM contains different complex and simple nutrients such as meat extract, yeast extract, glucose, starch and sodium chloride that would aid in microbial growth.

Hence the optimum growth observed in RCM compared to the other nutrients follows an expected trend. After the initial growth spurt, *E. cloacae* growth in the feedstock derived from the EBRU consortium levelled off at around 15 hours and in RCM levelled off after 16 hours.

The best growth for *E. cloacae* was observed in RCM medium. This is because, amongst other things, a result of the high carbohydrate and protein concentrations compared to the other media. *E. cloacae* in sonicated and autoclaved *Arthrospira* feedstock had similar growth with EBRU consortium autoclaved and sonicated medium. The carbohydrate and protein concentrations in *Arthrospira* medium that was autoclaved and sonicated were 5.01 $g.l^{-1}$ and 6.29 $g.l^{-1}$ respectively. The carbohydrate and protein concentrations in EBRU consortium medium that had been autoclaved and sonicated were 5.64 $g.l^{-1}$ and 6.73 $g.l^{-1}$ respectively. The carbohydrate and protein concentrations between the media were very similar, which may explain the similar growth. *Arthrospira* feedstock medium that had been autoclaved had slightly lower growth compared to EBRU consortium sonicated and autoclaved as well as *Arthrospira* sonicated and autoclaved. The carbohydrate concentration was 3.54 $g.l^{-1}$ and the protein concentration was 6.01 $g.l^{-1}$. Compared to sonicated and autoclaved *Arthrospira* medium and sonicated and autoclaved EBRU consortium medium, the protein concentrations are similar but the carbohydrate concentrations are different.

E. cloacae in *Chlorella* medium that had been autoclaved and in *Chlorella* medium that had been autoclaved and sonicated had similar growth rates with *E. cloacae* in EBRU consortium that had been autoclaved. The protein concentrations were 5.27 $g.l^{-1}$, 5.45 $g.l^{-1}$ and 4.43 $g.l^{-1}$ respectively. These feedstocks had the lowest growth observed, with absorbance peaks being approximately half of the *Arthrospira* autoclaved, *Arthrospira* autoclaved and sonicated and EBRU consortium autoclaved and sonicated media. The protein concentration for both the Chlorella based media is relatively high but the growth for *E. cloacae* is low. The carbohydrate concentrations for *Chlorella* autoclaved medium and *Chlorella* autoclaved and sonicated medium were 2.85 $g.l^{-1}$ and 4.10 $g.l^{-1}$. These carbohydrate concentrations were relatively lower than for the other algal based media, which would account for the low peak in growth for *E. cloacae* in *Chlorella* based media.

For all the algal-based media, the autoclaved media had supported lower growth responses of *E. cloacae* when there was no sonication treatment. The growth at the stationary phase were less than 0.25 OD units. The microscopy images show some loss of cell integrity after autoclaving but not as much as when sonicated. The exception is in the case of *Arthrospira*, which is also susceptible to disruption through autoclaving. For medium derived from sonicated and autoclaved *Chlorella*, growth of *E. cloacae* was significantly lower compared to sonicated and autoclaved EBRU consortium medium or *Arthrospira* medium. From the nutrient analysis, it can be observed from the effects on *E. cloacae* growth that the autoclaved carbohydrates nutrient available in the supernatant from the EBRU consortium and *Arthrospira* are similar to that of sonicated and autoclaved *Chlorella* carbohydrate concentrations. However, this does not take account of the different complexity of carbohydrate based nutrients such as hemicellulose and saccharides, which minimise the availability for utilisation by *E. cloacae*.

The growth cannot be explained by just the carbohydrate and protein concentrations. The carbohydrate and protein assays help to give a limited view on observed trends. Other factors that may affect results include the main elements and trace elements that may be found in the different media, as well as the molarity of the concentrations due to the salt concentrations differing which may in turn affect metabolic pathways of *E. cloacae*. To give greater insight into the metabolic pathways, a full analysis of the nutrients and the metabolic pathways of *E. cloacae* would be required.

Figure 3.8 shows the growth of *E. cloacae*; with the absorbance values converted to log 10 and from the straight logarithmic growth log 2 graphs were plotted. The straight line graphs from the log 2 graph have a reciprocal of the gradient showing the doubling time of *E. cloacae* in each of the feedstock media. The doubling time is the time required for the *E. cloacae* to double in quantity during logarithmic growth.

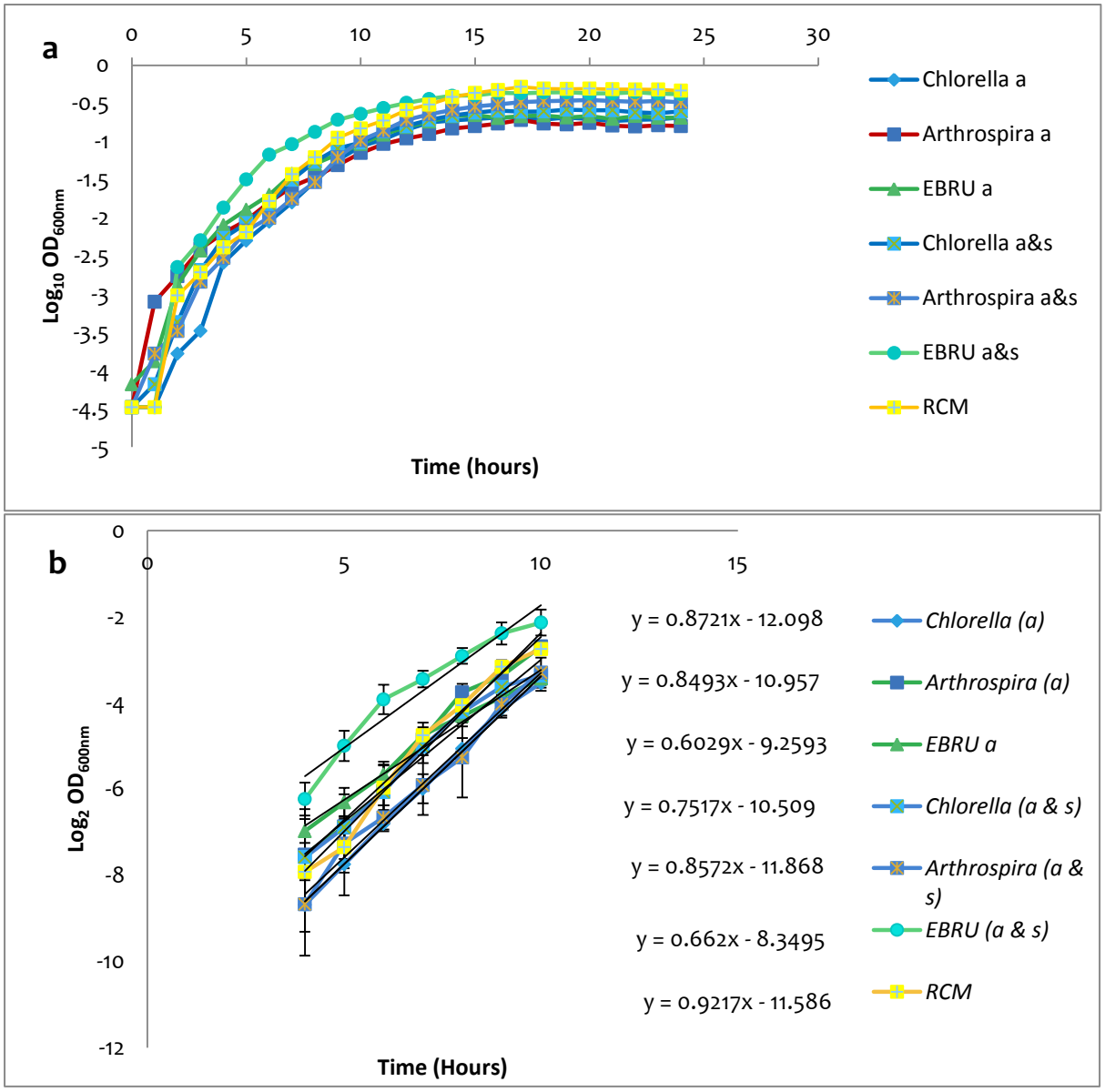

Figure 3.8: The logarithmic plotting of growth from figure 3.8, with absorbance values converted to $\log_{10}$ (a) and $\log_2$ (b).

From figure 3.8 b, the reciprocal of the gradient of the graphs gives the doubling time. It can be observed that the doubling time for *E. cloacae* was shortest in RCM medium with a doubling time of about 1 hour 5 minutes (± 3 minutes). The longest doubling time was measured in EBRU consortium feedstock (autoclaved) medium which had a time of about 1 hour 40 minutes (± 4 minutes), showing that acclimation to the EBRU consortium autoclaved medium was lowest. Growth of *E. cloacae* in *Chlorella* (autoclaved), *Arthrospira* (autoclaved) and *Arthrospira* (autoclaved and sonicated) feedstock media demonstrated

doubling times of around 1 hour 9 minutes (± 9 minutes) 1 hour 11 minutes (± 11 minutes) and 1 hour 10 minutes (± 10 minutes) respectively. The low doubling time for *E. cloacae* in the *Chlorella* medium relative to the growth rates, could be a result of the release of lipids after autoclaving the cells (Lee *et al*., 2010) which would provide ready nutrient for the microbe but not in such a large quantity that would allow much growth. The low doubling time for *E. cloacae* in *Arthrospira* media could be a result of the less complex nutrients released after pretreatment which lack cellulose (Gershwin and Belay, 2012).

The peak absorbance's from the different nutrient media were then compared to the peak absorbance observed in RCM medium. Maximum growth of *E. cloacae* in the different nutrient media was shown as a percentage compared to the maximum growth in RCM medium and the results were tabulated and presented in table 3.2.

Table 3-2: The peak absorbance of *E. cloacae* in the different nutrient media was recorded and tabulated.

Feedstock	Peak Absorbance (OD_{600nm})	Time taken to reach peak absorbance (Hours)	Percentage peak absorbance relative to RCM peak
RCM	0.522 (± 0.02)	17 (± 0)	100 (± 0.0)
Chlorella autoclaved	0.207 (± 0.04)	17 (± 0)	39.7 (± 0.8)
Chlorella sonicated and autoclaved	0.264 (± 0.04)	19 (± 1)	49.4 (± 1.1)
Arthrospira autoclaved	0.414 (± 0.01)	17 (± 4)	79.3 (± 0.3)
Arthrospira sonicated and autoclaved	0.429 (± 0.04)	22 (± 2)	82.1 (± 1.1)
EBRU consortium autoclaved	0.224 (± 0.02)	15 (± 2)	42.9 (± 0.5)
EBRU consortium sonicated and autoclaved	0.446 (± 0.01)	22 (± 0)	85.2 (± 0.8)

The data observed in table 3.2 indicates the growth of *E. cloacae* in the different medium and the time taken to reach the peak growth. The results were compared to those of RCM nutrient medium. Sonicated and autoclaved EBRU consortia showed a higher percentage of growth of 85.2 % (± 0.8), compared to *E. cloacae* grown in *Chlorella* (autoclaved and autoclaved and sonicated) and *Arthrospira* (autoclaved and autoclaved and sonicated) media with respect to RCM medium at its peak. This suggests that after treatment of the EBRU consortium, *E. cloacae* was able to utilise the nutrients in the medium more efficiently for growth and metabolic processes.

There is a direct correlation between the carbohydrate concentrations observed in table 3.1 and the growth of *E. cloacae* in the different media. An assumption can thus be made that carbohydrate availability for metabolic use plays an important role in initial growth of the bacteria culture. The lowest absorbance for *E. cloacae* was observed in autoclaved *Chlorella* of 0.207 (± 0.04) and the carbohydrate concentration in this medium was 2.85 (± 0.28) $g.l^{-1}$. EBRU consortium that had been autoclaved had an *E. cloacae* absorbance of 0.224 (± 0.02) and the carbohydrate concentration was 3.81 (± 0.31) $g.l^{-1}$. Sonicated and autoclaved *Chlorella* medium resulted in an absorbance of 0.264 (± 0.04) for *E. cloacae* in the medium and the carbohydrate concentration was 4.10 (± 0.30) $g.l^{-1}$. In RCM growth were more than in all the other media at 0.522 (± 0.02) and the carbohydrate concentration was 6.36 (± 0.39) $g.l^{-1}$. This trend is not observed for protein concentrations in the media, with sonicated and autoclaved *Chlorella* as well as sonicated and autoclaved EBRU consortium having no significant protein concentrations differences with RCM but the growth were different.

3.3.4 The performance of the MFC using algal based feedstock with *E. cloacae* as biocatalyst.

Figure 3.9 shows the power density values when log phase *E. cloacae* were inoculated in the respective researched media in an MFC. MFC runs were done at 35° C for a length of 14 hours.

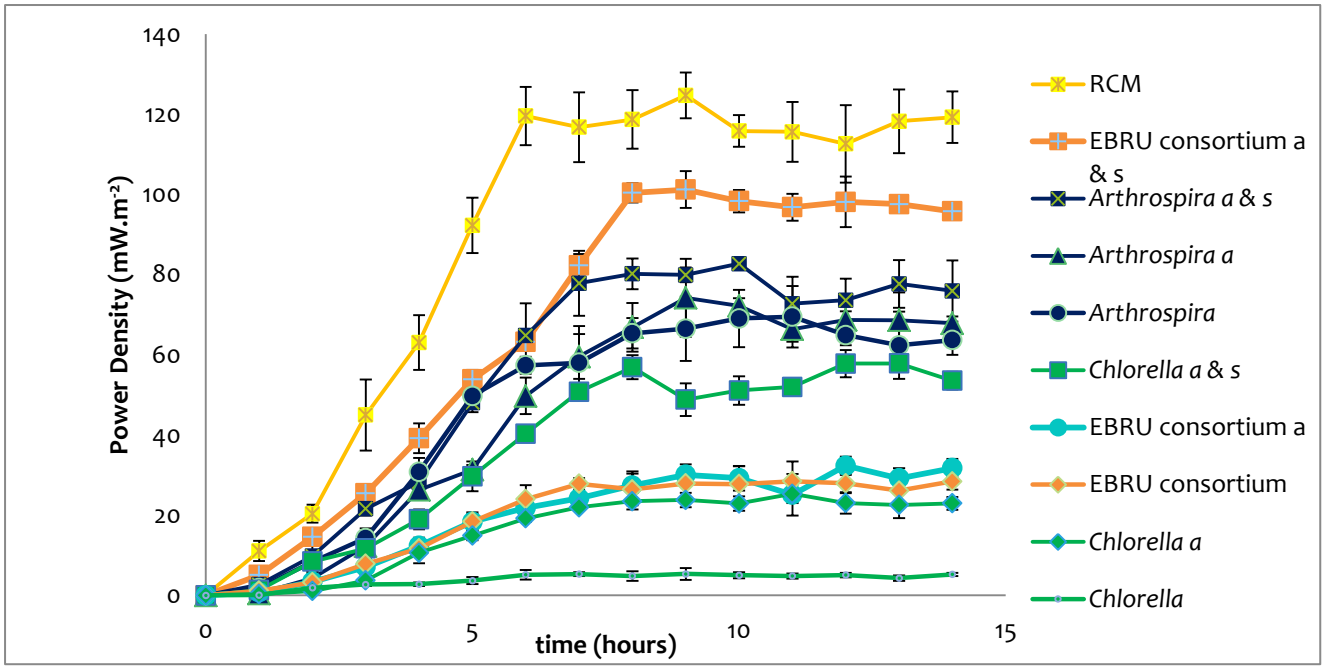

Figure 3.9: Power density curves versus time for MFC utilising different substrates. MFCs studies were performed in triplicate at 35° C with *E. cloacae* as the biocatalyst. Algal-based feedstock and RCM were used as the substrates. Studies were performed for 14 hours with readings taken hourly.

The performance of the MFCs using different feedstock at 35° C is shown in figure 3.9. In the figure the increase in power density on an hourly basis is represented. RCM is used as the baseline for the study and the performance of the different treatments on the algal-based feedstock is compared to the performance in RCM. The different treatments for the algal based feedstock included autoclaving (a) and autoclaving and sonicating (a & s). These treatments were also compared to untreated media.

The peak power density in each of the different feedstocks was tabulated and for the different treatment the peaks were shown as a percentage of the peak power density in RCM. The tabulated results are shown in table 3.3.

Table 3-3: **The peak power density for each of the nutrients is shown as per gram of dry weight.**

Nutrient	Peak power density ($mW.m^{-2}$)	Percentage peak power density relative to RCM
RCM	124.7 (± 5.73)	100
Chlorella	5.3 (± 1.51) *#	4.23 (± 1.5)
Chlorella a	23.8 (± 1.78) *#	19.0 (± 2.5)
Chlorella a & s	56.9 (± 2.05) *#	45.5 (± 4.0)
Arthrospira	69.5 (± 7.65) *+	55.8 (± 9.1)
Arthrospira a	77.2 (± 3.65) *+	61.6 (± 6.4)
Arthrospira a & s	82.8 (± 0.71) *+	66.4 (± 4.7)
EBRU consortium	28.5 (± 4.93) *+	22.8 (± 5.3)
EBRU consortium a	32.3 (± 2.29) *+	25.9 (± 4.2)
EBRU consortium a & s	101.2 (± 4.58) *#	81.2 (± 7.7)

The asterisk * shows the results of the Tukey HSD test of each of the feedstock compared to RCM where $p < 0.01$. The hash symbol # shows the results of the Tukey HSD test of each of the same feedstock treatments compared to each other when $p < 0.01$. + shows the results of the Tukey HSD test of each of the same feedstock treatments when $p > 0.1$.

Statistical analysis on the results from table 3.3 was performed using ANOVA and the Tukey HSD test. Each of the feedstock was compared to RCM. For each feedstock the different treatments were also compared.

From table 3.3, it can be noted that all the algal based feedstock, yielded significantly different performances compared to RCM medium in an MFC. For *Chlorella*, the different treatments had a major impact on the performance of the MFC, with significantly different results observed when treatment steps were taken compared to untreated cultures. Using *Arthrospira* as the feedstock in an MFC, the different treatments have no significant

difference on the performance. Therefore in terms of *Arthrospira* use, minimum treatment to the feedstock does not greatly affect MFC performance. EBRU consortium feedstock had no significant difference in MFC performance between autoclaved and untreated media. However, autoclaving and sonicating the EBRU consortium, resulted in improved performance in the MFC. The latter results in a highly significant performance difference in an MFC. The highest peak power density for algal-based medium was observed in sonicated and autoclaved EBRU consortium, which was about 81.2 % of the peak in RCM. *Chlorella* untreated medium had the lowest power density, at 4.23 (± 1.5) $mW.m^{-2}$. Without sonicating and autoclaving, excluding *Arthrospira* medium, the peak power density in algal-based feedstock was low. The peak in *Chlorella* autoclaved was 23.8 (± 1.78) $mW.m^{-2}$, in untreated EBRU consortium 28.5 (± 4.93) $mW.m^{-2}$ and in autoclaved EBRU consortium was 32.3 (± 2.29).

A comparison of the peak power densities in the different feedstock and the peak power absorbance shows a correlation as shown in figure 3.10.

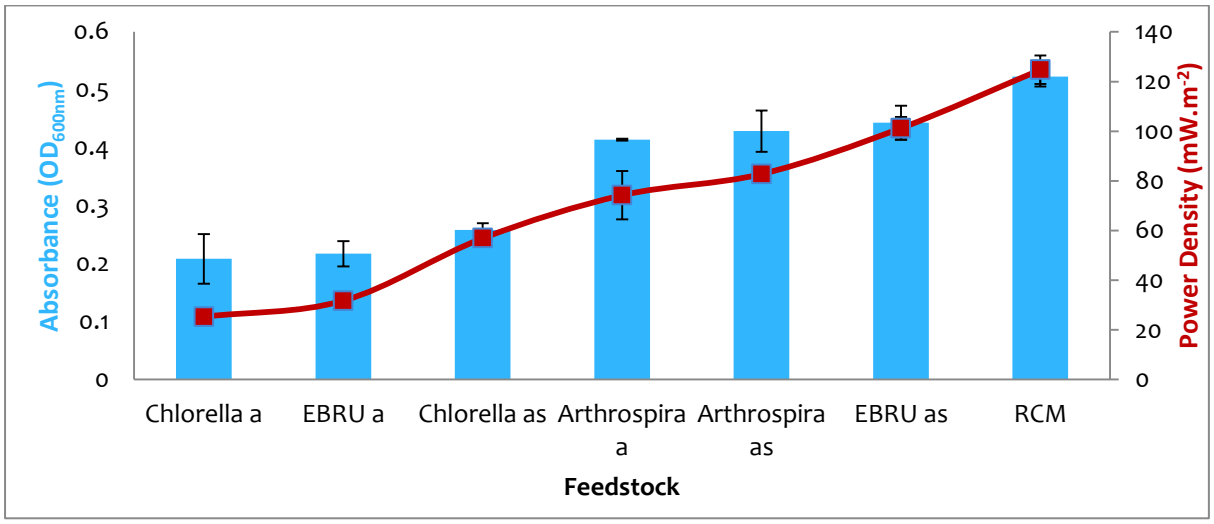

Figure 3.10: Bar graph comparing the growth of *E. cloacae* in the different feedstock and a line graph of the peak power density in the different feedstock.

Figure 3.10 shows the peak absorbance for growth kinetics for *E. cloacae* in different feedstock at OD_{600nm} and is represented as bar graphs. The peak power density for MFC studies in each of the feedstock is shown by the line graph. The figure shows trends similar to

those observed for the *E. cloacae* growth (figure 3.8). As can be observed in table 3.3, the peak absorbance also relates to the peak power density. There is a direct relationship between the peak power density and peak absorbance. *E. cloacae* in RCM had the greatest absorbance for growth with an absorbance at OD_{600nm} being 0.52 (± 0.02). The peak power density for MFC studies was also greatest in MFCs with RCM as feedstock with a peak power density of 124.73 (± 5.73) $mW.m^{-2}$. RCM contains L-cystein hydrochloride which is an oxygen scavenger, and which also improves performance of an MFC. Logan (2008) describes the need of an anaerobic chamber as oxygen inhibits the electricity generation. For the algal-based feedstock, EBRU consortium feedstock that has been sonicated and autoclaved had a peak power density of 101.21 (± 4.58) $mW.m^{-2}$ and for growth the peak absorbance observed was 0.45 (± 0.01). From figures 3.8, 3.9 and 3.10, EBRU consortium feedstock that had been autoclaved and sonicated resulted in the best performance for the algal-based feedstock. As can be observed in table 3.3, the trend observed for peak absorbance during growth, is also observed for the peak power densities in MFC studies.

Arthrospira (sonicated and autoclaved, autoclaved and untreated) media gave higher power density readings compared to *Chlorella* and EBRU autoclaved media. This demonstrates that *Arthrospira* when prepared as a feedstock in an MFC requires minimal treatment, and thus is a cost effective feedstock to use. *Chlorella* feedstock that was untreated demonstrated the least effective source of nutrient use in an MFC. The thick cell wall present in the *Chlorella* cell (Zheng *et al*., 2011) suggests that without any pre-treatment to rupture the algal cells, the power density generated in an MFC will be low. When the *Chlorella* feedstock was autoclaved the power density derived from the MFC increased and was similar to that of the EBRU consortium (untreated and autoclaved).

Figure 3.10 shows the relationship between the growth in the different feedstock and the MFC performance. The figure clearly shows the relationship between the growth of the microbial catalyst and the performance in the MFC. The relationship may not be direct, given that different systems have different limitations including generation of protons affecting pH, PEM fouling affecting reactor media and other reactor changes. The growth of the biocatalyst in the feedstock, however, gives an insight on the relative power density to be expected during an MFC study.

The main hurdle with the use of algal-based feedstock in MFCs, although it may prove to be abundant and a renewable source, is the energy input needed in upstream processing for the ensuring of the bioavailability of nutrients for the biocatalyst used in the MFCs. This requirement for input energy raises the cost of operating the MFC and therefore this makes feedstock such as *Arthrospira* that require less pre-treatment more promising for future use.

Chapter 3.4

Conclusions

The type and number of treatment steps for preparing the algal based feedstock prior to its use as a feedstock, influences, the nutrient availability in the medium for *E. cloacae* use. Sonicating and autoclaving have a synergistic effect on nutrient liberation. This was observed through nutrient assays, microscopy assays and *E. cloacae* growth as well as performance in an MFC. This in turn resulted in higher growth for the bacteria and also the peak power densities that are generated in the MFC. The source of algae used as feedstock also determined the availability of nutrients in the media after treatment. After some treatment steps using *Chlorella* as feedstock, more nutrients appear to be released into the medium compared to untreated *Chlorella* feedstock. However, this is not reflected in the doubling time of *E. cloacae*. *Chlorella* cells are recalcitrant and, even after sonication and autoclaving treatment, the nutritional content of the algae seems to be restricted. This may be the result of the type of nutrient that is released into the medium after treatment, where it is composed of a mixture of more complex nutrients, such as hemicellulose and saccharides. From these studies it was demonstrated that *E. cloacae* was able to utilise nutrients from all the different nutrient media tested, allowing further research to be carried on using *E. cloacae* as the biocatalyst and the various algae feedstock as nutrient media. Considering the energy input required for the preparation of algal based feedstock and the resulting power density derived from their use as feedstock for *E. cloacae*, the use of *Chlorella* as feedstock compared to EBRU consortium and *Arthrospira* is less desirable. The studies also showed that there is a relationship between the carbohydrate concentrations released into the medium from the different feedstock with the growth of the microbial biocatalyst. The growth of the microbial catalyst are also directly related to the MFC performance. Sonication and autoclaving of the EBRU consortium, resulted in an MFC performance that was about 80 % of that of RCM medium in an MFC. This study shows that sonication and autoclaving may make it possible to substitute commercial nutrient feedstock with complex algal-based feedstock for these purposes.

Chapter 4 : Factors affecting MFC performance: pH, temperature and PEM

4.1 Introduction

The performance of microbial fuel cells (MFC) has several limiting factors that affect its performance besides architecture including temperature, proton exchange membrane (PEM), substrate type and pH (Behera *et al*., 2010). These parameters are very specific to each type of fuel cell, a key determinant being the microbial community.

4.1.1 pH and temperature effects

For the biocatalyst in the MFC, pH and temperature are important parameters to enable efficient fuel oxidation and electron transfer (Gil *et al*., 2003). The anodic pH microenvironment is an important factor that greatly affects the performance of the MFC Slightly acidic conditions (pH 5 and 6) have been reported to result in higher proton release by different microbes, including *Enterobacter cloacae* and *Clostridum beijerinckii*, under anaerobic conditions in bioelectrochemical systems (Khanna *et al*., 2011). Nimje *et al.* (2011) observed how the MFC system at pH 6 outperformed similar systems operated at alkaline pH when *E. cloacae* was used as the biocatalyst. This was attributed to a high electron discharge at neutral or acidic pH. At a lower pH there are more protons (Bates and Durst, 1985) in the MFC system, which increases the proton gradient between the anode and cathode, leading to an increase in transfer of protons to the cathode. This in turn makes the cathodic reaction go faster. However, although more protons will be available at lower pH, the microbial activities need to be balanced, and the optimal pH of *E. cloacae* is 7.0 (Catal *et al.,* 2010; Kumar and Das, 2001), therefore, a lower pH that is close to pH 7 would be required for efficient MFC performance (Nimje *et al*., 2011).

An increase in temperature from 20 to 35° C was shown to increase MFC performance when *E. cloacae* was used as the biocatalyst with optimum efficiency being reported at 35° C (Edwards *et al*., 2012). Biological processes are often modelled as an empirical function of temperature (Liu *et al*., 2005), therefore, bacterial activities are also affected by temperature (Liu *et al.,* 2005). Anaerobic metabolism of microbes in bioreactors, where the system is not buffered or temperature controlled, results in changes in pH and temperature due to

exothermic reactions and secondary metabolites (Ratledge and Kristiansen, 2002). This in turn affects the performance of the bioreactor over time (Nimje *et al*., 2011). The cathode potential has also been shown to be lower at low temperatures, therefore proving to be the main limiting factor in power generations when temperature is concerned (Liu *et al.,* 2005).

4.1.2 Proton exchange membrane

Some studies have been conducted on the fouling of the proton exchange membrane and its effects on power production. Bio-fouling of the PEM affects ion transport, electrical resistance and MFC performance. Membrane fouling is thought to be caused by organic foulants and bio-foulants (Choi *et al.,* 2011) which are found in the media. The long term operation of an MFC inevitably results in membrane fouling (Xu *et al*., 2012). The membrane is negatively charged to aid in the binding and transfer of protons (Choi *et al*., 2011). The negative charge of the membrane is a result of negatively charged sulfonate groups attached to the hydrophobic fluorocarbon backbone (Chae *et al*., 2008 a). However, the Nafion® membrane, also has a high affinity for other cations that maybe found in the system such as Na^{+}, Ca^{2+} and K^{+}, and the binding of these cations inhibits the migration of the protons (Chae *et al*., 2008 a). Transport of cations through the membrane also increases the pH of the cathode, which in turn reduces the MFC voltage (Kim *et al*., 2007). Cations existing in large quantities in the nutrient solution containing bacteria also cause an increase in electrical resistance through irreversible chemisorption to the negatively-charged membrane (Choi *et al.,* 2011). This limits the effectiveness of the PEM, resulting in power density falls. Membrane fouling results in intermolecular bridging between organic foulants and the fouling layer by the cations. Accumulation of bio-foulants leads to the formation of a dense bio-film on the PEM surface which in turn results in greater electrical resistance (Choi *et al.,* 2011). The Nafion® membrane also has been shown to be prone to substrate losses, which aid in fouling and lowering of the PEM performance (Chae *et al*., 2011). Specifically, the proton exchange capacity (PEC) is affected. The physical and chemical biointeraction of the PEM with the media during and after fouling changes (Xu *et al*., 2012) has been known to affect the ion and electron balance with fouling resulting in greater electrical resistance.

There is little information on the change of the anodic microenvironment during MFC operation with *E. cloacae* as the biocatalyst in terms of pH and temperature nor how the

anodic microenvironment may affect proton exchange membrane fouling and electrode biofilm formation. The effect of the change would be better studied over a longer period than the experimental 14 hour MFC study.

From chapter 3 MFC studies and growth of *E. cloacae* as the biocatalyst, some significant differences were observed for the different feedstocks in terms of power density. Observing the change in pH of the anode microenvironment could give further insight into the MFC performance. In chapter 3, the performance of the MFC using *Chlorella* as the medium, even after the treatment, was least favourable. All further research was thus performed without the use of *Chlorella* as a feedstock, concentrating instead on *Arthrospira* and EBRU consortium.

The aim of the study was therefore to monitor pH and temperature change in the anode microenvironment during MFC operation and growth of *E. cloacae* in RCM, *Arthrospira* and EBRU consortium media. The change in pH and temperature in the MFCs for each of the feedstock could then be compared against the change in pH and temperature for the *E. cloacae* growth under anaerobic conditions.

The role of pH in MFC performance was also studied through controlling the pH of the feedstock utilised (for this purpose, *Arthrospira* feedstock). The change in COD and nutrient concentrations and how utilisation of the nutrients differs under different pH conditions were also studied.

Finally, the study also examined biofilm formation and proton exchange capacity of the PEM under conditions in which pH was controlled or not controlled (unbuffered) as described further.

4.2 Methodology and materials

Studies were performed using RCM, EBRU consortium and *Arthrospira* as feedstock. The anode microenvironment was sampled for changes in nutrient content, pH, temperature and fouling of PEM. Further studies were performed using buffered *Arthrospira*, to control the pH.

4.2.1 Studies in MFC and growth where pH is not controlled

i. Monitoring and effect of pH change in *E. cloacae* MFC

Two-chambered H-type MFCs (chapter 2 section 2.1.1) were operated in controlled environment (CE) rooms at 32° C (± 3° C). Anodes were prepared as described in chapter 2, section 2.2.3 and cathodes were prepared as described in chapter 2, section 2.2.4. MFCs were operated for 14 hours and 120 hours. The pH and temperature of the anode feedstock (RCM, EBRU consortium feedstock and *Arthrospira* feedstock) was measured hourly and daily using a pH meter (WTW series Inolab pH 730, Germany). pH and temperature measurements were carried out under sterile conditions to minimise contamination of the anode chamber. Studies were performed without buffering the media. Temperature readings were found to be the same in all the media, at 30° C, throughout the study. The cathode chamber was maintained at pH 7.0 using 0.25 M phosphate buffer, and adjusted accordingly to maintain a pH of 7.0 using 0.1 M HCl or NaOH. Feedstocks were prepared as described in chapter 2, section 2.3.1, 2.3.2 and 2.3.4

ii. Monitoring of growth of *E.cloacae* against pH fluctuations

The growth of *E. cloacae* in the feedstock studied (without pH buffering) were performed in batch mode, in sealed 250 ml Schott bottles. Measurements were performed using the turbidimetric method by measuring the hourly change in absorbance at a wavelength of 600 nm of *E. cloacae* in each of the nutrients feedstocks (RCM, EBRU consortium and *Arthrospira* section 2.1.1 to 2.1.4) and pH was measured simultaneously.

iii. Monitoring of biofilm formation in an MFC

a Stereo Microscopy

Anode electrodes from the MFC studies in which pH in the anodic chamber was not buffered (utilising RCM, EBRU consortium and *Arthrospira* media as feedstocks) were removed after a 120 hour MFC study and lightly rinsed using milliQ water. The electrodes were then placed on a petri dish surface and viewed using a stereo microscope (Olympus SZX16) at different magnifications to observe biofilm formation on the electrode surface. Images of the algae were captured using an Olympus DP72 camera.

b Scanning Electron Microscopy

As above, (section 4.2.1.3.1), anode electrodes were removed after a 120 hour MFC operation (unbuffered anodic media) and prepared for SEM studies. This was done by fixing the biolayer first using the method adapted from Xu *et al.* (2012). In this method, the anode electrodes were placed in 2.5 M gluteraldehyde in 0.1 M phosphate buffer and incubated overnight at 4° C. The electrodes were then rinsed using 0.1 M phosphate buffer for 10 minutes (twice). After rinsing, the electrodes were dehydrated using an ethanol dehydration ladder by placing them in 30 %, 50 %, 70 %, 80 % and 90 % ($^{v}/_{v}$) ethanolic solutions for 5 minutes at each concentration. A final dehydration step was performed by placing the electrodes in absolute ethanol for 10 minutes (twice). The electrodes were then placed in absolute ethanol for 1 hour 30 minutes, during which the ethanol was evaporated till the electrodes were dried at critical point. The electrodes were sputter coated with gold particles using a Quorum Q150R S, for 15 minutes, prior to SEM (Tescan, Germany).

4.2.2 Studies where the pH is controlled through buffering

i. Effect of pH buffering on MFC performance

Commercially purchased *Arthrospira* was used for studies in which the pH of the anodic microenvironment was controlled by buffering, denoted as 'buffered pH studies'. *Arthrospira* was selected for this studies here due to the good power density exhibited with minimal pre-treatment (Chapter 3 section 3.3.4). Buffer solutions were prepared that ranged from pH 4 to pH 9 with a molar concentration of 0.1 M. For pH 4 to 6, acetate buffer was used which was made by mixing 0.1 molar concentrations of acetic acid and sodium acetate until the desired

pH was achieved. For pH 7 to 9 phosphate buffer was used, in which 0.1 molar concentrations of sodium dihydrogen phosphate and di-sodium hydrogen phosphate were mixed until the desired pH was achieved. To a 900 ml of each of the buffers, 33 g of *Arthrospira* dry weight was added and mixed and the pH of the samples was measured and adjusted to the required pH using the acidic or basic buffer solutions, before adjusting to a litre with milliQ water and autoclaving. The differently buffered *Arthrospira* media was then used as the anode substrate for *E. cloacae* in MFC studies. MFCs were setup as described in chapter 2, section 2.1.1. The pH of the anode compartment was monitored using a pH meter and corrected using 0.1 M NaOH or 0.1 M HCl that had been diluted in milliQ water that had been autoclaved under sterile conditions to maintain the required pH of the anode during analysis.

ii. Effect of pH on nutrient utilisation

a Carbohydrate assays

Carbohydrate assays as described in chapter 2, section 2.5.1, was conducted on the buffered pH *Arthrospira* feedstock (drawn from the anodic chamber) before and after a 120 hour continuous operation in an MFC, using the phenol:sulphuric acid method for total carbohydrates.

b Protein assays

Protein assays were also conducted on the buffered pH *Arthrospira* feedstock before and after 120 hours of continuous operation in an MFC, as described in chapter 2, section 2.5.2.

4.2.3 PEM studies under presence and absence of pH control

i. Proton exchange membrane preparation and cleaning

The PEM was prepared and cleaned as described in the methodology section (chapter 2, section 2.3.2). The cleaned PEM were used for comparison to used and pristine PEM for the PEC calculations.

ii. Proton exchange capacity

Proton exchange capacity (PEC) of the PEM (Nafion 117) (from both buffered and unbuffered media) was calculated using the method adapted from Xu *et al*., (2012). PEC was measured for unused Nafion, cleaned Nafion and Nafion from the MFCs that had been run

for 120 hours continuously using buffered *Arthrospira*, unbuffered *Arthrospira* and RCM feedstock. The active site of the PEM was cut (the area covering the bridge opening) and cleaned. Unused PEMs were also cut and used as reference material. A solution of 2.5 M NaCl was prepared and each of the membranes were soaked in the 10 ml of the NaCl solution and left overnight at room temperature. The solutions were neutralised with 0.05 M NaOH, with the reactions being monitored using a pH meter until a pH of between 7.2 and 7.5 was reached. The PEC was calculated using the following formula $PEC = \frac{a\,x\,b}{m}$ where a is the added titrant volume in litres, b is the molar concentration of the titrant (0.05 M) and m is the dry membrane weight in grams.

iii. Scanning electron microscopy of the Nafion® proton exchange membrane

The PEM from the MFC studies where *Arthrospira* buffered pH (pH 5-7), unbuffered *Arthrospira* pH and RCM feedstock were used in a 5 day continuous MFC study, were taken and prepared for SEM studies. This was done by fixing the biolayer first using the method adapted from Xu *et al.* (2012). The PEM were placed in 2.5 M gluteraldehyde in 0.1 M phosphate buffer and incubated overnight at 4° C. The PEM kept overnight were then rinsed using 0.1 M phosphate buffer for 10 minutes (twice). After rinsing the PEM were dehydrated using an ethanol dehydration ladder by placing them in 30 %, 50 %, 70 %, 80 % and 90 % ethanol, for 5 minutes at each concentration. A final dehydration step was performed by placing the electrodes in absolute ethanol for 10 minutes (twice). The PEM were then placed in absolute ethanol for 1 hour 30 minutes, during which the ethanol was evaporated at critical point until the PEM were dry The PEM were sputter coated with gold particles using a Quorum Q150R S, for 15 minutes, before SEM (Tescan, Germany).

4.2.4 Analysis of buffered and unbuffered media after MFC operation

i. Light Microscopy

From the MFC operations using buffered *Arthrospira* pH (pH 5-7), unbuffered *Arthrospira* and RCM feedstock was harvested and visualised under a light microscope to observe the visible difference between fresh nutrient media and media after the 5 day run. An Olympus

BX50 light microscope was used and the images were captured using an Olympus DP72 camera.

ii. COD studies

COD of the buffered *Arthrospira* (pH 5-7), unbuffered *Arthrospira* and RCM was measured before and after a 120 hour MFC operation. Procedure used was from the COD testing kit, from MERCK (spectroquant®) for the COD Cell Test 14 690. To 2 ml of the test sample (fresh media and 120 hour MFC operation used media), 0.3 ml COD solution A (Merck, South Africa) and 2.3 ml COD solution B (Merck, South Africa) were added in a test tube. Solutions were mixed vigorously until hot and heated for 2 hours at 148° C on a thermoreactor (Spectroquant® TR420, Merck, Germany). The solutions were subsequently left at room temperature for 10 mins. Afterwards, the solutions were shaken, and left to cool to room temperature. The resulting solutions were measured for COD concentrations using a spectrophotometer (Spectroquant® NOVA 60, Merck, Germany).

4.3 Results

4.3.1 Studies in MFC and growth where pH is not controlled

4.3.1.1 MFC and *E. cloacae* growth kinetic studies monitoring pH with RCM as feedstock

Figure 4.1 shows power density output against pH change for time periods of 14 hours and 120 hours when RCM medium was used.

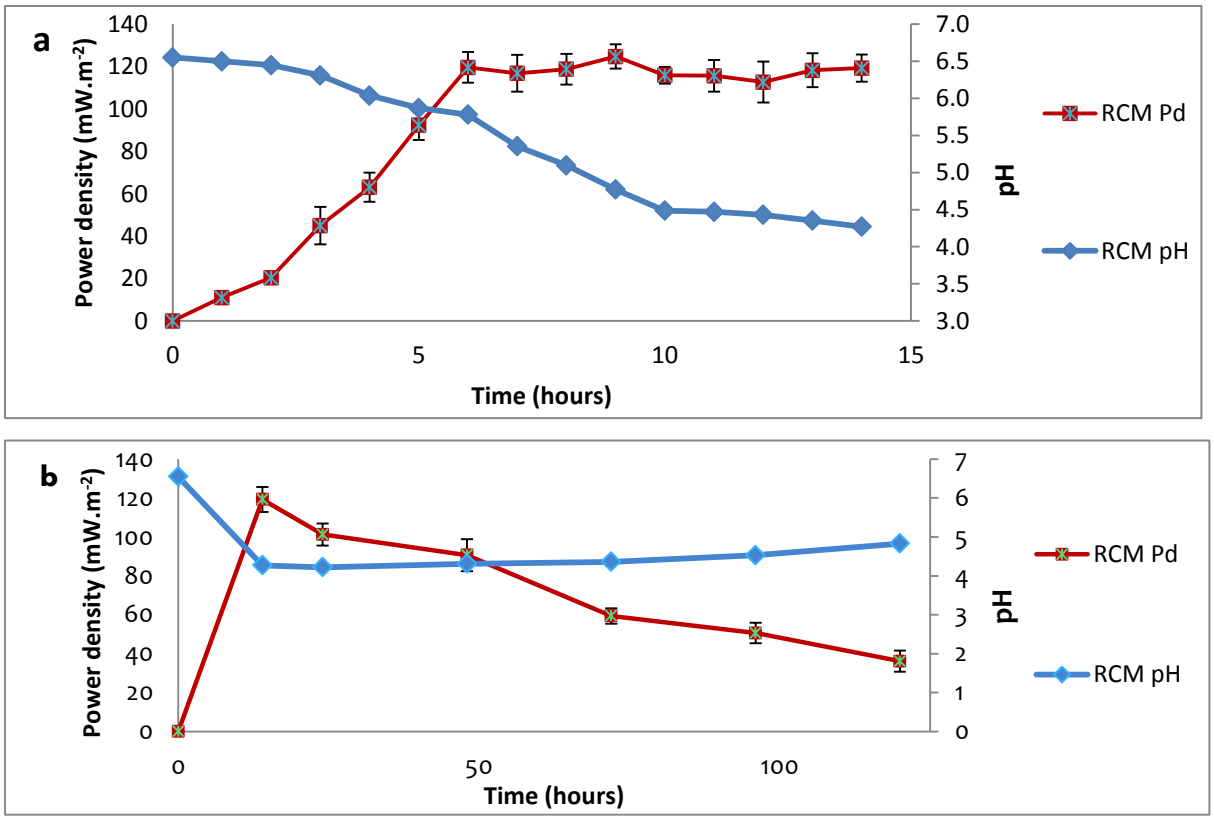

Figure 4.1: pH and Power density (Pd) changes of MFCs containing RCM as the anode medium during a short-term 14 hour study (a) and a long-term 120 hour study (b). MFCs were set up in a CE room at 35° C.

Figure 4.1 shows that the pH of the RCM media decreases with time. During peak performance of the MFC using RCM as a substrate, the pH is slightly acidic. From the MFC study over 14 hours, it can be observed that as power density increases, pH decreases constantly. A possible explanation for this is organic acid build up, as secondary metabolites from the anaerobic processes of the biocatalyst (Wise, 1980) in the anode chamber. Additionally, pH lowering could also be a result of proton transfer limitations through the

PEM, which results in lower proton exchange leading to an accumulation of protons which in turn decreases the pH. When the peak power density is reached the pH starts to decline more rapidly from a pH of about 5.6 at the peak to about 4.3 at the end of the run (14 hours) which could be a result of the bacteria entering exponential growth phase as shown in figure 2.1 (chapter 2) with associated increases in organic acid build up. When the study was initiated, the initial pH observed in figure 4.1a was 6.5. After 6 hours of the study, the power density plateaued and the pH reached 5.6. From the 6th to the 10th hour, the power density was constant with slight variations, however, the pH continued declining from 5.6 units to 4.4 units. The low pH does not negatively affect the current generation, with *E. cloacae* being reported to maintain its metabolic pathway at pH ranges between 4.5 and 7.0 (Daz and Veziroglu, 2008). The slightly acidic pH corresponds to high power densities, possibly showing a link between current generation and pH (figure 4.1).

After 24 hours (figure 4.1b), the power density started to decrease, and this corresponded with an increase in the pH of the media in the anode chamber. As the protons are depleted and less are produced with the decrease in either substrate, or where other depleting factors such as fouling of the PEM minimise further proton release, it can be inferred that this may act as a negative feedback resulting in an increase in pH and decrease in power density.

Figure 4.2 shows the growth of *E. cloacae* measured as absorbance (at OD_{600nm}) in RCM medium and the change in pH over time grown in batch flasks. This figure shows how pH changes over a period of 120 hours when RCM was used as the substrate.

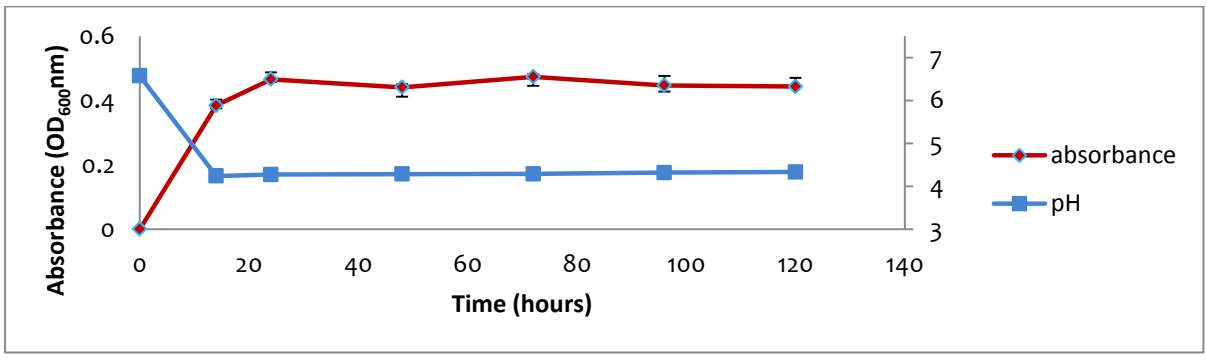

Figure 4.2: The growth kinetics of *E. cloacae* in RCM medium. The absorbance was measure at OD_{600nm}. The pH is plotted against the absorbance over time. Growth was performed under anaerobic conditions at 35° C.

Figure 4.2 shows a decrease in pH from 6.6 at the start of the study to 4.2 after 14 hours and an increase in absorbance until 20 hours. When the pH levels off after 14 hours, the absorbance values peak at 24 hours before levelling off showing a decline in growth kinetics possibly due to nutrient limitations or suppressed metabolic processes at pH 4.2. This follows the trend observed for the MFC study with RCM as the feedstock, with an initial decline in pH as power density increases (figure 4.1b). The results show that anabolic and catabolic process for *E. cloacae* in RCM can occur under acidic conditions and the organic acid build up under anaerobic conditions does not have a large detrimental effect. After the initial 24 hours, the pH remains constant at about 4.3. The maintenance of a constant low pH in the batch studies of the growth of *E. cloacae* may be a result of the accumulation of protons which, unlike in the MFC, are not transported to the cathode.

4.3.1.2 MFC and *E. cloacae* growth kinetic studies monitoring pH with EBRU consortium media as feedstock

Figure 4.3 shows the power densities of MFCs with EBRU consortium feedstock at 35° C both when the feedstock was autoclaved and when it was autoclaved and sonicated. The change in pH over time was also monitored and plotted against time in relation to power density.

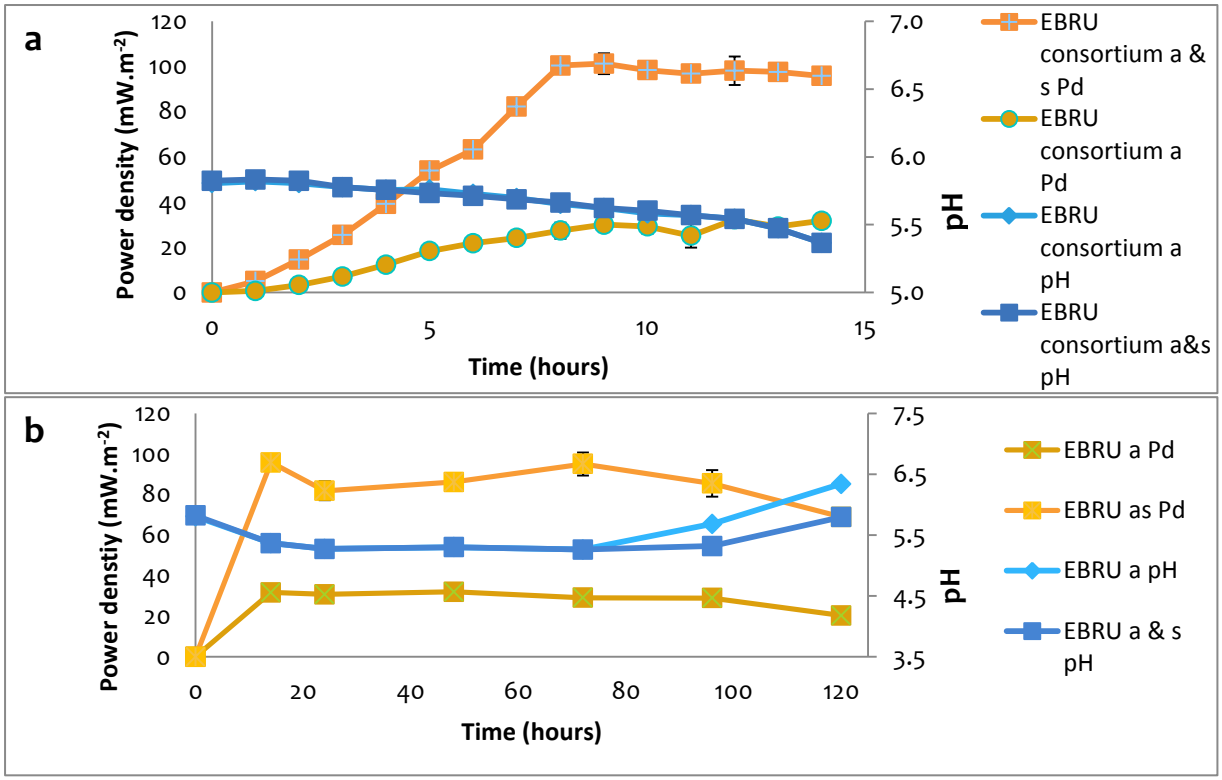

Figure 4.3: MFC studies with *E. cloacae* as the biocatalyst measuring the change in pH and power density over time. EBRU consortium feedstock that was autoclaved (EBRU a) and EBRU consortium feedstock autoclaved and sonicated (EBRU a & s) were used as the anolytes for short-term 14 hour MFC studies (a) and long-term 120 hour MFC studies (b).

Figure 4.3 shows that the pH for the EBRU consortium medium MFC study was initially approximately 5.7. As the power density increased the pH gradually decreased. After the 14 hour run the pH reached about 5.2. This was different from the RCM medium (figure 4.1) MFC study where the pH changed by over 2 pH units over the 14 hour run. The pH change was similar for both the autoclaved and the autoclaved and sonicated EBRU consortium media used in the MFCs. The data suggests that like for RCM medium, current generation under anaerobic conditions for *E. cloacae* was preferentially carried out under slightly acidic conditions.

For the MFC studies in EBRU consortium feedstock over 120 hours, the initial trend observed for RCM medium (figure 4.1) of an increase in pH corresponding with a decreased power density (figure 4.3) was also observed. However, unlike in RCM medium where the decline was observed after the first 24 hours (figure 4.1), the decline in power density in EBRU consortium medium started at 72 hours. After 120 hours (figure 4.3b) of the sonicated

and autoclaved EBRU consortium medium, a 20 % decline on the final power density from the peak power density was observed. For the EBRU consortium (autoclaved) medium the final power density showed a decline of approximately 20 % from the peak power density as well. This was much less than the decline in the final power density from the peak power density in RCM medium MFC runs where the decline was over 50 %.

Figure 4.4 shows the growth kinetics of *E. cloacae* in EBRU consortium (both autoclaved medium and autoclaved and sonicated) at 35° C under anaerobic conditions. The growth kinetics was observed by measuring the absorbance at OD_{600nm} and change in pH was noted by plotting these against time.

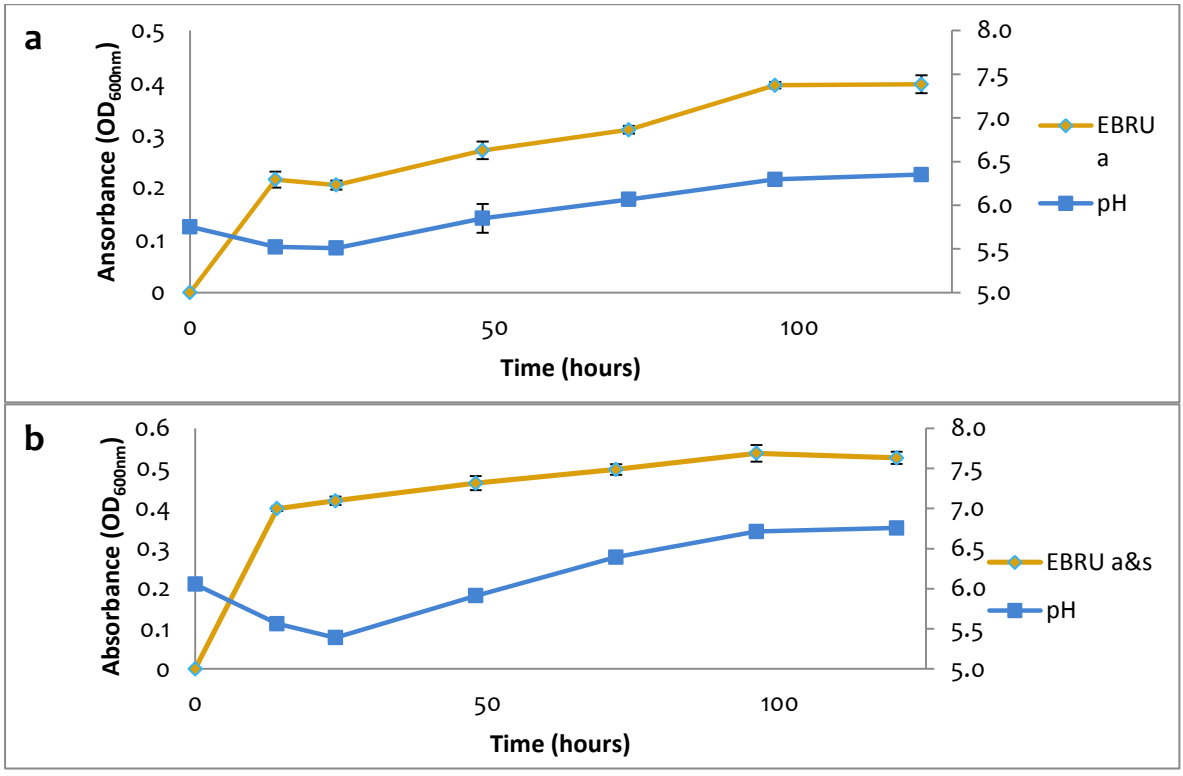

Figure 4.4: The growth kinetics of *E. cloacae* in batch flasks were measured by measuring change in absorbance at OD_{600nm}. The change in pH in EBRU consortium feedstocks were also measured. Studies were conducted at 35° C under anaerobic conditions. Substrate medium was autoclaved (a) or autoclaved and sonicated (b).

In figure 4.4, the initial growth of *E. cloacae* resulted in a lowering in the pH from 6.0 to 5.6 after 14 hours. When growth kinetics levelled off after 14 hours, the pH continued to decline

to a pH of 5.6 up till 24 hours. After 24 hours, growth kinetics, show a steady increase coinciding with an increase in pH. After 48, 72 and 120 hours the pH reached was 5.9, 6.4 and 6.8 respectively. Unlike the RCM medium study where the pH was level after the initial decline, the pH increased after the initial growth spurt in EBRU consortium medium. The increase in pH towards the optimum of *E. cloacae* (Catal *et al.,* 2010; Kumar and Das, 2001), which is 7.0, could in theory improve metabolic processes hence contributing to increase in biomass. The initial metabolic processes, when growth is initiated and proceeds in the first 24 hours, would have resulted in organic acids and other secondary metabolites (Wise, 1980). The organic acids, would have made the media, acidic, which, would have aided in release of further nutrients from the algae (Zheng *et al*., 2011), and therefore different conditions in the complex media which might have increased the pH.

4.3.1.3 MFC and *E. cloacae* growth kinetic studies monitoring pH with *Arthrospira* media as feedstock

Figure 4.5 shows the power densities of MFCs with *Arthrospira* feedstock at 35° C when the feedstock was autoclaved and when it was autoclaved and sonicated. The change in pH over time was also monitored and plotted against time in relation to power density.

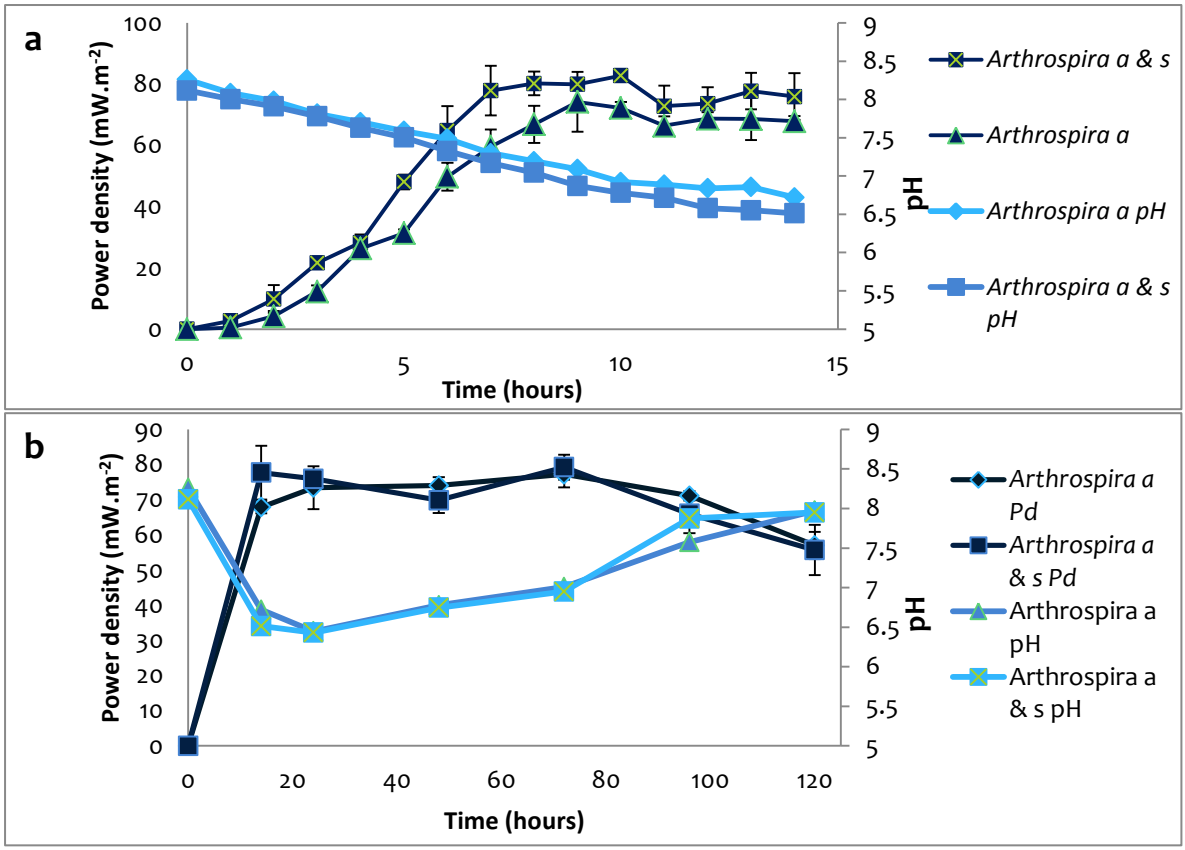

Figure 4.5: Short-term 14 hour MFC studies (a) and long-term 120 hour MFC studies (b) with *E. cloacae* as the biocatalyst were conducted. *Arthrospira* feedstock that was autoclaved and *Arthrospira* feedstock autoclaved and sonicated were studied as the anolytes and the change in pH and power densities were measured against time.

The initial pH for *Arthrospira* feedstock was alkaline with a pH of 8.0 as shown in figure 4.5. Using *Arthrospira* as the feedstock for MFC studies resulted in an initial decline in pH, associated with microbial metabolism and release of organic acids (Wise, 1980), along with an increase in power density. The initial pH was 8.0 and during the study it declined to a pH of about 6.6 after 14 hours. In the *Arthrospira* feedstock, the power density and pH trends recorded were similar to the EBRU consortium feedstock, namely, the first 24 hours, pH rapidly decreased while the power density increased, and then pH steadily increases with power density remaining constant up until 72 hours. Thereafter, the pH increase is more pronounced, and the power density steadily declines. From the peak power density to the final power density, a decrease of about 25 % was observed, with the final pH returning to its starting pH. This shows that even under alkaline conditions, *E. cloacae* is capable of maintaining current generation. The nutrient availability also decreases with time, which

affects the metabolic processes. From 14 hours to 72 hours when pH is in the range between 6.5 and 7.0, optimum MFC performance is observed. Depletion of readily available nutrients, may have resulted in the more complex nutrients being digested, and release of the metabolites to the media. Considering that the optimum pH for *Arthrospira* growth and maintenance is 9.0 (Ogbonda *et al*., 2007), *Arthrospira* nutrients may be alkaline, with studies showing the intracellular average pH to be between 8.0 and 8.5 (Kim *et al*., 2007). The preferential uptake of nitrogen in *Arthrospira* is when it is in the form of ammonia (Sanchez-Luna et al., 2006), therefore the metabolism of Arthrospira cells may result in the release of alkaline based by-products which in turn will increase the pH of the media.

Figure 4.6 shows the growth kinetics of *E. cloacae* in autoclaved *Arthrospira* medium and sonicated and autoclaved *Arthrospira* medium at 35° C under anaerobic conditions. The growth kinetics were measured by measuring the absorbance at OD_{600nm} and pH, and plotting these against time.

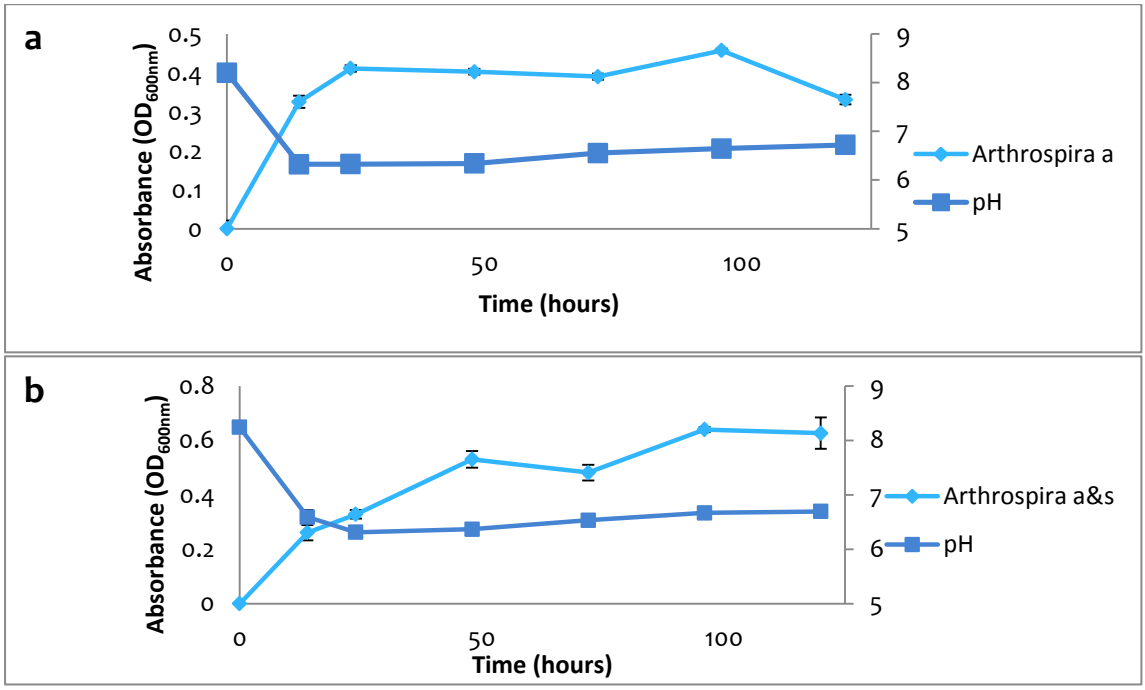

Figure 4.6: Growth kinetics of *E. cloacae* in batch flasks were measured by measuring the change in absorbance at OD_{600nm} *Arthrospira* feedstock. The change in pH over time was also measured. Studies were conducted at 35° C under anaerobic conditions. Substrate medium was autoclaved (a) or autoclaved and sonicated (b).

The *E. cloacae* growth kinetics in *Arthrospira* media (figure 4.6), show an initial decline in pH within the first 24 hours, during the log growth phase of *E. cloacae*. Over the next 96 hours, as pH increased, growth increased as well. The final pH of the autoclaved *Arthrospira* medium was about 6.2 with the final pH for the sonicated and autoclaved *Arthrospira* medium being around 6.7. The growth kinetics show that in the exponential growth phase, under anaerobic conditions, bacterial metabolism results in formation of organic acids, which lower the pH.

The studies were carried out for 120 hours because the method used to determine cell concentration, of absorbance at OD_{600nm} only gives limited insight into cell density. It does not account for the state of the cells. Extending MFC studies beyond 14 hours provided more insight into the state of the cells, with continuous power production after 14 hours showing continuous metabolic activity. The non-zero current generated by the MFC at times beyond 14 hours demonstrates active metabolism by the biocatalyst in the anodic compartment and studies investigating the longevity of the fuel cell were warranted.

For all three media, the pH fluctuates in the anode chamber of the MFC. This is also evident during growth curves studied during batch culture of the bacteria with the trend showing a decrease in pH during the onset of log phase growth of the bacteria. This period is also associated with increase in power density. It is difficult to distinguish the role that pH lowering plays on the power density or total power density as it impacts on both proton availability in the anode and also on microbial metabolic processes. At lower pH, there are more protons available in the system, therefore the proton shift from anode to cathode through the PEM would be more enhanced, which may contribute to increases in power densities. At a pH range, between 4.5 and 7.2, *E. cloacae* is able to maintain its metabolic pathways (Daz and Veziroglu, 2008), and the low pH may also enhance the proton transport. Daz and Veziroglu, (2008) also observed how fermentative bacteria produce hydrogen between the pH ranges of 4.5 and 6.5. The algaenans found in cells that are found in the EBRU consortium like *Scenedesmus* and *Pediastrum* (Blokker *et al.,* 1998) may also influence the release of protons after fermentation, resulting in higher power densities and lower pHs. Bacterial metabolism results in electron and proton release in an MFC, which drives the power density up (Logan, 2008). However, anaerobic metabolism, results in the

release and build-up of organic acids (Wise, 1980) as well as the decrease in nutrient availability. Acidic conditions also increase the fouling of the PEM with the organic acids and biofilm (Xu *et al*., 2012) which in turn impacts the performance of the MFC. The nutrients are also depleted during operation, which in turn would lower the availability of the nutrients to the biocatalyst, hence lower the performance. The low pH is beneficial to the MFC, because of the high proton gradient, which drives the reaction forward. However, the low pH, impacts on the metabolism of the *E. cloacae* as the optimum metabolism is at pH 7.0 (Daz and Veziroglu, 2008). The low pH, would thus result in less metabolism and biomass growth, which would eventually impact the MFC performance. The pH fluctuates but it does so within the defined limits of growth and metabolic processes for *E. cloacae* and the proton build up from the decreased pH may positively impact power density.

4.3.2 Anode electrode analysis using microscopy techniques

Figure 4.7 shows the carbon paper electrodes with MWCNTs that were used in MFC studies after 120 hours with RCM as the feedstock medium and *E. cloacae* as the biocatalyst.

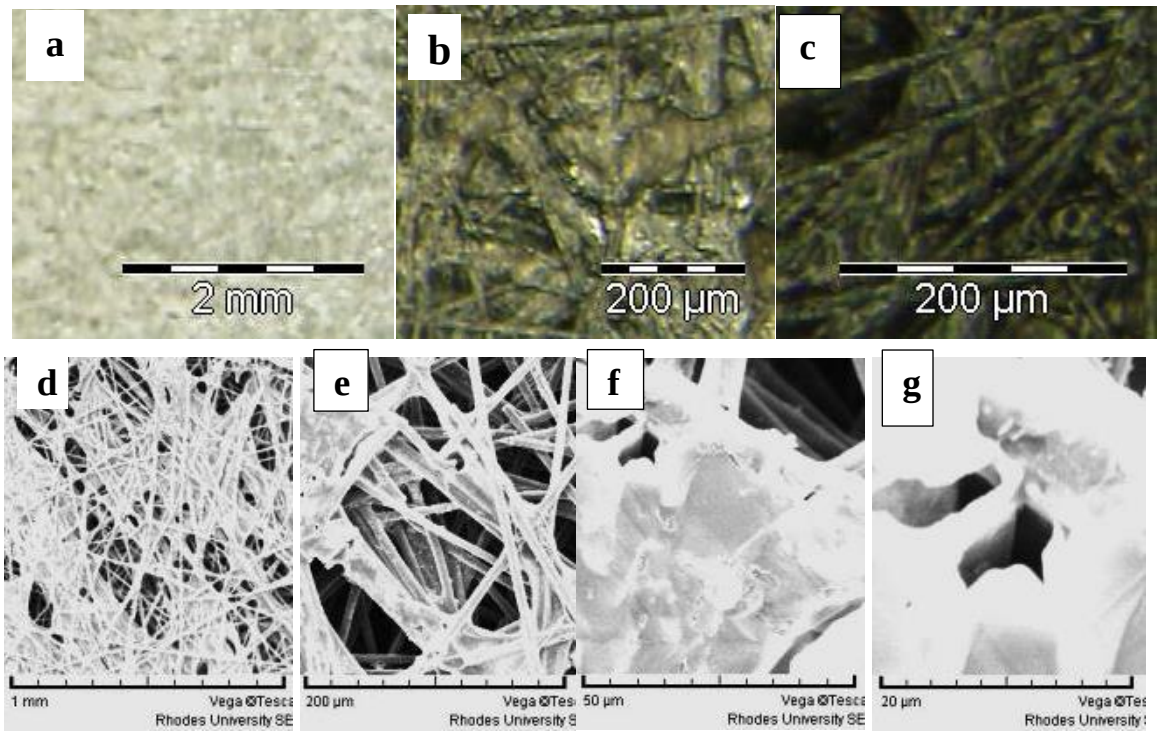

Figure 4.7: Stereo microscope images of carbon paper electrodes at 10 times magnification (a), 50 times magnification (b) and 100 times magnification (c) and SEM images with scale bar at 1 mm (d), 200 µm (e), 50 µm (f) and 20 µm (g) from MFC studies after 120 hours with RCM as anolyte. MFC studies were performed at 35° C and the substrate medium was under anaerobic conditions.

From the stereo microscopy images, very little electrode biofilm formation is visible. The 3D structure of the carbon paper electrode can be visualised in figure 4.7 c under the stereo microscope. The 3D structure of the carbon paper is more defined in figure 4.7 e after visualisation with SEM. Biofilm formation in the SEM images is more visible compared to the stereo microscope images as can be seen in fugure 4.8. This is because the SEM images provide more clarity.

Figure 4.8 shows images of the carbon paper electrodes with MWCNTs that were used in MFC studies after 120 hours, with *Arthrospira* autoclaved as the feedstock medium and *E. cloacae* as the biocatalyst. The images were observed using a stereo microscope at 10 times, 50 times and 100 times magnification and SEM.

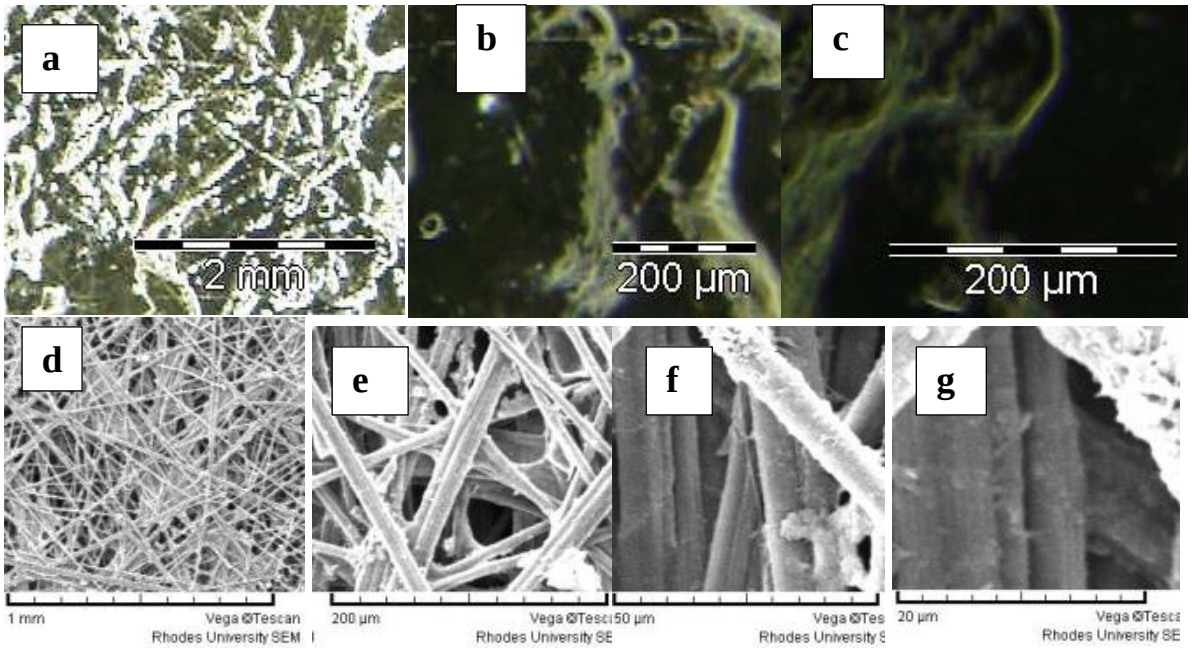

Figure 4.8: Stereo microscope images of carbon paper electrodes at 10 times magnification (a), 50 times magnification (b) and 100 times magnification (c) and SEM images with scale bar at 1 mm (d), 200 µm (e), 50 µm (f) and 20 µm (g) from MFC studies after 120 hours with *Arthrospira* autoclaved as anolyte. MFC studies were performed at 35° C and the substrate medium was maintained under anaerobic conditions.

Compared to figure 4.7, in figure 4.8 the 3D structure of the carbon paper electrode is not visible. Accumulation of the autoclaved *Arthrospira* particulates on the elecrode, under the

stereo microscope is clearly visible. Under SEM, the 3D structure of the electrode is visible as well as the biofilm layer on the electrode surfaces.

Figure 4.9 shows the carbon paper electrodes with MWCNTs that were used in MFC studies after 120 hours with EBRU consortium autoclaved as the feedstock medium and *E. cloacae* as the biocatalyst. The images were observed using a stereo microscope at 4 times, 10 times and 40 times magnification and SEM.

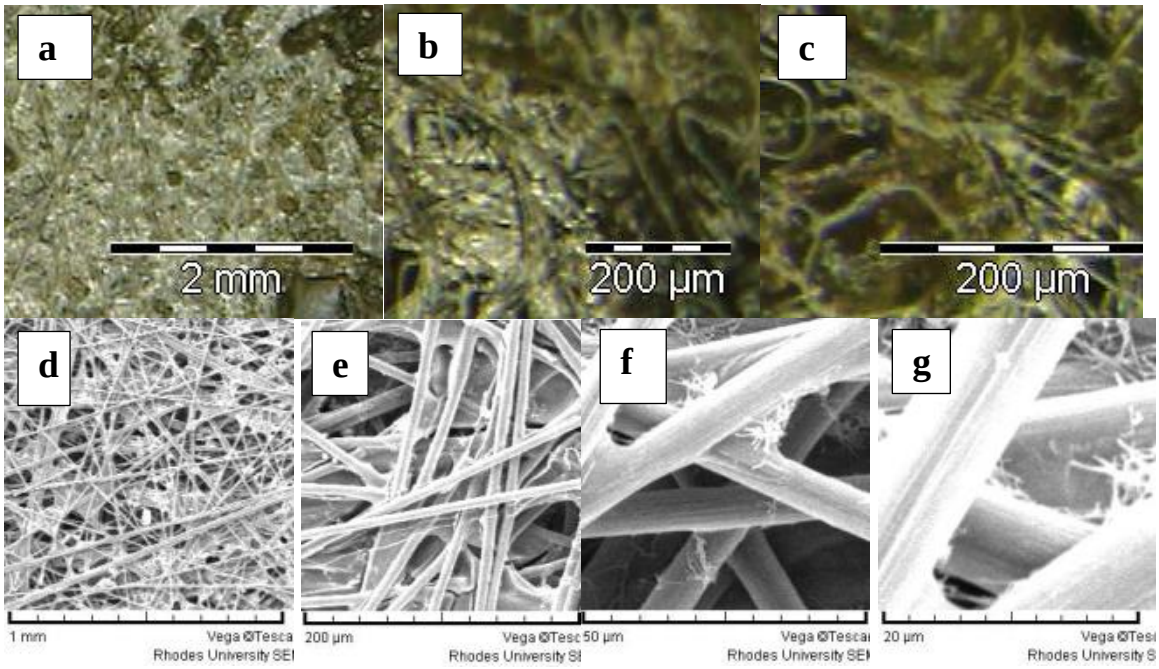

Figure 4.9: Stereo microscope images of carbon paper electrodes at 10 times magnification (a), 50 times magnification (b) and 100 times magnification (c) and SEM images with scale bar at 1 mm (d), 200 µm (e), 50 µm (f) and 20 µm (g) from MFC studies after 120 hours with EBRU consortium autoclaved medium as anolyte. MFC studies were performed at 35° C and the substrate medium was maintained under anaerobic conditions.

From figure 4.9, the 3D structure of the carbon paper electrode under the stereo microscope is barely visible. The fouling of the electrode is less compared to electrode from *Arthrospira* anolyte studies (figures 4.9 and 4.10). SEM shows the biofilm formation on the 3D structures of the carbon paper.

Figures 4.7, 4.8 and 4.9 show biofilm formation and organic fouling on the anode electrode surfaces from the different feedstock in the MFCs. For algal based media lower biofilm formation was observed on the electrode surface, under stereo microscopy. The algal-based feedstock accumulation on the electrode surface, would have resulted in minimising the area

for *E. cloacae* biofilm formation. This could have been responsible for the lower power densities observed when the algal matter was not sonicated because of the barrier that formed between the electrode surface and the *E. cloacae,* which minimises the exoelectrogenic transfer of electrons (Gil *et al*., 2003). Biofilm formation was observed on all the anode electrodes albeit to a different degree depending on the feedstock. For the SEM images, biofilm formation and fouling of the electrode surface can be observed. Biofilm on the electrode surface improves exoelectrogenic transfer from the bacteria to the electrode (Gil *et al*., 2003). The SEM and stereo microscopy images showed how the biofilm interacts with the electrode surface, suggesting that it forms a complex that readily releases the electrons to the electrode surface.

4.3.3 Buffered pH studies utilising *Arthrospira* based feedstock

MFC studies as well as growth kinetics of *E. cloacae* shows that pH fluctuations occurred in both anode chambers as well as in batch cultures for growth. Studies were thus conducted during MFC operation and in a batch culture in which pH was controlled through buffering, (figure 4.10). *Arthrospira* was selected as the nutrient medium as previous research (chapter 3, figure 3.7 and 3.9) demonstrated that good growth of the *E. cloacae* biocatalyst could be achieved without much pre-treatment, and that it could offer a cheaper alternative to RCM medium. From previous studies biocatalyst growth in *Arthrospira* medium was shown to be successful over a range of pH values, which included alkaline and acidic conditions (in chapter 4, section 4.3.1, figures 4.5 and 4.6)

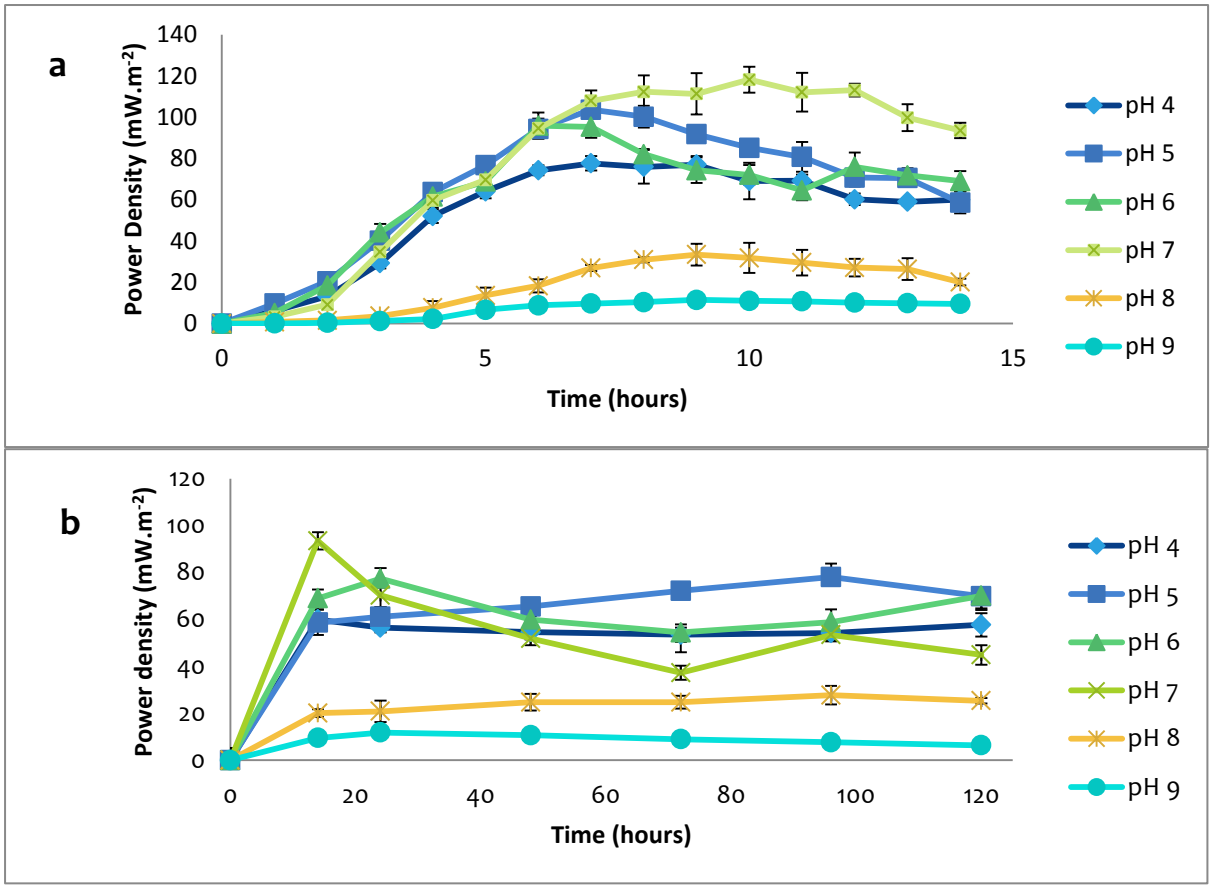

Figure 4.10: Power density curves of autoclaved *Arthrospira* feedstock at different pH values using phosphate buffer (pH 7 – 9) and acetate buffer (pH 4 – 6) for short-term MFC studies over 14 hours (a) and long-term MFC studies over 120 hours (b) are shown. pH was monitored during operation and maintained using 0.1 M NaOH or 0.1 M HCl. MFC studies were performed at 35° C with *E. cloacae* as the biocatalyst.

Figure 4.10 shows a change in the power density, over the period of 120 hours between pH 9. A bar graph shows the change in the daily peak power density for each pH treatment (Figure 4.11).

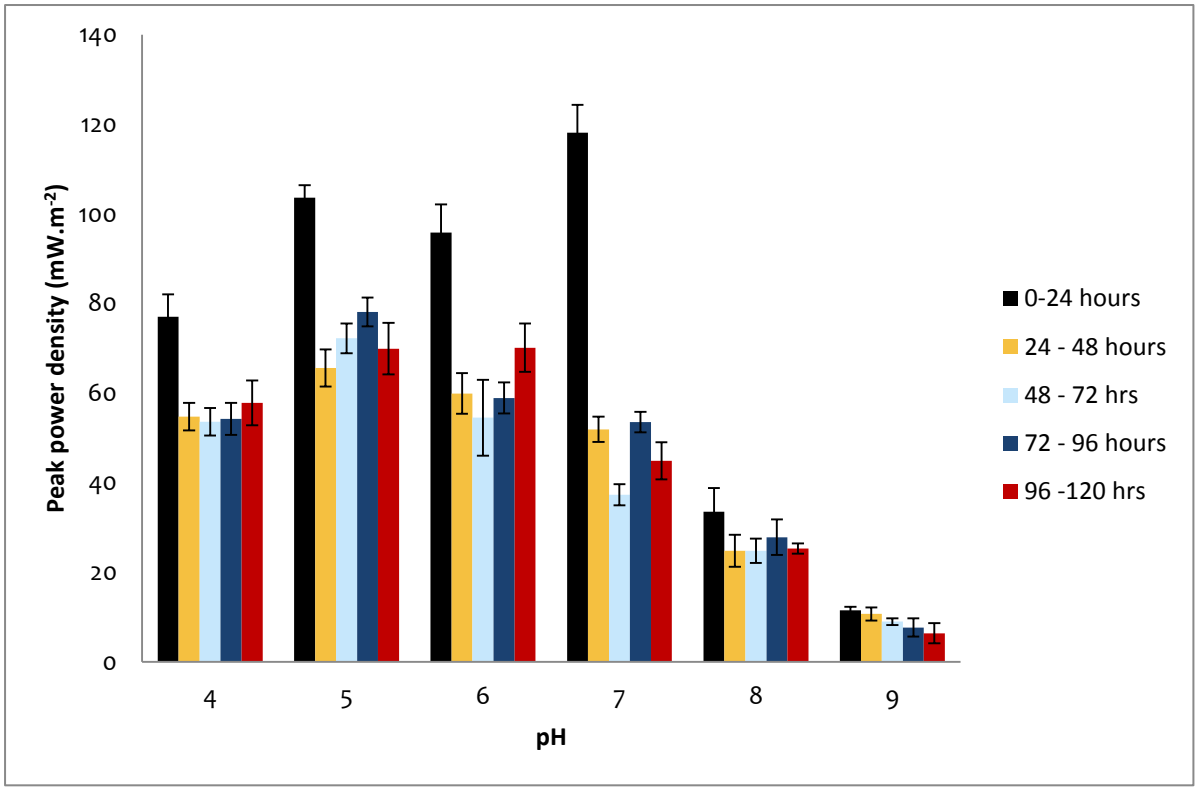

Figure 4.11: The daily peak power densities from each buffered pH treatment were plotted over the 120 hour period.

Figure 4.11 shows a representation of the peak power densities observed for each day for each of the pH values studied. It shows how the maximum power density over time changes for each of the studied media. From figure 4.11, it can be observed that very low peak power densities were observed in an MFC buffered to pH 9, with very little change in the daily peak power density being observed over the 120 hours (figure 4.11) and low total power output. The peak power density of 11.91 (± 2.34) $mW.m^{-2}$ was recorded during the first 24 hours in the pH 9 treatments. After the peak power density at 24 hours, the power density did not change significantly over the MFC operation period, with a final power density of 6.37 (± 2.25) $mW.m^{-2}$ being the lowest reading at 120 hours. In the pH 8 treatment, the power density was about double that of the peak power density in the pH 9 treatment, with a maximum power density of 33.54 (± 5.27) $mW.m^{-2}$ at 9 hours. The power density in the pH 8 treatment, unlike that in the pH 9 treatment, increased after the first 24 hours. This suggests that the biocatalyst adapted to the less alkaline system, probably through the change of metabolic pathways and systems. At 14 hours, the peak power density in the media buffered at pH 7 was higher than that at the other pH treatments. However, for the 120 hour run, after reaching

the peak power density at 14 hours, the power density declined from of 118.10 (± 6.21) $mW.m^{-2}$ to 70.31 (± 5.04) $mW.m^{-2}$ after 24 hours of the MFC operation. Thereafter, there was a steady decline in power density until at 72 hours, at which point the systems power generation rose again. For the acidic pH 5 and 6 treatments, the power densities measured were similar over the 14 hour run, while differences in power density measurements were observed over the 120 hour period. A statistical analysis of the results from pH 5 and pH 6 gave a result of $p = 0.88$. These results show that the pH 5 and pH 6 treatments have no significant difference. All other treatments had a p value < 0.01 compared to each other, showing the effect of pH on the MFC anode performance. For the pH 4 treatment, the peak and total power density was lower than the pH 5, 6 and 7 treatments for the 14 hour run. The power density for pH 4 treatment remained constant over the 120 hour run, with no major fluctuations being observed. There is an increase in power density after the initial drop for pH 4, 5 and 6, although they do not yield the highest peak power density. The power density in this pH range (4 - 6) is greater after 48 hours than at pH 7. The extracellular electron transfer at acidic and neutral pH from the cell to the anode is greatest, whereas at alkaline pH, there is a low proton production which also results in low electron discharge hence lower current generations (Nimje *et al.*, 2011).

In order to interrogate this further, the total power output at each pH is compared in Table 4.1 below. After the 5 day MFC run, the supernatant of each of the reactors was assayed for total carbohydrate and total protein (Table 4.1).The data was compared to fresh unused, media that had not been buffered.

Table 4-1: The nutrient assays of the buffered media after a 120 hour MFC study

assay	pH 4	pH 5	pH 6	pH 7	pH 8	pH 9	Fresh
Protein concentration ($g.l^{-1}$)	3.17 * (± 2.76)	3.26 * (± 1.79)	4.88 * (± 1.22)	3.68 * (± 1.13)	8.28 * (± 1.27)	10.46 # (± 1.51)	12.01 (± 1.63)
Carbohydrate concentration ($g.l^{-1}$)	1.99 * (± 0.29)	2.08 * (± 0.30)	2.48 * (± 0.27)	1.76 * (± 0.28)	1.83 * (± 0.31	1.78 * (± 0.30)	3.54 (± 0.29)
Approximate Total Power output (W)	6.64 (± 0.401)	8.33 (± 0.532)	7.70 (± 0.615)	6.19 (± 0.415)	2.96 (± 0.415)	1.09 (± 0.212)	N/A

Statistical analysis was performed on the results using one way ANOVA, with further tests performed using the Post Hoc analysis, Tukey HSD test. Results were compared to fresh *Arthrospira* medium. When $p < 0.01$ the results were denoted the sign * and when $0.01 < p < 0.05$, the results were denoted the sign #.

In table 4.1 it is clear that the highest total power output is at pH 5, followed by pH 6, 4 and finally 7. The lowest total power output occurs at pH 8 and 9. Considering that the optimal growth of *E.clocae* occurs at pH 7, this might lend strong support that the low pH supports higher power density potentially as a result of the proton accumulation at acidic conditions. There was a significant difference for all the pH treatment steps in nutrient use compared to unused *Arthrospira* medium for carbohydrate utilisation in the MFC. However, for protein utilisation, there was a significant difference between the pH 9 treatment and the unused *Arthrospira* medium, and the other treatments there was a highly significant difference. There was no significant difference in depletion of nutrients from the pH 4 to 7 treatments in terms of protein depletion. This could show that different mechanisms are being utilised by *E. cloacae* at the different pH conditions in utilising roughly the same amount of nutrients. This in turn resulted in the release of different metabolites, with more electron and proton discharge being observed for the neutral and low pH treatments. Protein structure and folding is also dependent on pH, which could make the proteins change their structure at low pH, and

making them more usable to the microbes. This could generate more protons and electrons which would result in higher power densities. Ogbonda *et al*. (2007) describe how the optimum protein production in *Arthrospira* growth is at pH 9.0. This information gives us a possible insight into how the *Arthrospira* proteins are likely to be alkaline. An acidic medium may result in the denaturation and conformational change in the protein's structure, which would therefore aid in degradation by the *E. cloacae* biocatalyst resulting in faster release of electrons and protons.

Carbohydrates concentrations are lowest in the neutral and alkaline pH treatments. Nimje *et al.* (2011) observed that under acidic anodic pH conditions, the MFC, system outperforms neutral and alkaline system in terms of current generation. However, substrate degradation is greater under neutral and alkaline pH. At neutral and alkaline pH conditions, nutrient utilisation favours the growth of the biocatalyst more, resulting in more substrate degradation and less current generations (Nimje *et al.,* 2011). This could explain the low carbohydrate concentration at neutral and alkaline pH conditions at the end of the MFC study compared to pH 5 and pH 6 treatments. The total power output for pH 5 and pH 6 treatments had no significant difference. The pH 5 and pH 6 treatments, in terms of total power output, compared to pH 7 and pH 4 treatments were significantly different, and compared to the alkaline treatments were highly significantly different.

The PEM is a major limiting factor for the generation of current in an MFC. However, factors that affect the performance of the PEM are not well characterised in literature. Although it has been shown in research that Nafion® membrane is a very good proton exchange membrane (Behera *et al.,* 2010), (Choi *et al.,* 2011), other research has shown that during the continuous operation of an MFC, it is the major limiting factor to power output (Edwards *et al*., 2012). The performance of the PEM after a 5 day MFC study was examined by measuring the ion exchange capacity (Table 4.2).

Table 4-2: After the 120 hour pH MFC operation, an analysis of the PEM was performed. The proton exchange capacity was measured to show how the capacity to retain protons in the membrane changes at the different pH rates.

	Unused	Cleaned	pH 4	pH 5	pH 6	pH 7	pH 8	pH 9
PEC in $mmol.g^{-1}$	0.6683 (± 0.0056)	0.6220 (± 0.0038)	0.0282 (± 0.0012)	0.0220 (± 0.0024)	0.0023 (± 0.0007)	0.0074 (± 0.0011)	0	0

The proton exchange capacity for the PEM declined with an increase in pH from 4 to 9. No values were obtained in alkaline pH treatments, because under alkaline solutions the protons in the membrane are replaced with hydroxyl ions (Xu *et al*., 2012). The lack of protons in the alkaline media resulted in possible proton transport from the membrane to the media. Xu *et al,* (2012) describes how during an MFC operation, the proton binding sites of the PEM are substituted by metal ions found in the MFC media which also affects biofouling and organic fouling of the membrane. The loss of protons from the membrane affects the proton exchange capacity (ion exchange capacity specifically for protons). The greater the PEC, the better the proton transport is from the anode to the cathode in an MFC (Xu *et al*., 2012). The PEC at the lower pH conditions (pH 4 – pH 5) is greater than that at neutral and pH 6, because at lower pH the media has more protons possibly leading to competitive absorption at the proton binding sites in the membrane (Xu *et al*., 2012). The cleaning of the membrane is done using sulphuric acid, which would aid in regeneration of protons to the membrane and sulfonation of the membrane (Zawadinski *et al*., 1993). The difference in PEC due to the loss of protonation under different pH conditions could aid in explaining the low power densities observed under alkaline conditions. However, since membranes used had been cleaned instead of being unused, the PEC gives no actual indication of biofouling, because of the difference in pH and absence of negative controls.

Further analyses were carried out using the top three performing *Arthrospira* substrate media under buffered pH treatments in terms of peak power density (pH 5-7) from figures 4.12 , and the performance was compared to the performance of unbuffered *Arthrospira* and RCM

(figures 4.1 and 4.5) nutrient media as shown in figure 4.12. The change in power density over time was observed for the media.

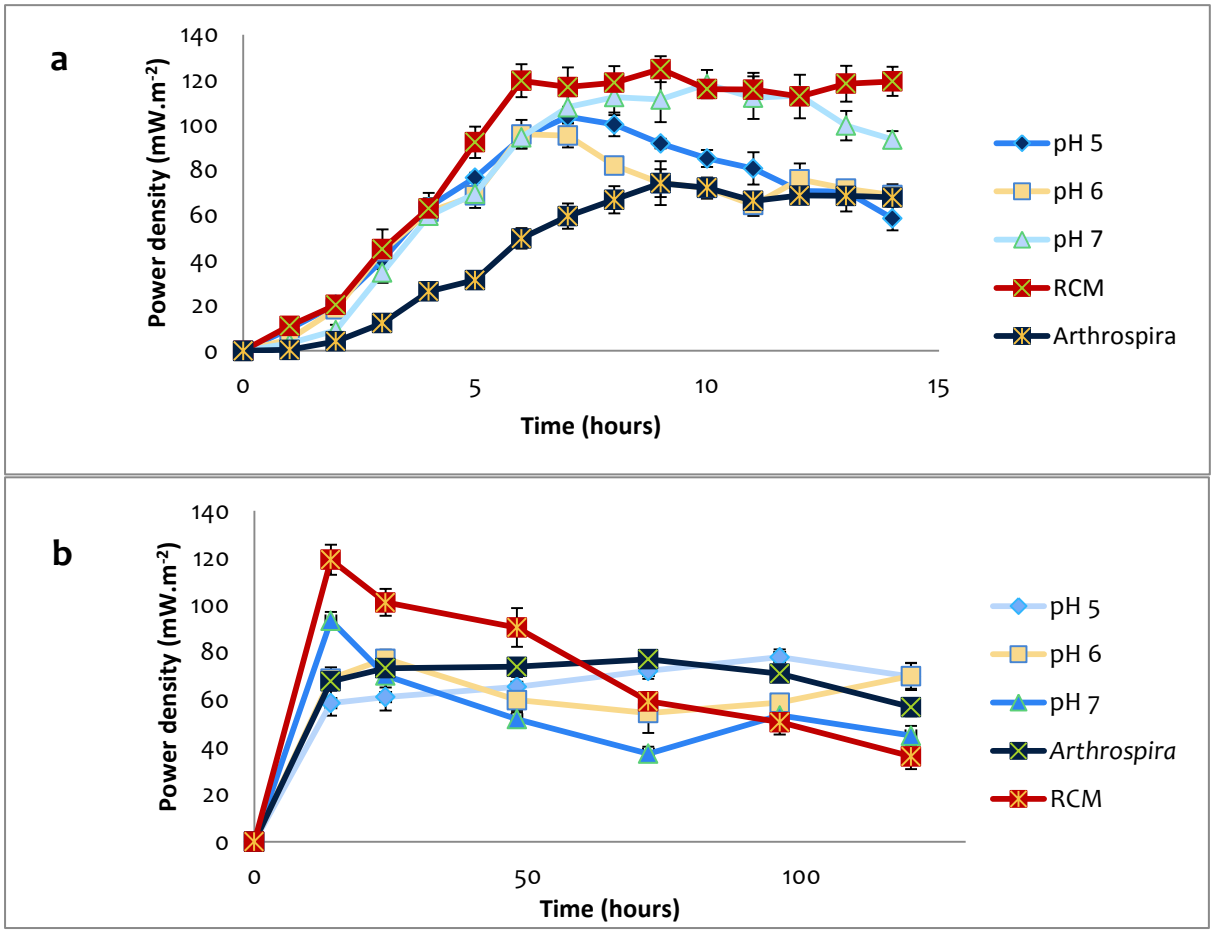

Figure 4.12: A comparison of buffered *Arthrospira* feedstock media, unbuffered *Arthrospira* feedstock medium and RCM medium in an MFC. Short-term MFC over 14 hours (a) and a long-term MFC studies over 120 hour (b). MFC studies were performed at 35° C and *E. cloacae* was used as the biocatalyst.

Figure 4.12a shows that the biocatalyst inoculated in the buffered *Arthrospira* feedstock treatment at pH 7, for a 14 hour MFC study produces similar power densities to that in RCM feedstock, which was used as the baseline for study. However, after 12 hours a rapid decline in power densities was observed for the pH 7 treatment, which can be a result of faster biocatalyst metabolism at pH 7 (Nimje *et al.*, 2011). This may have resulted in the initial release of electrons and protons that causes the spike in power density observed at 14 hours and the activation of other metabolic pathways. In the pH 5 and pH 6 treatments, there is an initial spike in the power density up to 7 hours (figure 4.12), then a decline in power density thereafter. For the unbuffered feedstock (RCM and *Arthrospira*), power densities stabilise

after the initial peak and did not decline further. From these results, it appears that the change in pH mediated by the biocatalyst is necessary in providing optimal conditions for metabolism and maybe crucial in the adaptation of the bacteria to the environment over the short term. After the initial peak power density was measured in RCM medium in the first 24 hours, the power density subsequently declined rapidly over the following 96 hours. At the conclusion of the experiment after 120 hours, power densities in RCM medium were the lowest, of all the treatments. RCM medium had a peak power density of 119.29 (± 6.41) $mW.m^{-2}$ in the first 14 hours and the final power density after 120 hours was 36.13 (± 5.41) $mW.m^{-2}$ which signifies a 83.16 (± 9.9) % fall in power density from the peak power density over a period of about 96 hours. The buffered pH feedstock treatments at pH 5 and 6 displayed consistent power densities throughout the 120 hour run. After the initial peak in the *Arthrospira* pH 5 treatment at 7 hours of 103.58 (± 2.79) $mW.m^{-2}$, a decline was observed to 58.64 (± 5.25) $mW.m^{-2}$ after 14 hours. An increase in power density is then observed after 14 hours, with a new peak of 78.11 (± 3.25) $mW.m^{-2}$ only observed after 96 hours. This is in contrast to the power density observations in RCM feedstock, where a decline was observed in power density after 24 hours. In the pH 6 treatment, the power density reached its peak after 6 hours of 95.93 (± 6.34) $mW.m^{-2}$. As for the pH 5 treatment a decline is observed with a final power density after 14 hours being 69.00 (± 4.82) $mW.m^{-2}$. After 24 hours the power density was 73.37 $mW.m^{-2}$ and the power density was constant with the final power density after 120 hours at 70.13 (± 5.40) $mW.m^{-2}$. Unbuffered *Arthrospira* feedstock treatment peaked after 9 hours to 74.19 (± 9.73) $mW.m^{-2}$ and was constant till 96 hours where the power density was 71.11 (± 1.31) $mW.m^{-2}$. The final power density at 120 hours was 57.06(± 3.84) $mW.m^{-2}$.

The change in COD between fresh media and after a 120 hour MFC study was studied (table 4.3). The difference in the PEC of the PEM from the different media was calculated as well, and shown in the table (table 4.3).

Table 4-3: The change in COD and the PEC after a 120 hour MFC study.

	pH 5	pH 6	pH 7	*Arthrospira*	RCM
COD initial ($mg.l^{-1}$)	N/A	335 (± 12)	388 (± 37)	178 (± 9)	572 (± 22)
COD Final ($mg.l^{-1}$)	N/A	298 (± 17)	230 (± 33)	133 (± 13)	477 (± 26)
PEC ($mmol.g^{-1}$)	0.0225 (± 0.0014) *+	0.0051 (± 0.0020) *#	0.0045 (± 0.0015) * #	0.0054 (± 0.0015) *#	0.0353 (± 0.0034)

Statistical analysis on the PEC was performed using one way ANOVA, with further tests done use Post Hoc test, Tukey HSD test. PEC values were compared to RCM PEC firstly, and results that were $p < 0.01$ were denoted *. The algae based PEC were then compared to each other and the PEC that were $p < 0.01$ were denoted + and if $p > 0.1$ denoted #.

Using the COD test kit, the COD for *Arthrospira* feedstock buffered at pH 5 exceeded the limit of detection probably as a result of the acetate buffer used which also contributes to COD, but was measured readily at pH 6 and 7. The COD removal for RCM was about a sixth of the original COD, while the COD removal in unbuffered pH *Arthrospira* feedstock was about a quarter of the original COD over a period of 120 hours. COD removal in pH 7 *Arthrospira* feedstock was about 41 % and in pH 6 *Arthrospira* feedstock, the COD removal was about 12 %. The change in pH in the feedstock media affected the COD removal by the biocatalyst. The results show that, COD removal is more effective at pH 7 than at pH 6 when *E. cloacae* is used as the biocatalyst.

The PEM that had been used in the MFC studies in the different feedstocks were analysed using SEM after 120 hours of operation in the MFC is shown in figure 4.13 to 4.17.

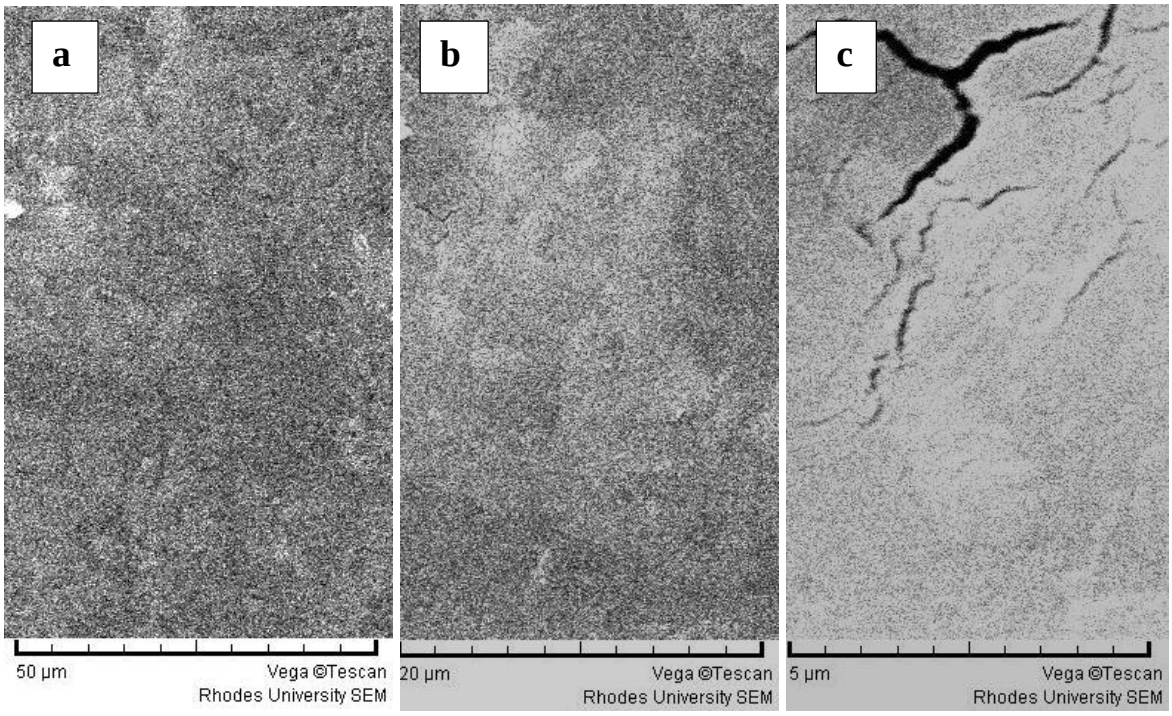

Figure 4.13: PEM fouling after 120 hours in an MFC with *Arthrospira* feedstock at pH 5 as the medium. SEM was used for visualisation with scale bars at 50 µm (a), 20µm (b) and 5 µm (c). MFC studies had been performed at 35° C.

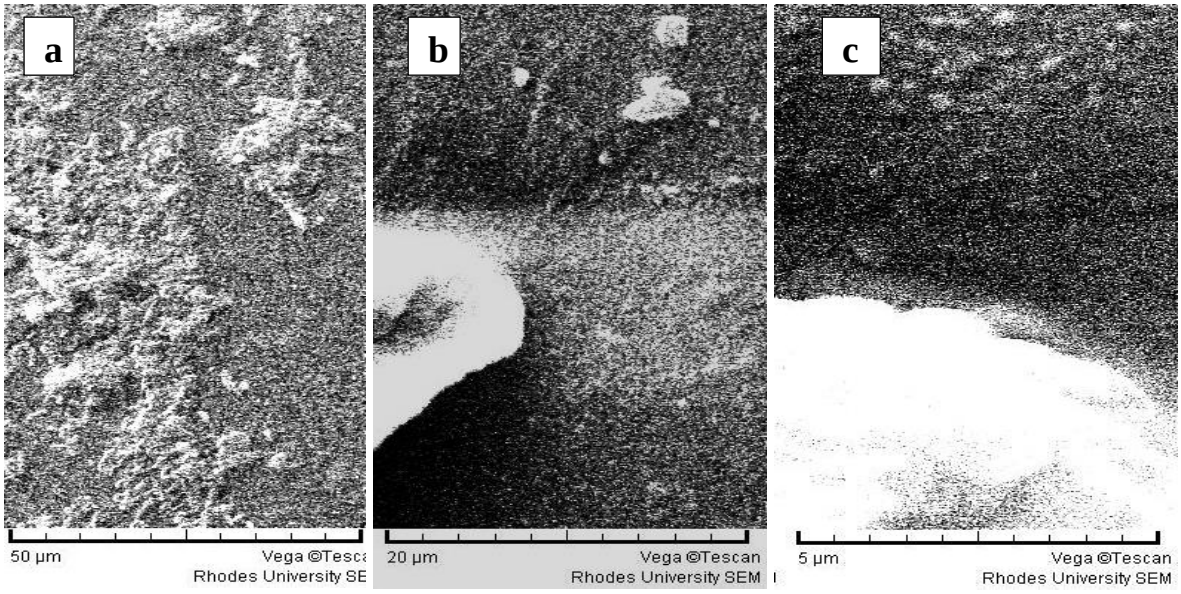

Figure 4.14: PEM fouling after 120 hours in an MFC with *Arthrospira* feedstock at pH 6 as the medium. SEM was used for visualisation with scale bars at 50 µm (a), 20µm (b) and 5 µm (c).MFC studies had been performed at 35° C.

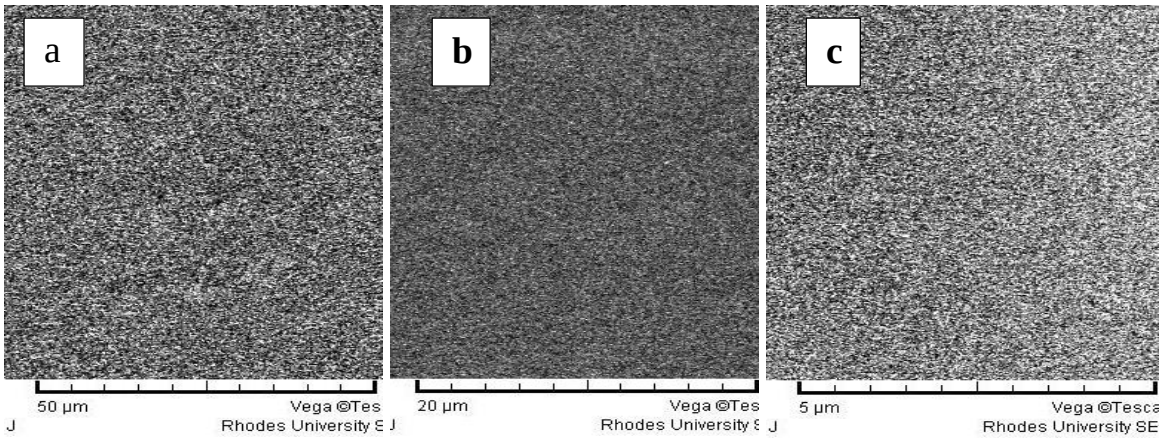

Figure 4.15: PEM fouling after 120 hours in an MFC with *Arthrospira* feedstock at pH 7 as the medium. SEM was used for visualisation with scale bars at 50 µm (a), 20µm (b) and 5 µm (c). MFC studies had been performed at 35° C.

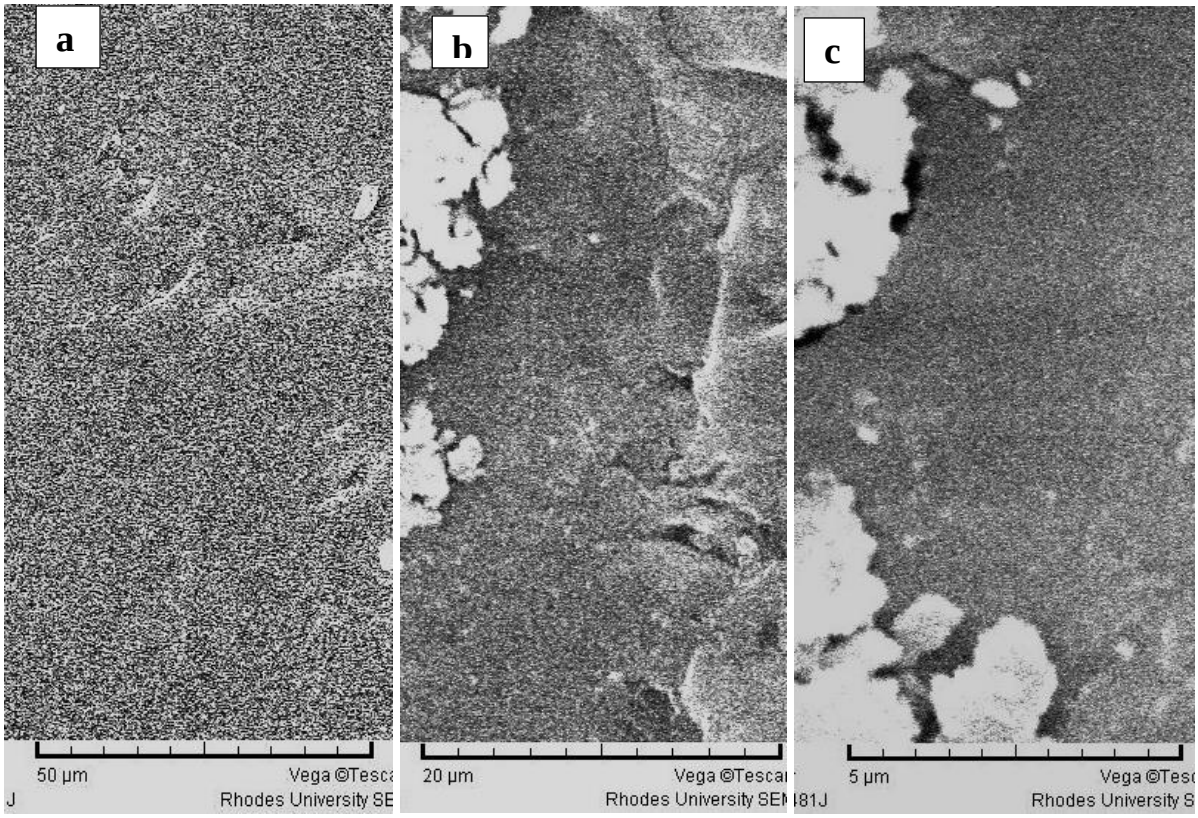

Figure 4.16: PEM fouling after 120 hours in an MFC with unbuffered *Arthrospira* feedstock as the medium. SEM was used for visualisation with scale bars at 50 µm (a), 20µm (b) and 5 µm (c). MFC studies had been performed at 35° C.

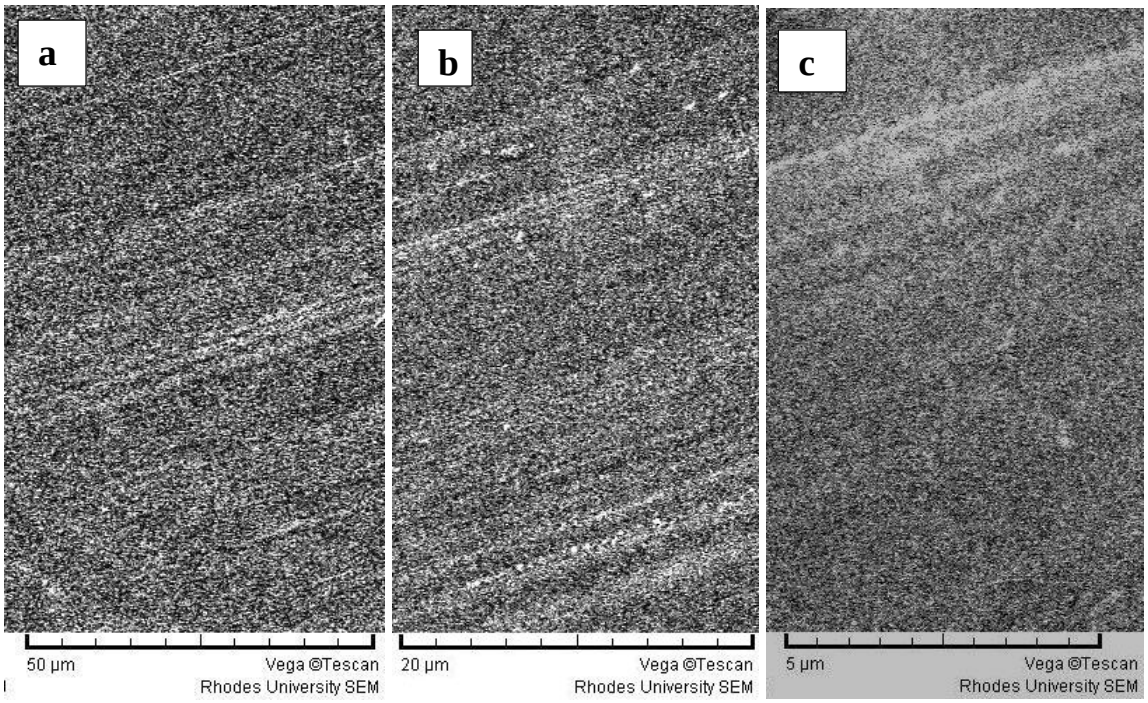

Figure 4.17: PEM fouling after 120 hours in an MFC with RCM as the medium. SEM was used for visualisation with scale bars at 50 µm (a), 20µm (b) and 5 µm (c). MFC studies had been performed at 35° C.

Figures 4.13 to 4.17 show the fouling of the PEM after operation at different pH (5- 7), unbuffered *Arthrospira* medium and in RCM medium. In the buffered *Arthrospira* medium at pH 7, fouling is minimal compared to pH 6, pH 5 and uncontrolled *Arthrospira* media treatments. Fouling on the PEM in RCM medium is low. The low fouling shown in the figures with *Arthrospira* media as feedstock could be a result of the large particulates of *Arthrospira* feedstock which could have formed a layer on the membrane surface, compared to RCM medium which does not contain large particulates. The fouling could explain why the PEC for the PEM from RCM medium is almost double that of the PEMs from the *Arthrospira* feedstocks. Xu *et al*. (2012) describes that fouling of the PEM occurs during long-term performance and how different anode feedstock affects biofilm formation. Biofouling affects proton binding sites on the membrane which results in substitution of the proton binding sites with metal ions and other ionic groups like hydroxyl and carbonate ions resulting in a lower PEC for the PEM (Xu *et al*., 2012) and also increases electrical resistance (Choi *et al*., 2011) with the SEM showing fouling which could explain the decline in power density over time of the MFC. From the SEM images, it can be observed that algal based feedstock results in more biofouling and organic fouling of the PEM than the less complex

feedstock such as RCM which are industrially prepared from refined products for commercial purposes. The fouling of the PEM presents a significant bottleneck in the operation and scale up of the MFC technology. A method of operating an MFC that may minimise fouling of the PEM or even circumvent the use of a PEM would be desirable.

Figure 4.18 shows the buffered feedstock media (pH 5 – pH 7) after a 120 hour study in an MFC. Visualisation was done under a light microscope at 400 times magnification. The feedstock was visualised before and after the 120 hour MFC study.

Unused feedstock **Feedstock after 120 hours study**

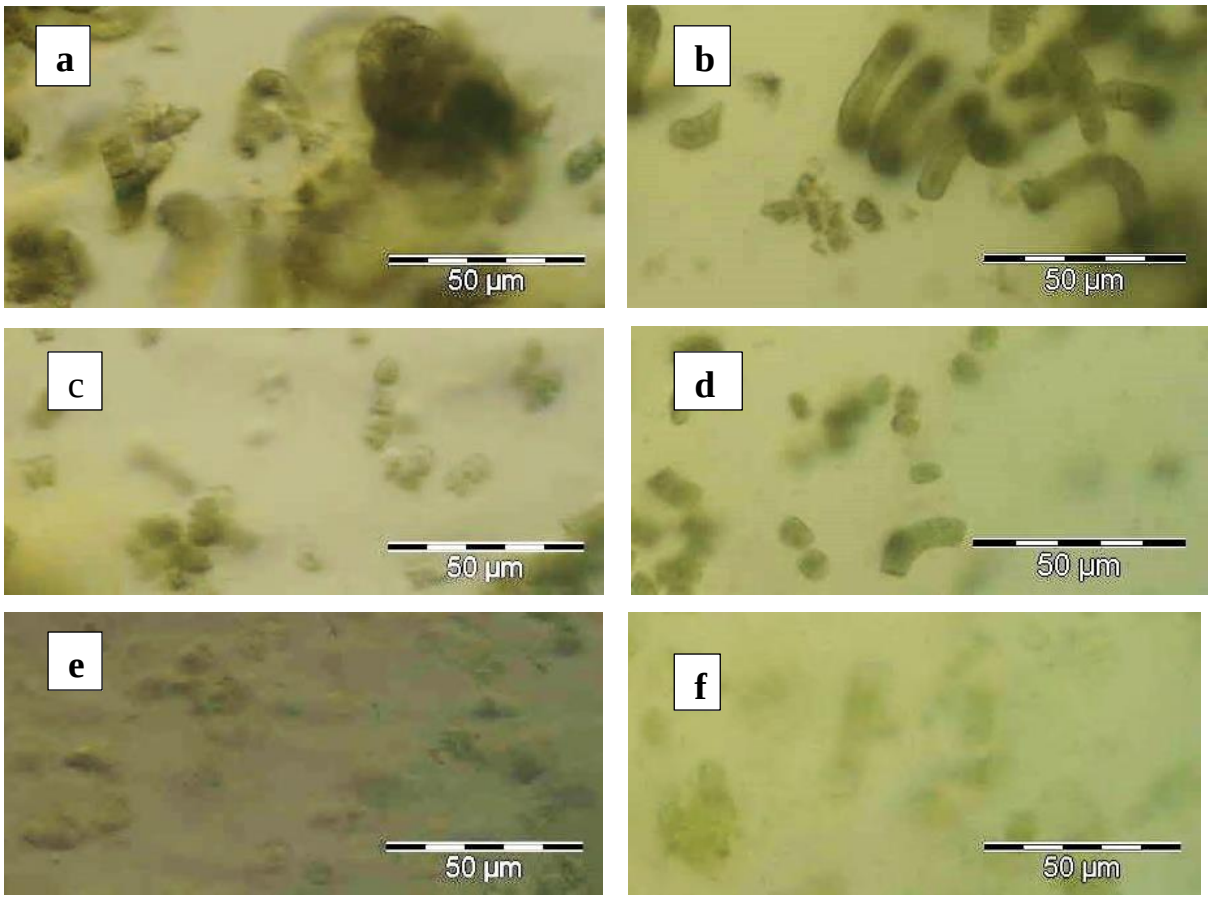

Figure 4.18: *Arthrospira* feedstock visualised at 400 times magnification using a light microscope. *Arthrospira* feedstock buffered at pH 5 before an MFC study (a) and after a 120 hour MFC study (b); *Arthrospira* feedstock buffered at pH 6 before an MFC study (c) and after a 120 hour MFC study (d); and *Arthrospira* feedstock buffered at pH 7 before an MFC study (e) and after a 120 hour MFC study (f).

Figure 4.19 shows the *Arthrospira* unbuffered feedstock and RCM after visualisation under a light microscope at 400 times magnification before and after a 120 hour MFC study.

Unused feedstock **feedstock after 120 hours study**

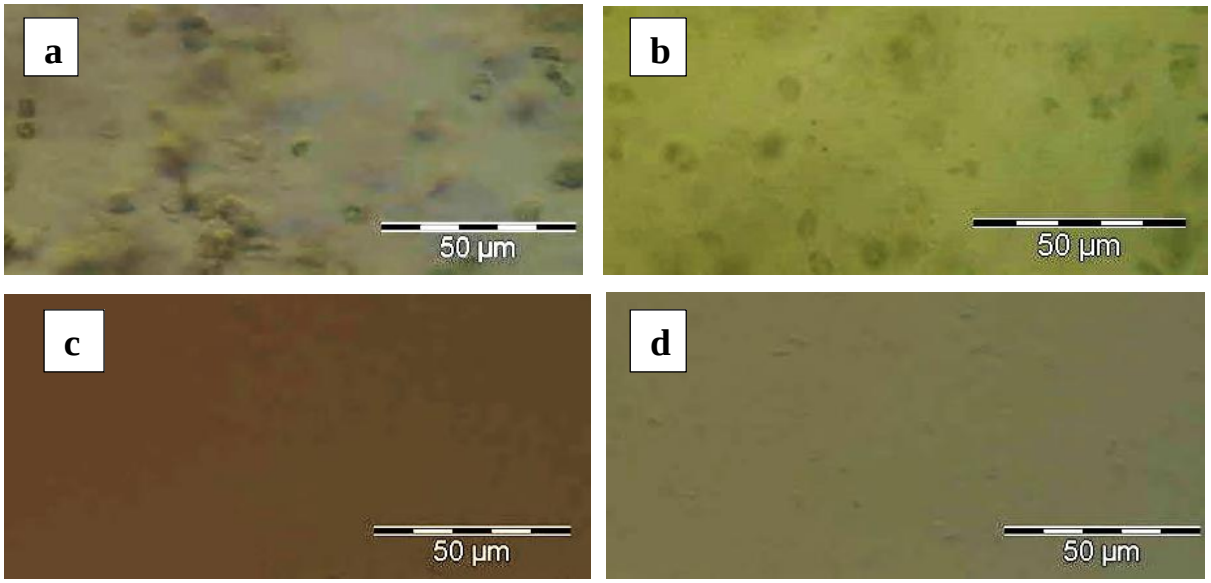

Figure 4.19: *Arthrospira* feedstock without controlled pH before an MFC study (a) and after a 120 hour MFC study (b); and RCM medium before an MFC study (c) and after a 120 hour MFC study (d) visualised at 400 times magnification using a light microscope. MFC studies were performed at 35° C.

From figures 4.20 and 4.21 it can be observed that after the 120 hour run in an MFC for the algal based feedstock, larger algal particulates are broken down and dispersed. These results coupled with the COD removal data and power density curves, provides further evidence that biodegradation does occur in the MFC with electricity harvesting being a by-product. The images from RCM show some particles which could be the clumping of the biocatalyst making them visible at 400 times magnification.

4.4 Conclusions

The pH of the microenvironment of the anode media during MFC operation using *E. cloacae* as the biocatalyst changes during the operation. Peak power densities for the biocatalyst, irrespective of the media occur under acidic pH conditions. Growth of the biocatalyst, under anaerobic conditions is at acidic pH during its log phase. Peak performance of the MFC at 35° C with *E. cloacae* as the biocatalyst is observed under acidic pH conditions and performance declines or levels off when the pH in the MFC anode microenvironment naturally increases. Buffering the anode microenvironment and controlling the pH gave a more in depth analysis of the MFC system and performance for the biocatalyst. Peak performance in the MFC over short operation lengths was observed under neutral pH however performance under neutral pH for the MFC declined after the first 24 hours. Under controlled pH studies, under alkaline conditions, the MFC performance is low compared to MFCs with acidic pH feedstock. Similar MFC performance was observed when the feedstock was not buffered, whereby peak power densities were observed under acidic conditions. The MFC pH studies show that performance is optimal in an MFC when the anode microenvironment is acidic and MFC performance is suppressed under alkaline conditions. The performance of the MFC was also shown to be related to the carbohydrate concentrations in the feedstock. The studies showed that growth kinetics of *E. cloacae* were directly related to MFC performance in terms of the peak power densities in the first 14 hours of operation. Metabolic pathways at the different pH of the feedstocks result in different proton and electron release in the MFC, as well as different substrate degradation. The different pH conditions also affect the proton exchange capacity of the PEM, with low capacity observed at neutral pH compared to acidic pH and very minimal capacity observed for alkaline pH. However, compared to unused and cleaned PEM, the proton exchange capacity after an MFC operation is greatly affected, with over 90 % loss in PEC observed under all the pH treatments. Controlling the pH of the *Arthrospira* feedstock increases the efficiency of electricity generation by the system. The pH also affects nutrient and COD removal from the system and plays a major role in the fouling and performance of the PEM.

Chapter 5 : Influence of electrode material on performance and study of microalgae as biocathodes in an MFC

5.1 Introduction

Electrode material in microbial fuel cells (MFC) shoudly ideally be biocompatible and have a high surface area (Zhu *et al*., 2011; Lee *et al*., 2008). Activated carbon fibre (ACF) is used in biological systems such as waste water treatment systems for the adsorption of polluted fluids (Deng *et al.,* 2010) showing its biocompatibility. It also has an enhanced 3D conformation. This in theory enhances the exposed surface area (He *et al*., 2011) allowing more biofilm surface interaction. The use of fibre with small diameters has also been shown to favour the formation of thick and continuous biofilms which improves biofilm-electrode interaction and possibly current densities (He *et al*., 2011).

The use of algae in MFCs can be expanded beyond the use of the algae as nutrient feed for microbial biocatalysts in the anode. Microalgae can be used as a bio-electron acceptor in the cathode, whereby it can sequestrate some of the electrons from the MFC anode reaction. Powell *et al*. (2009) used *Chlorella* as the bio-electron acceptor and Fu *et al*., (2009) used *Arthrospira* as a bio-cathode in MFC studies. Algae are photosynthetic under light conditions producing oxygen and acting as a CO_2 sink. This makes it theoretically possible to use algae as aerobic bio-cathodes, responsible for oxygen supply and also acting as bio-electron acceptors (Gonzalez *et al*., 2013). Microalgae also have the potential to decrease the over-potential of the ORR (Wu *et al*., 2014). Microalgae as bio-cathodes have the advantage of having low operation cost and self-generation capabilities (Wu *et al*., 2014). Light intensity affects the rate of photosynthesis, with higher light irradiance resulting in higher rates of photosynthesis, which in turn affects the dissolved oxygen content in the medium containing the algae (Juang *et al*., 2012). If photosynthesis is too high, the dissolved oxygen in the medium can reach a critical point where oxygen is leaked to the anode which in turn affects the power generation in the MFC (Juang *et al*., 2012). Fu *et al*., (2009) in their research showed how an increase in biomass areal density increases power density in the MFC.

The aim of the study was to compare and contrast the use of ACF in MFCs and how performance may differ from MFCs utilising carbon paper. Using the same modification

methods for carbon paper with MWCNTs and FePc, the activated carbon fibre was modified and the power density from MFCs was observed and compared. The second aim of the study was to observe the use of algae as biocathodes in an MFC under different light and temperature conditions and how this would affect MFC performance.

5.2 Methodology and materials

5.2.1 Carbon electrodes

i. Carbon paper

Toray carbon paper (TGP-060) (Alfa Aesar GmbH & Co. KG) was used for certain MFC experiments (2 cm x 2 xm). Modification was performed using MWCNTs and FePc when required as described in the methodology section (chapter 2.2.3.6 and 2.2.3.5).

ii. Activated Carbon Fibre

Activated Carbon Fibre (ACF) Non-Woven Fabrics (SO-EN CO., LTD) with a BET (Brunauer–Emmett–Teller theory) of 1000 ± 50 $m^2.g^{-1}$ was used as an alternative electrode material. From the BET, the surface area required was calculated to be 8 cm^2, which is similar to the surface area of CP used. The area required from the calculations measured about 4 mm x 4 mm. Bare ACF was used for the experiments and when modification was required it was done using MWCNTs and FePc. The drip-dry method of application was used as described for carbon paper modification (chapter 2.2.3.6 and 2.2.3.5).

5.2.2 Cyclic voltammetry

Cyclic voltammetry was performed on the carbon electrodes which were attached to the apparatus via an external copper wire. A Potentiostat/Galvanostat 30 (PGSTAT 30) (Autolab) was used and the data were gathered and analysed using NOVA 1.9 software. A standard three-cell system was utilised for all cyclic voltammetry work with copper wire connecting the sample carbon electrode in 10 mM phosphate buffer to the working electrode. To minimise interference of the data from copper, long pieces of carbon paper and carbon fibre were used, so that a substantial portion of the carbon material could be immersed in the liquid without exposing the copper wire to the liquid. A reference electrode which had been stored in 3 M KCl (Ag/AgCl vs. 0.225 (Bioanalytical Systems, USA) was used as the counter electrode and a platinum electrode. Before all analyses, nitrogen gas (purity 99.999 % with impurities less than 5 ppm, Afrox) was used to degas the solutions.

5.2.3 Electrode cleaning of carbon paper

Carbon paper that had been used in MFCs was cleaned and reused in further MFC studies. A combination of cleaning methods adapted from Harewood *et al*. (1973) Perfol *et al*. (2002) and Q-sense Handbook were used. Used carbon paper electrodes where immersed in absolute ethanol and sonicated (Elmasonic S10H, Elma® D-78224, Singen/HTW, Germany) for 5 minutes to remove bacteria and other biofilms. A rinse step was carried out using milliQ water. This step was followed by a 30 minute immersion in 2 % SDS (≥98.5 % purity, Sigma Aldrich, Japan) at room temperature to remove thiols and proteins. The electrodes were rinsed with milliQ water afterwards and left to try in a fumehood, with UV light turned on.

5.2.4 Microbial fuel cells

Two-chambered H-type MFCs were assembled and operated in controlled environment (CE) rooms at 35° C (as described in chapter 2, section 2.2.3.1).

5.2.5 Anode biocatalyst

Enterobacter cloacae strain 16657 was used as the biocatalyst (chapter 2.2.2).

5.2.6 Algae growth kinetics

Luminance was measured using a nokia Lumia 720 cellphone, Carl Zeiss 6.3 mp camera lense, using the light meter app.

i. *Chlorella* growth

A *Chlorella* culture in its log phase of growth was provided by EBRU. The culture was inoculated and grown in modified Bolds Basic media (BBM) as described by Powell *et al.,* (2009). Modified BBM was prepared by adding the following salts to one litre milliQ water; 75 mg KH_2PO_4, 50 mg K_2HPO_4, 75 mg NH_4Cl, 25 mg $MgSO_4.7H_2O$, 12.5 mg $CaCl_2$, 12.5 mg NaCl, 60 mg $NaHCO_3$, 25 mg EDTA (sodium salt), 2.5 mg $FeSO_4.7H_2O$ and adding 0.5 ml trace mineral solution. The trace mineral solution was made up by adding 1.25 mg H_2BO_3, 882 mg $ZnSO_4$, 70 mg MoO_3, 50 mg $Co(NO_3)_2$, 140 mg $MnCl_2$ and 160 mg $CuSO_4.5H_2O$ to 100 ml milliQ water. To 200 ml BBM in a conical flask, 20 ml log phase *Chlorella* was inoculated. The reactors were set-up in a 27° C CE room with a luminance of 228 $cd.m^{-2}$ and placed on a shaker at 100 rpm. An alternating photoperiod of 12 hours light and 12 hours dark was used.

ii. *Arthrospira* growth

A log phase *Arthrospira* culture was provided by EBRU. Different batches of *Arthrospira* used in this study were grown in Zarrouk's or Schlösser's media.

a. Arthrospira growth in Zarrouk's medium

Arthrospira was grown in Zarrouk's liquid medium using the method adapted from Chojnacka and Noworyta, (2004). Zarrouk's medium was prepared by adding 2.5 g $NaNO_3$, 0.5 g K_2HPO_4, 10 g $NaHCO_3$, 1 g NaCl, 0.2 g $MgSO_4.7H_2O$, 0.02 g $CaCl_2.2H_2O$ and 0.01 g $FeSO_4.7H_2O$ in a litre of milliQ water. To 200 ml of the media, 20 ml log phase *Arthrospira* was inoculated. The reactors were set-up in a 27° C CE room with a luminance of 228 $cd.m^{-2}$ and placed on a shaker at 100 rpm. An alternating photoperiod of 12 hours light and 12 hours dark was used.

b. Arthrospira growth in Schlösser's medium

Arthrospira was grown in Schlösser's medium using the method adapted from Celekli and Yavuzatmaca, (2009). Schlösser's was prepared by adding to a litre of milliQ water 13.61 g $NaHCO_3$, 4.03 g Na_2CO_3, 0.50 g K_2HPO_4, 2.50 g $NaNO_3$, 1.00 g K_2SO_4, 1.00 g NaCl, 0.20 g $MgSO_4.7H_2O$, 0.04 g $CaCl_2.2H_2O$ and autoclaving. After the solution had cooled off, 6 ml of metal solution containing 97 mg $FeCl_3.6H_2O$, 41 mg $MnCl_2.4H_2O$, 5 mg $ZnCl_2$, 2 mg $CoCl_2.6H_2O$ and 4 mg $Na_2MoO_4.2H_2O$, 1 ml of micronutrient containing 50 mg Na_2EDTA, 618 mg H_3BO_3, 19.6 mg $CuSO_4.5H_2O$, 44 mg $ZnSO_4.7H_2O$, 20 mg $CoCl_2.6H_2O$, 12.6 mg $MnCl_2.4H_2O$, and 12.6 $Na_2MoO_4.2H_2O$ and 0.15 mg of B12 vitamin were also added. To 200 ml of the Schlösser's solution, 20 ml of *Arthrospira* in log phase was added. Arthrospira were cultured in a conical flask placed on a shaker at 100 rpm in a 27° C CE room illuminated at 228 $cd.m^{-2}$.

Chlorella growth kinetics were very low and were not studied. The growth kinetics for *Arthrospira* were studied by measuring the daily absorbance at OD_{560nm} using a UVmini-1240 spectrophotometer (SHIMADZU).

c. Mass versus absorbance for *Arthrospira*

The medium with the best growth kinetics for *Arthrospira* was used in further absorbance against mass studies. One millilitre of *Arthrospira* was taken daily from the Zarrouk's

medium reactor and dried in an oven at 70° C for 48 hours. The mass was measured after drying and plotted against the absorbance (in growth medium).

5.2.7. MFCs for biocathode studies

i. Electrode material

After the successful use of ACF as a potential electrode material substitute for carbon paper, and with good readings obtained without modification of the ACF, ACF was used as the cathode and anode electrode material.

ii. Nutrient medium

RCM was used as the nutrient medium in the anode for the MFC biocathode studies (chapter 2.2.1.1).

iii. Cathode media

Algae in its log phase during growth were used as the catholyte. *Arthrospira*, *Chlorella* or a mixture of the two algae was used in the studies. For some of the studies an unsealed cathode was used whereby the cathode side was open to the atmosphere and for other studies where specified, the cathode was sealed in the same way as for the anode.

iv. MFC setup

Two-chambered H-type MFCs were assembled and operated. Activated carbon fibre was used as the anode and cathode electrodes. The cathode medium contained a growing culture of algae. Studies were conducted in a 35° C CE room with a luminance of 83 $cd.m^{-2}$. Other studies were done in the 27° C CE room with a luminance of 228 $cd.m^{-2}$. The final studies were conducted in the 27° C CE room in total darkness.

5.3 Results

5.3.1 Carbon based electrodes

Different carbon material can successfully be used as electrode material in MFCs including carbon paper and activated carbon fibre as shown in figure 5.1. The performance of bare carbon paper and bare activated carbon fibre were compared against the performance of modified electrodes in an MFC at 35° C.

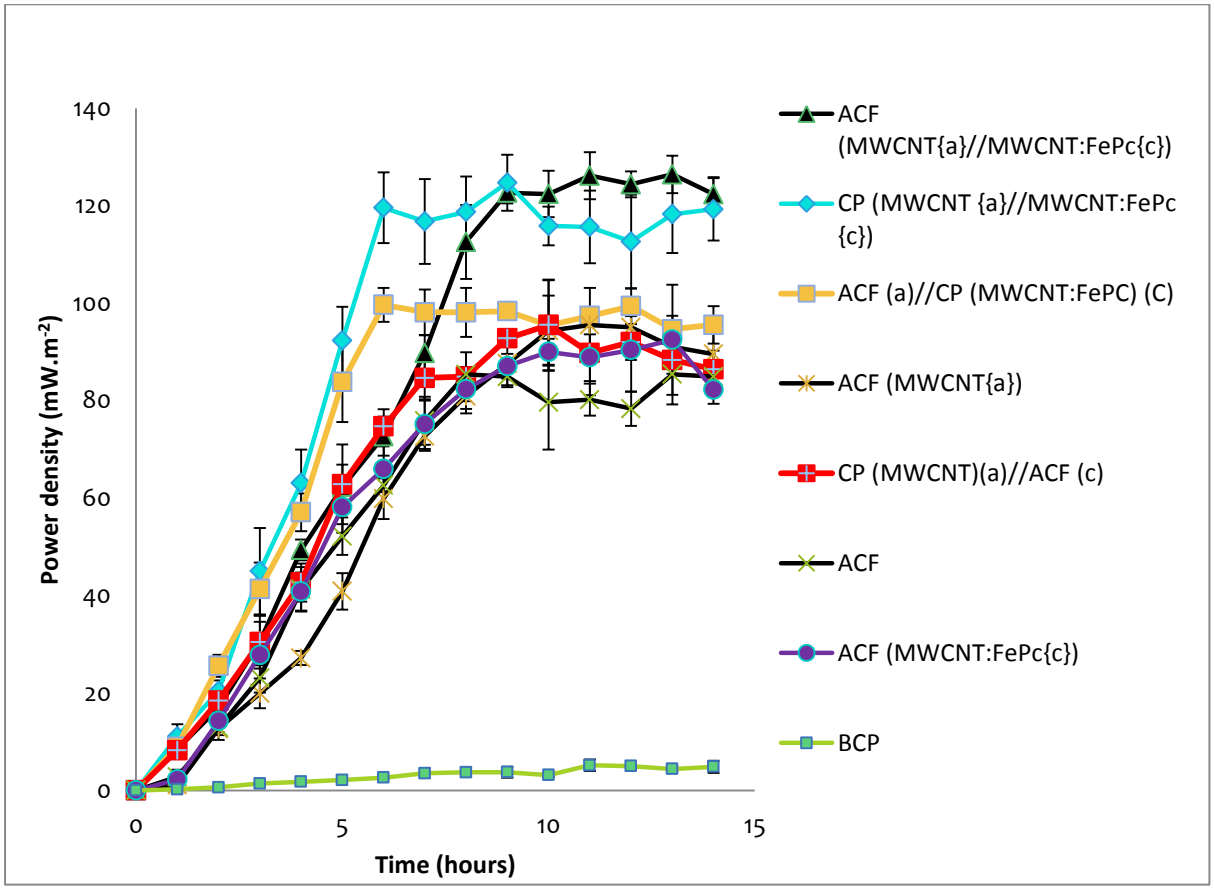

Figure 5.1: Power densities for different electrode material in MFCs using RCM medium as the feedstock. Electrodes used as the anode were denoted (a) and electrodes used as the cathode were denoted (c). CP – carbon paper; ACF – activated carbon fiber; BCP – bare carbon paper; MWCNT – multi-walled carbon nanotubes; FePc – iron (ii) phthalocyanine. MFCs were set up at 35° C in a CE room. *E. cloacae* were used as the biocatalyst.

Table 5-1: Peak power density for different electrode configurations with the time taken to reach peak power density output.

Electrode material used (anode)	Electrode material used (cathode)	Time taken to reach peak power density (hours)	Peak power density ($mW.m^2$)
Bare carbon paper	Bare carbon paper	11	5.16 (± 1.17) *#
CP (MWCNT)	CP (MWCNT:FePc)	9	122.7 (± 5.73) #
ACF	ACF	8	85.4 (± 1.50) *
ACF (MWCNT)	ACF	11	95.5 (± 1.92) *#
ACF	ACF (MWCNT:FePc)	13	92.5 (± 3.77) *
ACF (MWCNT)	ACF(MWCNT:FePc)	11	126.5 (± 3.84) #
ACF	CP (MWCNT:FePc)	6	99.7 (± 3.51) *#
CP (MWCNT)	ACF	10	95.5 (± 3.09) *#

Using ANOVA for statistical analysis, the Tukey HSD test, comparing results to the positive control of modified carbon paper electrodes, * shows the results of the electrodes that are highly significantly different to modified carbon paper for MFC performance where $p < 0.01$. Using ANOVA for statistical analysis, the Tukey HSD test, all electrode configurations were compared to bare ACF, where # shows the results when $p < 0.01$ and # shows the result when $0.01 < p < 0.05$.

Use of bare carbon paper as the electrode material for the anode and cathode resulted in low power density output with a peak power density of 5.16 (± 1.17) $mW.m^{-2}$ (figure 5.1). Modifying CP with MWCNT at the anode and MWCNT:FePc at the cathode resulted in an increase in catalytic efficiency which also increased the power density. The peak power density for the modified CP was 122.71 (± 5.73) $mW.m^{-2}$ which is about 24 times as much as bare CP. Zou *et al*. (2008) describe how carbon paper with a large surface area can be easily modified to improve catalytic efficiency. Carbon paper has poor oxygen reaction rate (Uria *et al.*, 2011) and the biocatalyst (bacteria) to electrode catalyst (bare carbon paper) electron transfer is minimal (Peng *et al*., 2010). This could explain why the bare CP has low power density outputs compared to the modified carbon paper. Modification of the carbon paper

results in an increase in current generation (Edwards *et al*., 2012). Use of MWCNTs as electrode enhancers results in an increased surface area and increased reactivity area for the biocatalyst (Zou *et al*., 2008). At the cathode, MWCNTs acting as the support materials for FePc on the electrode surface, improve the ORR and activity for the MFC (Yuan *et al.,* 2011; Mshoperi *et al*., 2013; Edwards et al., 2012). Modification of carbon electrodes has also been shown to improve biofilm-electrode interaction (He *et al*., 2011).

Bare ACF used as electrode material for the anode and cathode in MFC studies performed better than bare CP. Bare ACF had a peak power density of 85.4 (± 1.50) $mW.m^{-2}$. Compared to bare CP, bare ACF performance was about 17 times better. From figure 5.1 it can be observed that using carbon paper with MWCNTs on the anode and ACF at the cathode resulted in a lower power density output of 95.5 (± 3.09) $mW.m^{-2}$ compared to carbon paper with MWCNT:FePc mixture at the cathode, which had a peak power density of 122.71 (± 5.73) $mW.m^{-2}$. Modifying the ACF with the same MWCNT at the anode and MWCNT:FePc at the cathode resulted in similar power density with the modified CP having a peak power density output of 126.5 (± 3.84) $mW.m^{-2}$. Table 5.1 also shows the time taken to reach the peak power density output, with ACF at the anode and CP with MWCNT:FePc at the cathode had the shortest time of 6 hours. Bare ACF at the anode with modified ACF at the cathode had the longest time to reach peak power density of 13 hours.

Increasing the surface area and using material that increases surface area has been known to increase current generation and electrode efficiency (Liang *et al.,* 2011). ACF offers many potential benefits in use as electrode material in an MFC including having a high surface area and excellent adsorption (Deng *et al.,* 2010). Carbon fibre increases the active contact area for biofilm propagation (He *et al*., 2011) therefore its use is more effective as an anode electrode than a cathode electrode. These results show that ACF can be used as an effective electrode substitute for carbon paper in cost minimising efforts without drastically affecting current output.

5.3.2 Reuse of carbon paper during MFC studies

Carbon paper is brittle and variable costs such as transport have made it expensive (He *et al*., 2011). The reuse of used carbon paper, through recycling and re-modifying could minimise the overall cost of use in an MFC. Figure 5.2 shows the power density curves that were

observed when carbon paper was recycled during short term MFC studies. The plotted graph shows the reusability of carbon paper as electrode material in an MFC.

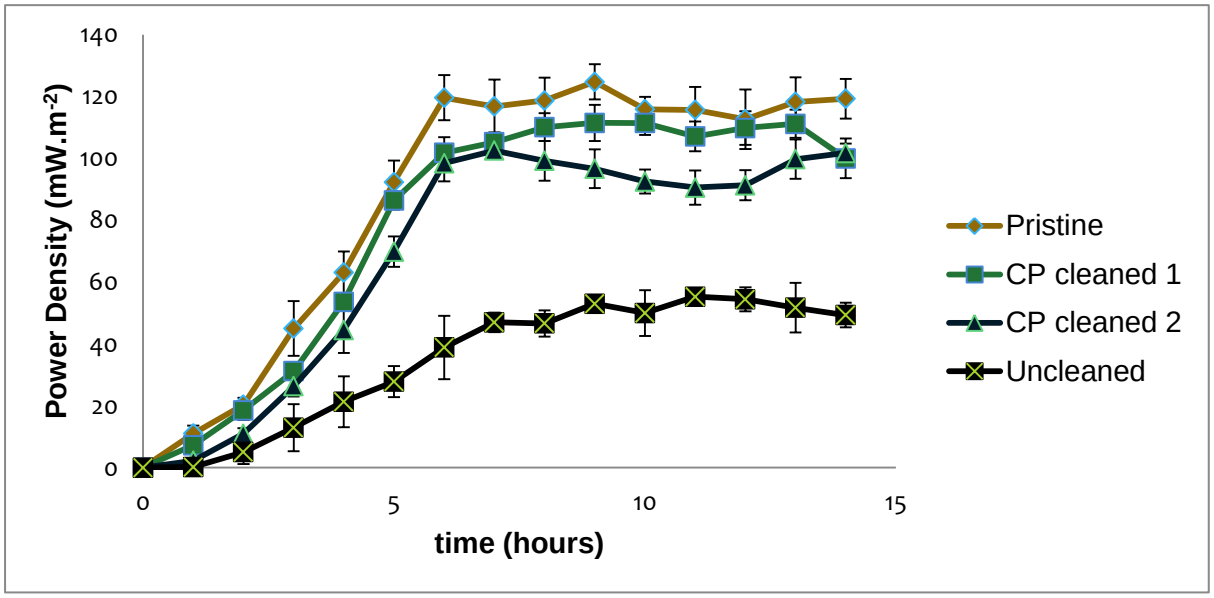

Figure 5.2: Power density output of MFCs with RCM medium as feedstock. A combination of cleaning methods where used to remove the biofilm layer. MFC studies were performed at 35° C with *E. cloacae* as the biocatalyst.

Table 5-2: Peak power density for pristine, cleaned and dirty modified carbon paper electrodes and the time taken to reach peak power density output for a 14 hour MFC study with RCM medium as feedstock at 35° C.

Electrode description (carbon paper)	Peak power density ($mW.m^{-2}$)	Time taken to reach peak power density (hours)
Pristine	124.7 (± 5.7)	9
Used (uncleaned)	55.3 (± 2.7)	11
CP cleaned 1 (used once and cleaned)	111.5 (± 5.9)	9
CP cleaned 2 (used once, cleaned, used again and cleaned, 2 cycles of use)	102.5 (± 1.6)	7

Figure 5.2 shows that it is possible to reuse carbon paper electrodes. Power density decreased slightly after each usage. The fresh modified carbon paper electrode had a peak power density of 124.7 (± 5.7) $mW.m^{-2}$ and after a single MFC run of 14 hours, recycling and reuse of these electrodes resulted in a fall of peak power density to 55.3 (± 2.7) $mW.m^{-2}$. This is a 55.7 % (± 6.8 %) fall in peak power density. From a single MFC run, cleaning the electrode resulted in a fall of peak power density from 124.7 (± 5.7) to 111.5 (± 5.9) $mW.m^{-2}$. Cleaning this electrode resulted in a 10.5 % (± 9.7 %) fall in power density compared to the reuse of an uncleaned carbon paper electrode which resulted in a 55.7 % (± 6.8 %) decline in peak power density. Recycling and cleaning the carbon paper electrode for reuse a second time resulted in a peak power density of 102.5 (± 1.6) $mW.m^{-2}$. The cleaning methods used were intended to remove most biological substances such as proteins and lipids (Harewood *et al*., 1973) and bacteria and biofilm from the electrode surface (Q-sense, 2002). A second round of cleaning after use resulted in a 17.8 % (± 5.9 %) decline in the original peak power density. This also signifies a further 8.2 % (± 6.9 %) decline in peak power density from the first round of cleaning. Even after the second cycle of cleaning the peak power density is still higher than a recycled and uncleaned electrode. With the relatively large cost of carbon paper (average R 1.20/cm^2, excluding transport: data averaged from Quintech, fuelcellearth and fuelcellsetc as of 25 November 2013), the single use of carbon paper in an MFC makes using such an electrode not as financially sound compared to reuse. Reuse of the electrodes was tested after the electrodes had been cleaned.

Figure 5.3 shows pristine carbon paper under SEM before use in an MFC. The 3D structure of the carbon paper is visible with no surface fouling observed.

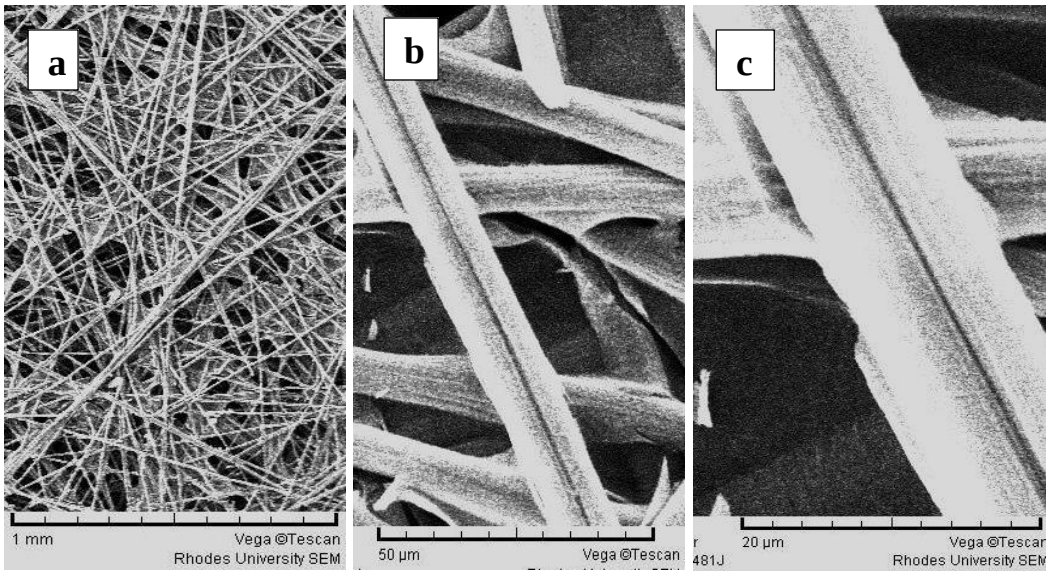

Figure 5.3: SEM of pristine carbon paper before use in an MFC with scalebars at 1 mm (a), 50 µm (b) and 20 µm (c).

The SEM images show the 3D structure of the carbon paper with no biofilm formed on the surfaces.

Figure 5.4 shows an SEM of carbon paper after a 14 hour MFC study with RCM as the feedstock in the anode. The carbon paper was used as the anode electrode.

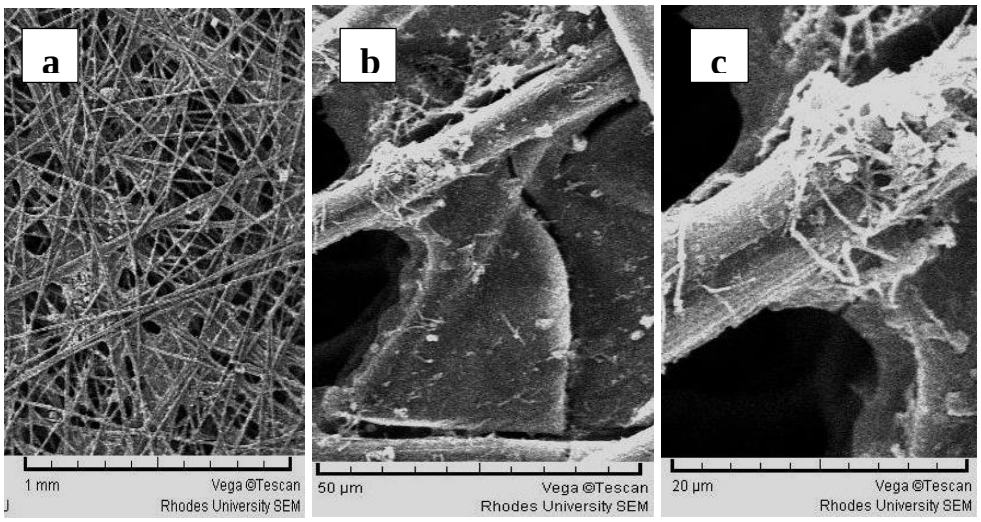

Figure 5.4: SEM of carbon paper after use in an MFC for 14 hours with scalebars at 1 mm (a), 50 µm (b) and 20 µm (c). RCM was the feedstock and *E. cloacae* was the biocatalyst. MFC studies were performed at 35° C.

Compared to figure 5.3, the SEM images in figure 5.4 show the structure of carbon paper with biofilm formed on the surfaces as well as MWCNTs used to modify the electrode.

Figure 5.5 shows carbon paper that had been used in an MFC study with RCM as feedstock for 14 hours after being cleaned, under SEM.

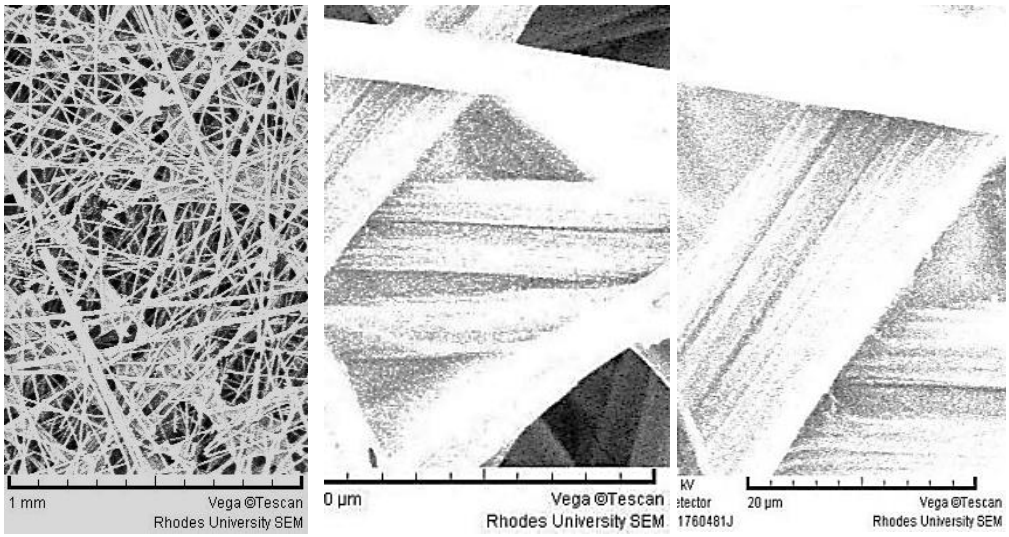

Figure 5.5: SEM of carbon paper that had been used as the anode electrode in a 14 hour MFC study with RCM medium after cleaning with scalebars at 1 mm (a), 50 µm (b) and 20 µm (c). After cleaning of the ekectrodes, *E. cloacae* was used as the biocatalyst.

The SEM images show the difference between a pristine electrode, a used electrode and a cleaned electrode, specifically how cleaning can be used as a tool to remove most of the biofilm and organic layer (Harewood *et al*., 1973). How the cleaning method affects the electrode surface which may result in the lowering of the current generation is unknown, but this could be due to the modification of electrode surface by the chemical procedure used to remove biofilm and bacteria, which could affect electrode surface interactions.

Compared to reusing an uncleaned electrode, the cleaning methods do improve current generation significantly, therefore allowing reuse and recycling of the electrodes and in turn minimising the cost of operation of the MFC.

5.3.4 *Chlorella* and *Arthrospira* biocathodes

Live *Chlorella* and *Arthrospira* cultures were inoculated and grown in Bolds Basal Medium for the former and Zarrouk's or Schlösser's media for the latter. As shown in figure 5.6. *Arthrospira* growth curves at 27° C under high illumination are shown over a period of 20 days.

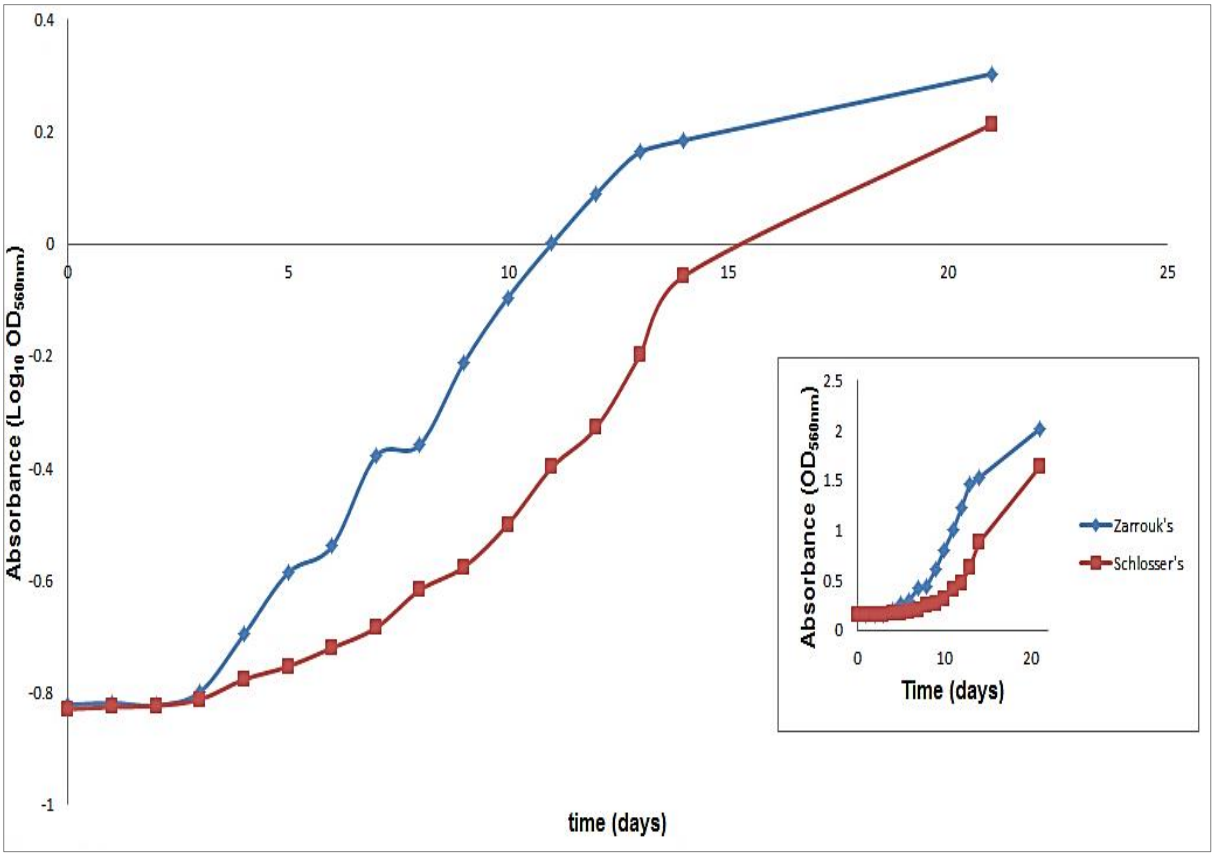

Figure 5.6: The growth kinetics of *Arthrospira* in Zarrouk's medium and in Schlösser's medium over a period of 20 days at 27° C and a luminance of 228 cd.m^{-2}. *Arthrospira* cultures were grown in 1 litre conical flasks. The rate of growth is shown as $\log_{10}$ OD_{560nm} absorbance and the inset shows growth kinetics as absorbance OD_{560nm} over time.

Figure 5.6 shows the growth kinetics of *Arthrospira* in Zarrouk's and Schlösser's media. Growth in Zarrouk's medium was more rapid compared to Schlösser's medium with earlier log phase observed for *Arthrospira* in Zarrouk's medium compared to Schlösser's medium. *Arthrospira* growth in Zarrouk's medium was more than in Schlösser's medium. The doubling time for *Arthrospira* in Zarrouk's medium was approximately 3.04 days compared

to the doubling time of Arthrospira in Schlösser's medium which was approximately 5.66 days. The standard deviations were negligible.

Arthrospira cultured in Zarrouk's medium was harvested daily and dried. The absorbance measurements of *Arthrospira* in Zarrouk's medium were plotted against the dry weight. A correlation of absorbance against dry weight of *Arthrospira* in Zarrouk's medium is shown in figure 5.7.

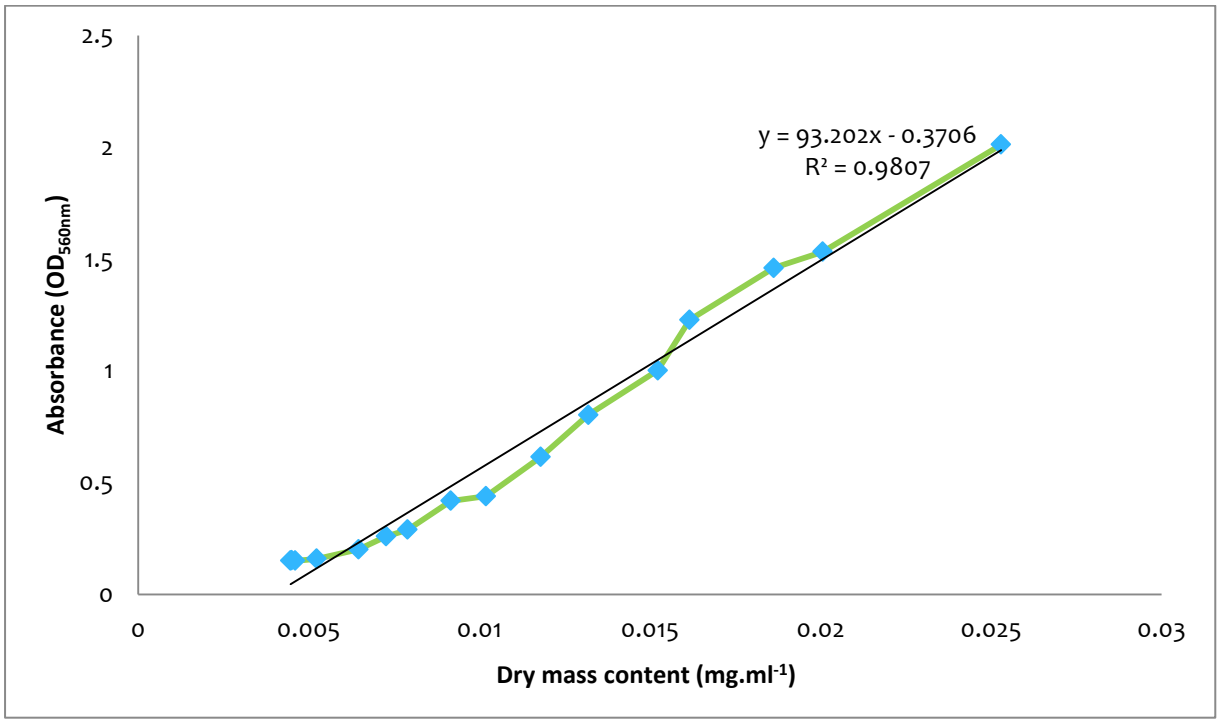

Figure 5.7: The absorbance measurements of growth in Zarrouk's medium was plotted against the dry weight concentration of *Arthrospira* in Zarrouk's medium. *Arthrospira* was cultured performed at 27° C under a luminance of 228 cd.m^{-2}.

Arthrospira cultures are mostly grown in either of two media, Zarrouk's or Schlösser's (Fu *et al.*, 2009; Celekli and Yavuzatmaca, 2009). Schlösser's medium is more complex to make (Celekli and Yavuzatmaca, 2009) compared to Zarrouk's medium (Fu *et al.*, 2009). Wu *et al.*, (2011) observed that the maximal growth rate for cyanobacteria occurs at temperatures around 28° C. From these results and considering the complexity of Schlösser's medium, further studies using *Arthrospira* were conducted using *Arthrospira* grown in Zarrouk's medium. Figure 5.7 shows the dry weight concentration of *Arthrospira* in Zarrouk's medium against absorbance measurements. From figure 5.7, an estimation of the concentration of the

Arthrospira cells in the medium can be done by measuring the absorbance. The R^2 value of 0.9807 shows that the estimated trendline corresponds closely to the actual data points (Walkenbach, 2007).

When the *Arthrospira* cultures in Zarrouk's medium were in their log growth phase, they were used as biocathodes in MFCs. MFCs were set up under conditions of low light illumination, high light illumination and no light illumination as shown in figures 5.8 and 5.9 respectively. After the successful use of ACF as electrode material without modification (figure 5.1), bare ACF had a peak power density of 85.4 (± 1.50) $mW.m^{-2}$, which was about 17 times better than bare carbon paper which had a peak power density of 5.16 (± 1.17) $mW.m^{-2}$. Further experiments were conducted using bare ACF as the electrode catalysts.

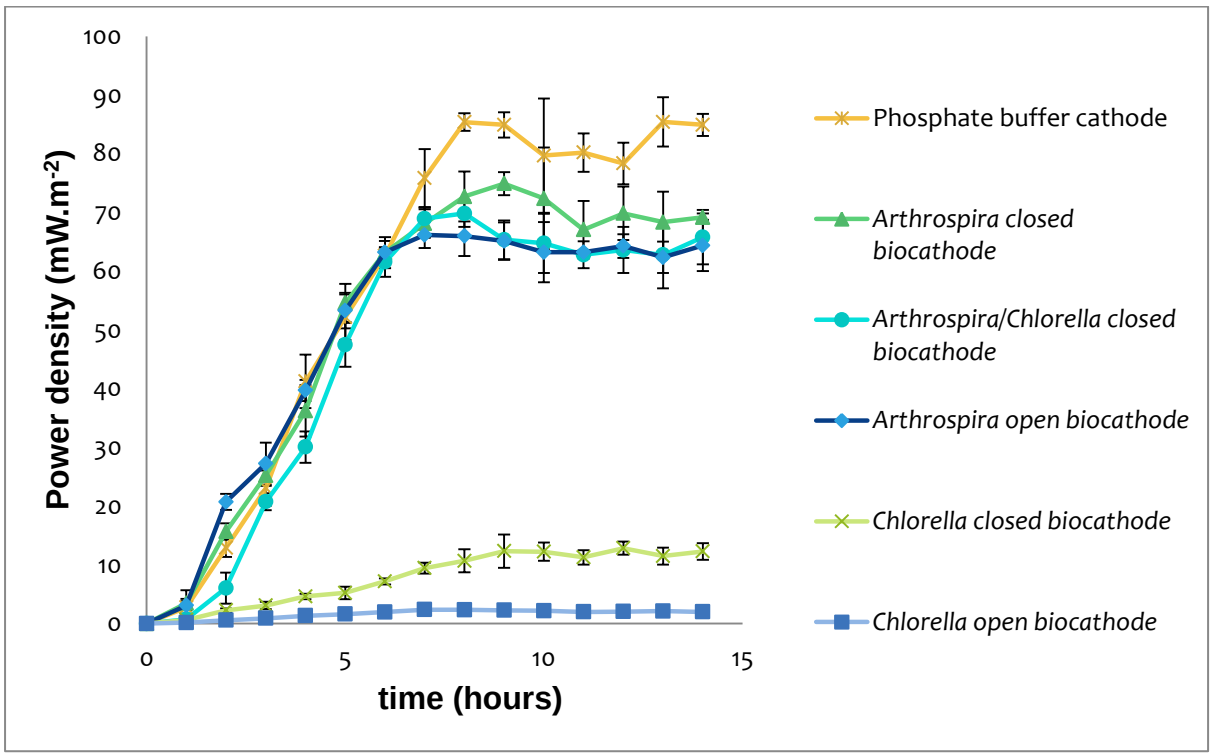

Figure 5.8: A comparison of algae based biocathodes to phosphate buffer in the cathode chamber in an MFC study at 35° C with a luminance (the measure of luminous intensity from a source with a measurable surface area) of 83 $cd.m^{-2}$. RCM medium was used as the anode feedstock and *E. cloacae* was the biocatalyst in the anode under anaerobic conditions. Bare ACF with a calculated exposed surface area of 8 cm^2 was used as the anode and cathode electrode catalysts. For some of the MFCs the cathode chamber was sealed like the anode chamber (closed) and for some of the MFCs the cathode chamber was not sealed (open) as indicated.

Table 5-3: The peak power densities that were observed for each different catholyte in the MFC biocathode studies in a CE room at 35° C, with a light luminance of 83 cd.m^{-2}.

Catholyte	Peak power density (mW.m^{-2})
Phosphate buffer	85.4 (± 4.20)
Arthrospira open cathode	66.2 (± 2.23) +#
Arthrospira sealed cathode	74.9 (± 1.96) +#
Chlorella open cathode	2.4 (± 0.30) + #
Chlorella closed cathode	12.3 (± 2.86) +#
Arthrospira/*Chlorella* closed cathode	69.8 (± 2.27) +

Statistical analysis was performed on the data using one-way ANOVA, and additional tests were done using Post-Hoc analysis, Tukey HSD test. All results were compared to the control, phosphate buffer catholyte and if $p < 0.01$, the sign + was placed next to the result. Algal-based catholytes were further compared to the mixed algae catholyte and when $p < 0.01$ the sign # was placed next to the result, when $p > 0.1$ the sign # was placed next to the results.

Figure 5.8 and table 5.3 shows that at 35° C, with a luminance of 83 cd.m^{-2}, power density is lower for the algal based biocathodes compared to phosphate buffer with a peak power density of 85.4 (± 4.20) mW.m^{-2}. The peak power density of the *Arthrospira* closed biocathode was 74.9 (± 1.96) mW.m^{-2} which is 10.5 mW.m^{-2} lower than for phosphate buffer. A mixture of *Chlorella* and *Arthrospira* in the biocathode, for a closed biocathode, gave a peak power density of 69.8 (± 2.27) mW.m^{-2}. The power density in the mixed algal-catholyte was lower than that for an *Arthrospira* based biocathode (closed), and higher than that for the Arthrospira based biocathode (open). However, the differences were not statistically significant as the p value for the former comparison was 0.44 and the latter was 0.16. The low power density observed for *Chlorella* biocathode compared to *Arthrospira* biocathode can be accounted for by the poor growth kinetics that were recorded for *Chlorella*, possibly due to the poor adaptation of *Chlorella* to the growth conditions and the BBM prepared. For

Chlorella open biocathode the peak power density was 2.4 (± 0.30) $mW.m^{-2}$ compared to the closed biocathode which had a peak power density of 12.3 (± 2.86) $mW.m^{-2}$.

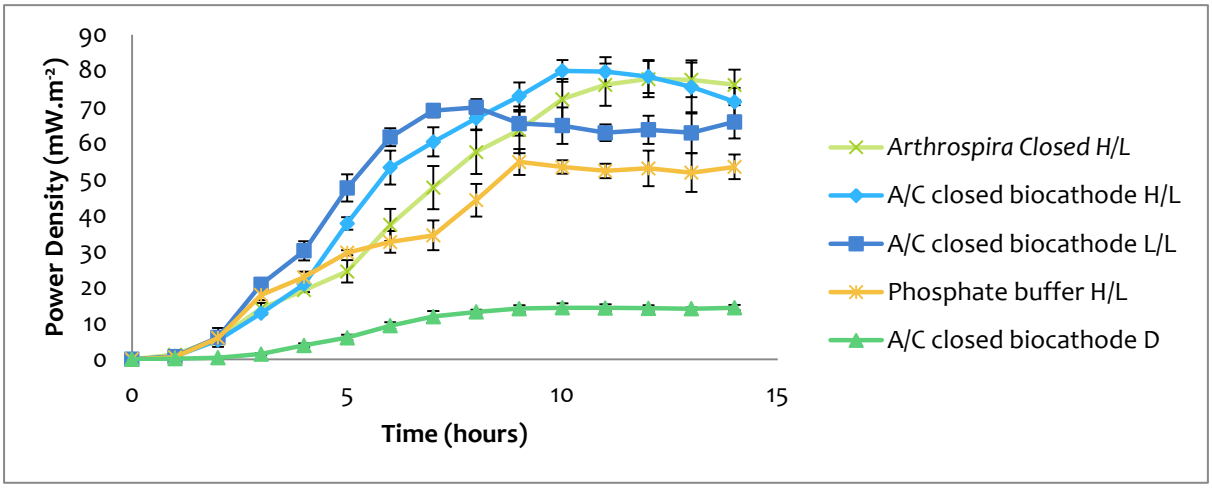

Figure 5.9: A comparison of algae based biocathodes under dark (D), low luminance (L/L) and high luminance (H/L) concentrations compared to phosphate buffer in the cathode under high light conditions at 27° C. A/C is a mixed consortium of *Chlorella* and *Arthrospira*. RCM medium was used as the feedstock and *E. cloacae* under anaerobic conditions was used as the biocatalyst. All biocathodes were sealed.

Table 5-4: The peak power densities that were observed for each different catholyte in the MFC biocathode studies in a CE room at 27° C, with a light luminance of 228 $cd.m^{-2}$.

Catholyte	Peak power density ($mW.m^{-2}$)
Phosphate buffer (H/L)	54.7 (± 3.58)
Arthrospira closed (H/L)	77.6 (± 5.02) +
Arthrospira/Chlorella closed (H/L)	80.0 (± 3.03) +#
Arthrospira/Chlorella closed (L/L)	69.8 (± 2.27) +#
Arthrospira/Chlorella closed (D)	14.3 (± 1.22) +#

Statistical analysis was performed on the data using one-way ANOVA, and additional tests were done using Post-Hoc analysis, Tukey HSD test. All results were compared to the control, phosphate buffer catholyte and if $p < 0.01$, the sign + was placed next to the result. The mixed algal-based catholytes were further compared to the *Arthrospira* catholyte and when $p < 0.01$ the sign # was placed next to the result, when $p > 0.1$ the sign # was placed next to the results.

Figure 5.9 and table 5.4, shows MFC runs at 27° C with a luminance of 228 $cd.m^{-2}$ for high luminance (H/L) conditions. Under these high light illumination conditions, phosphate buffer

media in the cathode gave the lowest peak power density. The peak power density was 54.7 (± 3.58) $mW.m^{-2}$. Unlike for phosphate buffer in the cathode, a decrease in temperature with a corresponding increase in luminance resulted in an increase in power density for the algal based biocathodes. For the MFC with mixed biocathode with *Chlorella* and *Arthrospira* an increase in luminance at 27° C from the low luminance at 35° C also resulted in an increase in the peak power density, from 69.8 (± 2.27) $mW.m^{-2}$ to 80.0 (± 3.03) $mW.m^{-2}$ which is about 4 (± 3.0) % increase in peak power density. Post Hoc test of the mixed algal-based catholyte at different light luminance, gave a p value of 0.023, which shows that the results were significantly different from each other. Under dark conditions at 27° C, the peak power density for the MFC with mixed biocathode that had both *Chlorella* and *Arthrospira* was low at 14.3 (± 1.22) $mW.m^{-2}$. Figures 5.8 and 5.9 show the importance of light intensity in algal biocathode performance compared to temperature. Temperature has been known to affect power density due to the performance of the anode biocatalyst at optimum temperatures which increase fermentation and hydrolysis and hence electron release (Edwards *et al*., 2012; Behera *et al.,* 2010). However with dissolved oxygen and the ORR being known limiting factors in power densities (Liu *et al*., 2010; Huang *et al*., 2011; Uria *et al*., 2011), an increase in luminance increases the rate of photosynthesis in algae which in turn increases the amount of dissolved oxygen in the cathode (Gonzalez del Campo *et al*., 2013; Juang et al., 2012) resulting in more oxygen for the ORR which increases the power density (Logan, 2008). Wu *et al*. (2014) saw an increase in the power density output from 60 $mW.m^{-2}$ to 120 $mW.m^{-2}$ when the luminance was doubled from 477 $cd.m^{-2}$ to 955 $cd.m^{-2}$, using *Desmodesmus spp*. algae as the biocathode. An increase in the illumination directly affects the performance of the biocathode, making it a photo-dependent MFC. Microalgae in the cathode also have been shown to decrease the over-potential of the ORR, which in turn increases the efficiency of the cathodic reaction and therefore increases the performance of the MFC (Wu *et al*., 2014). With adapting the use of algal-based biocathodes, the need for aeration is minimised therefore overally minimising the cost of the MFC (Gonzalez del Campo *et al.,* 2013). The algae also can act as bio-electron acceptors, therefore aiding in the consumption of electrons, creating an electron sink, which in turn improves the drive, increasing the power density (Gonzalez del Campo *et al*., 2013). Fu *et al.* (2009), describes how an increase in the *Arthrospira* biomass area density on the electrode resulted in an increase in power density.

This could be a result of direct electron transfer from the electrode to the *Arthrospira* as well as direct oxygen supply from the algae to the electrode catalyst.

Figure 5.10 represents the *Arthrospira* biomass attachment to the cathode electrode in an MFC at 35° C and at 27° C. The figure shows how for an MFC study the algal cells aggregate on the electrode.

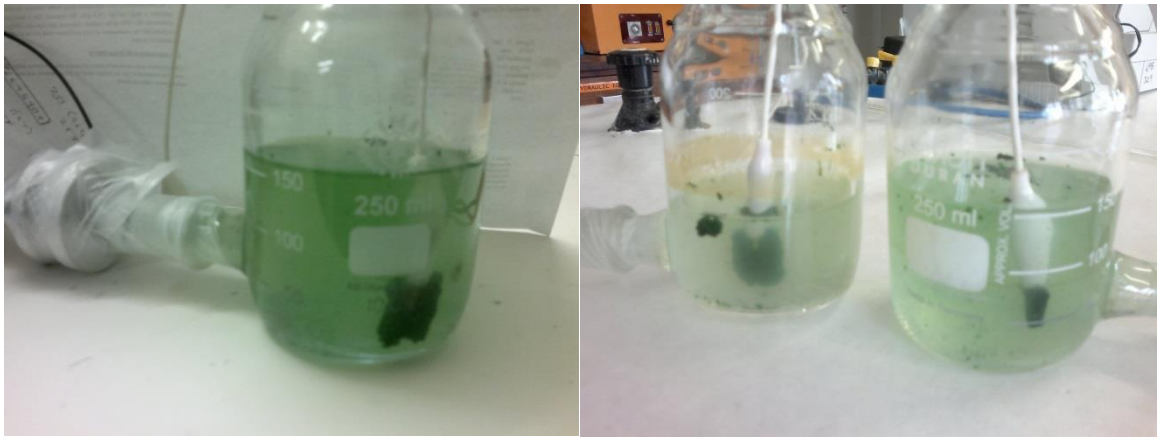

Figure 5.10: MFC biocathodes showing biomass densely attached to the electrode surface after a 14 hour MFC run at 35° C (left image) and at 27° C (right image).

Figure 5.10 shows formation of algal biomass on the electrodes. Fu *et al.*, (2009) showed how an increase in *Arthrospira* biomass on the electrode resulted in a direct increase in current generation and power density. This would account for the higher power density when light illumination is greater, as the biomass is attached to the electrodes and higher rates of photosynthesis would have resulted in increased oxygen production in the medium and release to the electrode.

5.4 Conclusions

Activated carbon fibre can be used in place of carbon paper based electrodes in an MFC, and positive results have been demonstrated when carbon paper was substituted with carbon fibre. Even without modification of the carbon fibre electrode with MWCNTs and FePc, high power densities are still observed, and this reduces the material used and therefore total cost of operating an MFC which is beneficial in the long run. Recycling and reusing carbon paper electrodes is possible when a cleaning step is included after each MFC run. Although this does result in a slight lowering in power density, it does minimise the costs associated with electrode use when reuse is possible. Algae cultures in their log phase that were used in the biocathode showed a light dependence more than temperature dependence for optimal MFC performance. *Arthrospira* cultures had better growth rates under the experimental conditions compared to *Chlorella* cultures, and in turn use of *Arthrospira* cultures in the biocathode outperformed MFCs with *Chlorella* cultures used as the biocathode. Sealing or unsealing the biocathode to atmospheric conditions affects performance of the MFC, with the sealed biocathode performing better in some instances than the unsealed biocathode. The sealing of the biocathode could act in minimising external contamination of the algae therefore not limiting biocathode performance. The use of ACF also helped and enhanced biocathode performance through the clumping of algae in the electrode.

Chapter 6 : Overall operational and cost analysis

6.1 Introduction

In order to contextualise the research into the use of algae as feedstock in MFCs, it is necessary to consider cost in terms of energy and materials as key factors.

It is understood that the prices used for the cost analyses, are not market related but relate more to the materials used in this study. More favourable prices could be obtained through bulk purchasing.

With any technology the analysis of the cost is important. Minimising costs may affect the quality. A way to minimise the costs would aid in making the technology economically viable (Russel *et al.*, 1996). Cost effectiveness evaluates the cost of the technology against the outcomes and shows the results as cost effectiveness ratios (Russel *et al*, 1996). This allows one to choose certain trade-offs to minimise cost and not quality, therefore allowing decision makers to get important data for informed judgements (Russel *et al*, 1996).

MFC have a low power density output compared to other fuel cells (Kim *et al.,* 2011). Therefore, in order to make the technology viable, the costs have to be lower than other related technologies. This has been the main disadvantage of using platinum as an effective cathode as the total cost of platinum as an electrode accounts for about 50 % of the whole MFC (Kim *et al.,* 2011). Substitutions for platinum and possibly other reactor configurations will benefit MFC research (Martin et al., 2011). Low cost materials like carbon have been used in research and its modification has shown to be effective in improving reactor performance (Liang *et al*., 2011) as evident in our research. Furthermore, iron phthalocyanines and multi-walled carbon nanotubes serve as effective cathode modifiers in our study to replace platinum. Portability of the MFC where it can be moved close to the biomass or waste source would also offset costs (Das and Veziroglu, 2008).

Using the results from the experiments, the cost effectiveness ratios were calculated to show how each configuration performs from a financial point of view.

6.2 Cost of raw material used

6.2.1. Sonication

Sonication was performed using a Vibra cell sonicator for a period of 30 minutes. The frequency used for sonication was 20 kHz and the power output for 30 minutes was 20 W. Two litre samples were sonicated which contained 66 g of substrate. For MFC studies, 150 ml were used of the samples which contained 4.95 g dry weight of sample. For each MFC operation, the effective power used for sonication was 0.6 W. The power output and the frequency for sonication were obtained from the Vibra cell sonicator manual.

6.2.2 Autoclaving

Autoclaving was performed using an RAU 530 D autoclave with a power output of 2 kW per hour. Autoclaving was done for 15 minutes resulting in the use of 500 W of power. All the samples were autoclaved at once, giving 10 litres of autoclaved material each round. For an MFC operation 150 ml of substrate media was needed (4.95 g dry weight of sample), which meant that for each MFC operated, 2.66 W was used during autoclaving. The power output for the autoclave were obtained from the RAU 530 D manual.

6.2.3 *Arthrospira*

Arthrospira (Superfoods, Ceres certified, India) was used for the studies. As of 5 February 2014, 1 kg of *Arthrospira* (*Spirulina*) costs R 599.00. For the purpose of this study, the currency of South Africa, the Rand (R) is employed.

6.2.4 *Chlorella*

Chlorella (The Real Thing, Pharmaceutical grade, South Africa) was used for the studies. As of 5 February 2014, 100 g of *Chlorella* costs R 172.00.

6.2.5 Carbon paper

Carbon paper (Toray TGP-060) (Alfa Aesar GmbH & Co. KG) electrodes were used for the studies. As of 5 February 2014, 1 600 cm^2 of carbon paper costs R 1 650.00 excluding shipping from the suppliers used. For each MFC setup, 4 cm^2 are needed for each electrode, which translates to R 4.13 per each electrode per MFC study.

6.2.6 Activated carbon fibre

Activated Carbon Fibre (ACF) Non-Woven Fabrics (SO-EN CO., LTD) with a BET of 1000 ± 50 $m^2.g^{-1}$ was used. As of 5 February 2014 the cost of a square metre of ACF was R8.20. For an MFC operation 4 cm^2 are needed which equal to R 0.03 for each electrode.

6.2.7 MWCNT

MWCNTs (diameter = 110 nm – 170 nm, length = 5-9 nm; >90 % purity) (Sigma-Aldrich) were used. As of 5 February 2014, MWCNTs cost R 6000.00 per 100 g. For electrode modification, 1 mg is required which is equal to R 0.06.

6.2.8 FePc

Iron (II) phthalocyanines (FePc) (Dye content ~ 90 %) (Sigma-Aldrich) were used for the MFC studies. The cost as of 5 February 2014 for 10 g is R 1 431.00. For each MFC operation, for the cathode electrode, 1 mg is required. This gives a cost of R 0.14 per MFC operation.

6.3.2 Cost benefit analysis of experimental results

Table 6-1: Analysis of carbon paper studies versus activated carbon fibre for an MFC run over 14 hours at 35° C. Temperature of the room was not factored in as a cost. Monetary values were expressed using the South African currency, Rand (R) and cents (c).

Anode material	Cathode material	Cost of anode material used (in c)	Cost of cathode material used (in c)	Total cost of MFC electrode (in c)	Total power output (mW)	Total average energy (mW.h)	Total cost (c/mW.h)
BCP	BCP	413	413	826	33.51	2.39	24.69
CP (MWCNT)	CP (MWCNT: FePC)	419	433	852	1034	73.83	0.82
CP (MWCNT)	ACF	419	3	422	760	54.31	0.56
ACF	CP (MWCNT: FePc)	3	433	436	874	62.43	0.50
ACF	ACF	3	3	6	679	48.50	0.01
ACF (MWCNT)	ACF	9	3	12	810	57.85	0.01
ACF	ACF (MWCNT: FePc)	3	23	26	718	51.27	0.04
ACF (MWCNT)	ACF (MWCNT: FePc)	9	23	32	1 106	79.07	0.03

The cost effectiveness ratio is shown in table 6.1, as a calculation of the cost required to produce a mW of power per hour. The results show that higher power density was achieved

from modified carbon paper when compared to ACF. When factoring in the cost, ACF is a comparable substitute for carbon paper which not only greatly affects performance but also substantially minimises costs.

Table 6-2: Analysis of the estimated external total power input vs estimated total power output required for the operation of an MFC at 35° C for 120 hours. Estimates were calculated from the power input from the autoclave and sonication according to the specifications listed in the respective manuals.

Substrate	Estimated Power Input (W) for 14 hr run	Estimated power output (W) for 14 hr run	Gross power output (W) after 14 hr run	Estimated power input (W) for 120 hr run	Estimated power output (W) for 120 hr run	Gross power output (W) after 120 hr
RCM	1.33	1.04	-0.29	1.33	6.48	5.15
Chlorella	0	0.04	0.04	N/A	N/A	N/A
Chlorella (a)	1.33	0.19	-1.14	N/A	N/A	N/A
Chlorella (a & s)	1.93	0.43	-1.50	N/A	N/A	N/A
Arthrospira	0	0.54	0.54	N/A	N/A	N/A
Arthrospira (a)	1.33	0.53	-0.80	1.33	6.77	5.44
Arthrospira (a & s)	1.93	0.64	-1.29	1.93	6.16	4.23
EBRU	0	0.23	0.23	N/A	N/A	N/A
EBRU (a)	1.33	0.23	-1.10	1.33	2.71	1.38
EBRU (a & s)	1.93	0.77	1.16	1.93	8.01	6.08

From the feedstock, *a* denotes autoclaved and *s* denotes sonicated.

Table 6.2 shows that when more upstream processing is done for a 14 hour MFC study, the gross power input is likely to exceed that of the gross power output. The extension of the MFC operation from 14 hours to 120 hours makes the gross power input insignificant

compared to the gross power output. This makes the case for extended operations in this case being more economical and energy positive. The advantage of using algae recovered from a wastewater treatment facility as feedstock for an MFC, such as is in the case of the EBRU consortium, is that it is sustainable and very cheap. Therefore the input cost of the feedstock for an MFC is considerably reduced. However the EBRU consortium medium requires more upstream processing compared to *Arthrospira* medium, which after only a single autoclaving step results is about four times the gross output of autoclaved EBRU consortium medium. This analysis shows that *Arthrospira* is a viable feedstock and efficient RCM medium substitute in an MFC. Nevertheless, there needs to be further consideration when accounting for the cost of using algal feedstock in the operation of MFCs, since harvesting algae incurs considerable capital and operational costs. *Arthrospira* is possibly the most economically harvested alga as it requires, at maximum, a coarse mesh (50 µm) for harvesting (Celekli and Yavuzatmaca, 2009).

Table 6-3: Cost-benefit analysis of the different feedstock use in an MFC run of 14 hours

Substrate	Total cost of MFC run (in c)	Total average power output (14 hours) (mW)	Total cost (14 hour run) (c.mW^{-1})	Total average power output (14 hours) (mW-h)	Total cost (14 hours) (c.mW-h^{-1})
RCM	3006	1 034	3	73.9	41
Chlorella	2173	45	48	3.21	677
Chlorella (a)	2173	188	12	13.4	162
Chlorella (a & s)	2173	431	5	30.8	71
Arthrospira	2149	545	4	38.9	55
Arthrospira (a)	2149	534	4	38.1	56
Arthrospira (a & s)	2149	636	3	45.4	47
EBRU	2026	229	9	16.4	124
EBRU (a)	2026	233	9	16.6	122
EBRU (a & s)	2026	777	3	55.5	37

From the feedstock, *a* denotes autoclaved and *s* denotes sonicated.

Table 6.3 represents the economic cost of MFC runs for a 14 hour run. The input required was converted to monetary terms using current average rates as of February 2014. The use of untreated *Chlorella* as feedstock in an MFC is unfeasible as it results in a low power density output, which translates into higher costs for the power output of R 6.77 per mW.h. The use of *Arthrospira* untreated, autoclaved and sonicated and autoclaved media as feedstock for the

14 hour run results in low cost for the power output, but slightly higher than that of RCM medium with the former between R 0.47 and R 0.56 per mW.h and the latter at R 0.41 per mW.h. The EBRU consortium media that are not sonicated (autoclaved and untreated) results in costs in excess of R 1.00 which is more than double the cost per mW.h of *Arthrospira* sonicated and autoclaved, autoclaved and untreated media and RCM medium. Sonication of the EBRU consortium medium results in a higher power output which translates into a lower output cost of R 0.37 which is the lowest of all the feedstock tested.

Table 6-4: Cost-benefit analysis of the different feedstock use in an MFC for a 120 hour run

Substrate	Total cost of MFC run (in c)	Total average power output (120 hours) (mW)	Total cost (120 hour run) ($c.mW^{-1}$)	Total average power output (120 hours) (mW.h)	Total cost (120 hours) ($c.mW.h^{-1}$)
RCM	3006	6 481	0.5	54.0	56
Arthrospira (a)	2149	6 769	0.3	56.4	38
Arthrospira (a & s)	2149	6 154	0.3	51.3	42
EBRU (a)	2026	2 711	0.7	22.6	90
EBRU (a & s)	2026	8 012	0.3	66.8	30

For the feedstock, *a* denotes autoclaved and *s* denotes sonicated.

Table 12 shows that longer operation times for the MFC, with greater total power density outputs, lowers the cost per unit of power produced. This reduces the overall cost of the MFC operation. For the longer run times, the algal-based media derived from *Arthrospira* and the EBRU consortium (sonicated and autoclaved) are more efficient and cost effective compared to RCM.

Current prepaid electricity costs in Grahamstown, South Africa, as of 30 March 2014, are R 1.42 per kW-h. While the current costs of the MFC are not feasible, the concomitant biodegradation of waste in an MFC is an attractive benefit supporting its larger scale application. Nevertheless, comparison of costs here serves as useful benchmark for further studies in the use of algae as feedstock in MFCs.

Chapter 7 : Overall conclusions and future studies

7.1 Conclusions

Chapter 3 examined the potential use of selected microalgae as feedstocks in the anodic chamber of a microbial fuel cells (MFC). In this study *Chlorella*, *Arthrospira* and a mixed algae consortium from the high rate algal ponds from an integrated algal pond system (EBRU consortium) were studied utilising *Enterobacter cloacae* as a biocatalyst in an MFC. The aim of the study was to examine sonication and heat for treating the algal based feedstock for cultivating *E. cloacae* in an MFC and to observe how the treatments would affect utilisation of the algal feedstock compared to a control using standard media preparation for reinforced clostridial media (RCM) as feedstock.

Heat treatment through autoclaving and treatment through sonication had a disruptive effect on the integrity of the algal cells. Autoclaving resulted in a loss of pigment colour for all the algal based feedstock. For *Chlorella*, the autoclaving step including a loss of pigment colour and also resulted in larger and less dense clumps compared to untreated *Chlorella*. For *Arthrospira*, autoclaving resulted in fragmentation of the *Arthrospira* trichomes, into smaller particulates that were distributed evenly in the medium compared to the large filamentous spiral cells of the untreated *Arthrospira*. For the mixed EBRU consortium (comprising of microalgae including *Chlorella*, *Pediastrum*, *Scenedesmus* and *Micractinium*), autoclaving had a similar result to the autoclaved *Chlorella* medium. For *Chlorella, Arthrospira* and the mixed consortium, sonication proved to be a more effective pre-treatment method, resulting in disintegration of the cells and visible cell disruption. A carbohydrate and protein assay of the pre-treated media compared to untreated media showed that the process of autoclaving resulted in an increase in the carbohydrate and protein concentration in the medium. Sonicating the media resulted in further release of carbohydrates and proteins to the media.

Growth kinetics of *E. cloacae* at 35° C under anaerobic conditions showed that the *E. cloacae* was able to proliferate in all the media studied. Growth was most favourable in RCM, which had the highest absorbance at peak growth and was least favourable in the autoclaved *Chlorella* feedstock and the autoclaved EBRU consortium feedstock. For the autoclaved and sonicated *Arthrospira* feedstock, as well as the autoclaved and sonicated EBRU consortium

feedstock, the peak absorbances were similar. Unlike the other sonicated and autoclaved algae-based media, the peak absorbance measurements in the *Chlorella* feedstock was low, being almost half of the autoclaved and sonicated mixed consortium and autoclaved and sonicated *Arthrospira* media. This result showed that the complexity of the different feedstock and the released nutrients result in different effects on *E. cloacae* activity for the study, with *Chlorella* feedstock utilisation being low also possibly due to the different bioavailability of the released nutrients. The doubling time for *E. cloacae* was shortest in RCM medium. As this medium had been set up specifically for microbial growth this was expected. However, doubling time was longest in the EBRU mixed consortium media (both autoclaved and sonicated and autoclaved) as well as in the autoclaved *Arthrospira* medium. Of all the algal-based media, growth was lowest in the autoclaved *Chlorella* medium. This result showed that although growth may differ in the different algal-based media, the adaptation of *E. cloacae* in the media over a period of time was also different, with *E. cloacae* adapting faster to the autoclaved *Chlorella* media compared to the other algal based media.

MFC studies using the different feedstocks, showed greatest power density from the RCM medium and lowest power density from untreated *Chlorella* medium. The autoclaved and sonicated EBRU consortium had the greatest power density of all the algal-based media. For the autoclaved and sonicated algal-based media, sonicated and autoclaved *Chlorella* medium had the lowest power density compared to the sonicated and autoclaved EBRU mixed consortium medium and sonicated and autoclaved *Arthrospira* medium. *Arthrospira* autoclaved and untreated *Arthrospira* media however, outperformed the other algal based media with the same pre-treatment. These results showed that, the power density from autoclaved or untreated *Arthrospira* media were favourably comparable to algal-based media with more pre-treatment steps and outperformed the other algal-based media with the same treatment steps.

Chapter 4 examined the internal factors that affected the MFC performance such as pH of the anode media, temperature of the anode media and the performance of the proton exchange membrane. The aim of the study was to monitor the change in pH and temperature of the

anodic microenvironment during MFC operation and how the change affects MFC performance. The fouling of the PEM after MFC operation was also examined.

From the study of the pH microenvironment using RCM medium, the EBRU mixed consortium media and the *Arthrospira* media was used as feedstock in MFCs and anaerobic growth reactors. It was shown that in the first 14- 24 hours, the pH of the anodic microenvironment and the anaerobic growth reactors tended to decline to slightly acidic pH. After 24 hours, in MFCs for all the media studied the pH started to increase. The fall in pH for the MFC studies coincided with an increase in power density and the increase in pH after 24 hours coincided with a levelling off as well as a subsequent decrease in power density. The peak power density was observed in the feedstock buffered at pH 7. However, over a 120 hour MFC operation, the total power output, was the most at pH 5. Total power output at pH 6 and pH 4 was more than the total power output at pH 7. These results confirmed that *E. cloacae* in an MFC performs under slightly acidic pH and low performance at alkaline pH. The low pH supports protons and this appears to have a greater impact on power density in the longer term than any negative impact of *E. cloacae* growth at sub optimal conditions. An increase in pH results in lower proton availability for the system. The low availability of protons results in a fall for the forward drive for proton transfer through the PEM lowering power density.

In chapter 5 the use of alternative carbon based electrodes and the use of algal-based biocathodes were examined. The aim of the study was to compare the use of carbon paper to activated carbon fibre (ACF) in an MFC at 35° C and how the different electrode material affects performance. The other aim was to study the use of algal based biocathodes and how they affect performance under different temperature and light intensity conditions.

ACF was successfully used in an MFC, with modification of the ACF with MWCNTs and FePc resulting in the ACF having similar performance to carbon paper with the same modifications. The peak power density for the modified ACF was 126.2 $mW.m^{-2}$ and the peak power density for the modified carbon paper was 124.7 $mW.m^{-2}$. Unmodified ACF outperformed unmodified carbon paper with a peak power density of 85.4 $mW.m^{-2}$ for the bare CF compared to a peak power density of 5.2 $mW.m^{-2}$ for the bare carbon paper. These

results showed that ACF could successfully be used as a substitute for carbon paper in an MFC. The use of ACF in an MFC is substantially cheaper than the use of carbon paper.

The use of *Arthrospira* and *Chlorella* as biocathodes showed that the main limiting factor for performance of the biocathode was light intensity. An increase in light intensity from 83 $cd.m^{-2}$ to 227 $cd.m^{-2}$ resulted in an increase in power density for the algal based biocathodes, although the temperature was decreased.

Microalgae were successfully used as feedstock in MFCs albeit to varying degrees. Pre-treatment of the microalgae using sonication and autoclaving aided in nutrient release from the cells. *E. cloacae* growth kinetics and MFC performance were favourable in *Arthrospira* and the EBRU consortium media and were least favourable in *Chlorella* medium after pre-treatment.

After the successful use of microalgae in the MFC, the change in pH and temperature of the anodic microenvironment during an MFC operation was examined. It was observed that MFC performance was peak when the feedstock was under acidic conditions of between 4.5 and 6.5. Further studies into the role of pH, by buffering the feedstock, showed that peak *E. cloacae* performance in terms of growth kinetics were at neutral pH. Over a short MFC operation (14 hours), the peak performance of the MFC was also at pH 7. However, over longer periods, MFCs with feedstock under acidic conditions (pH 4, 5 and 6 respectively) outperformed the neutral and alkaline feedstock (pH 7, 8 and 9). Nutrient utilisation was also specific to the pH of the anode microenvironment, showing that different metabolism by the biocatalyst occurred at the different pH.

ACF was successfully used as electrode material in an MFC with and without modification using MWCNTs and FePc. Results were comparable to carbon paper when both ACF and carbon paper were modified with MWCNTs and FePc. However, ACF outperformed carbon paper when no modification was applied. Use of live algal cultures as biocathodes was shown to be more dependent on light intensity more than temperature.

7.2 Future studies

Algal pre-treatment demonstrated an improvement in the utilisation of algal-based media by *E. cloacae* for growth and during MFC operations. Sonication and heat treatment through autoclaving were studied. Further pre-treatment studies for algal cell disruption to improve nutrient release and minimise overall cost and energy input in treatment would be necessary.

During MFC anodic microenvironment studies, it was observed that the pH changes with progression of MFC operation. The pH greatly influenced the power density output. Further pH studies over longer periods which are not controlled would be necessary in order to get insight into the pH regulation of the reactor over a prolonged period. Controlled pH studies showed an improvement in MFC performance. However, the effect of pH over a prolonged period versus short periods on the fouling of the PEM are not known, and investigations of this would be necessary.

The use of ACF was successfully implemented in an MFC and power density generations were more favourable than for carbon paper. ACF is a cheaper alternative to carbon paper and is not as brittle as carbon paper. Further studies on the effective modification of ACF would be required. Other studies such as microbial activity on the ACF should be performed using SEM studies.

Bio-cathode studies gave insight into the potential use of algae as bio-cathodes. The light intensity was shown to affect the power density. Further studies would be required on the use of algae-based biocathodes, including expanding the range of algae used for the biocathode studies. Further investigations into the effect of irradiance intensity and spectral quality on performance of algae-based biocathodes would advance the understanding of this field of study.

Chapter 8 : References

Barghbani R., Rezaei K. and Javanshir A. (2012), Investigating the effects of several parameters on the growth of *Chlorella vulgaris* using Taguchi's experimental approach, International Journal of Biotechnology for Wellness Industries, Volume 1, pp 128-133

Barsanti L., and Gualtieri P., (2005), Algae: Anatomy, Biochemistry, and Biotechnology, General overview, 2nd edition, Barsanti L. and Gualtieri P., pp 1-4, CRC Press, Fl, USA

Bates R.G. and Darst R.A. (1985), Definition of pH scales, standard reference values, measurement of pH and related terminology, Pure and Applied Chemistry, Volume 57, Issue 3, pp 531-542

Becker E.W., (1995), Algae production systems; Culture media Microalgae: Biotechnology and Microbiology, illustrated, pp 5-41, Cambridge University Press, Great Britain

Behera M., Jana P.S., More T.T. and Ghangrekar M.M., (2010), Rice mill wastewater treatment in microbial fuel cells fabricated using proton exchange membrane and earthen pot at different pH, Bioelectrochemistry, Volume 79, Issue 2, pp 228-233

Blokker P., Schouten S., van de Ende H., de Leeuw J.W., Hatcher P.G. and Damste J.S.S., (1998), Chemical structure of algaenans from the fresh water algae *Tetraedron minimum*, *Scenedesmus communis* and *Pediastrum boryanum*, Organic Chemistry, Volume 29, issues 5-7, pp 1453 - 1468

Bradford M.M., (1976), A rapid and sensitive method for the quantitation of microgram quantities of protein utilizing the principle of protein-dye binding, Analytical Biochemistry, Volume 72, Issues 1–2, pp 248–254

Catal T., Cysneiros D., O'Flaherty V., and Leech D., (2011), Electricity generation in single-chamber microbial fuel cells using a carbon source sampled from anaerobic reactors utilizing grass silage, Bioresource Technology, Volume 102, Issue 1, pp 404-410

Celekli A., and Yavuzatmaca M., (2009), Predictive modelling of biomass production by *Spirulina platensis* as function of nitrate and NaCl concentrations, Bioresource Technology, volume 100, issue 5, pp 1847-1851

Chae K., Choi M., Ajayi F.F., Park W., Chang I.S. and Kim I.S. (2008), Mass transport through a proton exchange membrane (Nafion) in microbial fuel cells, Energy and Fuels, Volume 22, pp 169 - 176

Cheng Y.L., Juang Y.C., Liao G.Y., Tsai P.W., Ho S.H., Yeta K.L., Chen C.Y., Chang J.S., Liu J.C., Chen W.M. and Lee D.J. (2011), Harvesting of *Scenedesmus obliquus* FSP-3 using dispersed ozone flotation, Bioresource Technology, Volume 102, Issue 1, pp 82-87

Choi M, Chae K, Ajayi F.F., Kim K., Yu H., Kim C and Kim I.S., (2011), Effects of biofouling on ion transport through the cation exchange membranes and microbial fuel cell performance, Bioresource Technology, Volume 102, Issue 1, pp 298-303

Christens L. and Sim R. (2011), Production and harvesting of microalgae for wastewater treatment, biofuels and bioproducts, Biotechnology Advances, Volume 29, Issue 6, pp 686 – 702

Cooney S., O'Brien S., Iversen C. and Fanning S., (2014), Other pathogenic Enterobacteriaceae – Enterobacter and other genera, Encyclopedia of food safety, Motarjemi Y., Moy G. and Todd E., (Ed.), pp 433-442, Academic Press, USA

Das D. and Veziroglu T.N. (2008), Advances in biological hydrogen production processes, International Journal of Hydrogen Energy, Volume 33 Issue 21, pp 6046 – 6057

Deng Q., Li X., Zuo J., Ling A. and Logan B.E., (2010), Power generation using an activated carbon fibre felt cathode in an upflow microbial fuel cell, Journal of Power Sources, Volume 195, Issue 4, pp 1130 - 1135

Ditzig J., Liu H., and Logan B.E., (2007), Production of hydrogen from domestic wastewater using a bioelectrochemically assisted microbial reactor (BEAMR), International Journal of Hydrogen Energy, Volume 32, Issue 13, pp 2296-2304

Du Z., Li H., and Gu T., (2007), A state of the art review on microbial fuel cells: A promising technology for wastewater treatment and bioenergy, Biotechnology Advances, Volume 25, Issue 5, pp 464 – 482

Edwards S.L., Fogel R., Mtambanengwe K., Togo C., Laubscher R. and Limson J. (2012), Metallophtalocyanine/carbon nanotubes hybrids: extending applications to microbial fuel cells, Journal of Porphyrins and Phthalocyanines, Volume 16, Issue 07/08, pp 917 - 926

Farret F.A., and Simoes M.G., (2006), Integration of alternative sources, Alternative sources of energy, illustrated, In Farret F.A and Simoes M.G., pp 4-8, John Wiley and sons, USA

FengY., Yang Q., Wang X. and Logan B.E., (2010), Treatment of carbon fibre brush anodes for improving power generation in air–cathode microbial fuel cells, Journal of Power Sources, Volume 175 Issue 7, pp 1841-1844

Fu C.C., Su C.H., Hung T. C., Hsieh C.H., Suryani D. and Wu W.T., (2009), Effects of biomass weight and light intensity on the performance of photosynthetic microbial fuel cells with *Spirulina platensis*, Bioresource Technology, Volume 100, Issue 18, pp 4183 - 4186

Gershwin M.E., and Belay A., (2012), *Spirulina* in Human Nutrition and Health, Environmental aspects of *Spirulina* production, Belay A., pp 21, CRC Press, Fl., USA

Gil G., Chang I., Kim B.H., Kim M., Jang J., Park H.S., and Kim H.J., (2003), Operational parameters affecting the performance of a mediator-less microbial fuel cell, Biosensors and Bioelectronics, Volume 18, Issue 4, pp 327-334

Girguis P.R., Nielsen M.E., and Figueroa I., (2010), Harnessing energy from marine productivity using bioelectrochemical systems, Current Opinion in Biotechnology, Volume 21, Issue 3, pp 252 – 258

Gonzalez del Campo A., Canizares P., Rodrigo M.A., Fernandez F.J. and Lobato J., (2013), Microbial fuel cells with an algae-assisted cathode, A preliminary assessment, Journal of Power Sources, Volume 242, pp 638 -645

Gouveia L., (2011), in Microalgae as a Feedstock for biofuels, Microalgae and Biofuels production, Gouveia L., pp 2-19, New York: Springer Heidelberg Dordrecht London

Hallenbeck P.C., and Ghosh D., (2009), Advances in fermentative hydrogen production: the way forward? Trends in Biotechnology, Volume 27, Issue 5, pp 287-297

Harewood K., and Wolff J.S., (1973), A rapid electrophoretic procedure for the detection of SDS-released oncorna-viral RNA using polyacrylamide-agarose gels, Analytical Biochemistry, Volume 55, Issue 2, pp 573-581

He G., Gu Y., He S., Schroder U., Chen S. and Hou H. (2011), Effect of fibre diameter on the behaviour of biofilm and anodic performance of fibre electrodes in microbial fuel cells, Bioresource Technology, Volume 102, Issue 22, pp 10763-10766

He Z. and Angenent L.T. (2006), Application of bacterial biocathodes in microbial fuel cells, Electroanalysis, Volume 18, Issue 19-2-, pp 2009 - 2015

Huang L., Regan J.M., and Quan X., (2011), Electron transfer mechanisms, new applications and performance of biocathode microbial fuel cells, Bioresource technology, Volume 102, Issue 1, pp 316-323

Juang D.F., Lee C.H. and Hsueh S.C. (2012), Comparison of electrogenic capabilities of microbial fuel cell with different light power on algae grown cathode, Bioresource Technology, Volume 123, pp 23 - 29

Khanna N., Katay S.M., Gilbert J.J., and Das D., (2011), Improvement of biohydrogen production by *Enterobacter cloacae* IIT-BT 08 under regulated pH, Journal of Biotechnology, Volume 152, Issue1-2, pp 9-15

Kiely P.D., Cusick R., Call D.F., Selembo P.A., Regan J.M., and Logan B.E., (2011a), Anode microbial communities produced by changing from microbial fuel cell to microbial electrolysis cell operation using two different wastewaters, Bioresource Technology, Volume 102, Issue 1, pp 388-394

Kiely P.D., Rader G., Regan J.M., and Logan B.E., (2011b), Long-term cathode performance and the microbial communities that develop in microbial fuel cells fed different fermentation end products, Bioresource Technology, Volume 102, Issue 1, pp 361-366

Kim C-J, Jung Y-H and Oh H-M., (2007), Factors indicating culture status during cultivation of *Spirulina* (*Arthrospira*) *platensis*, The Journal of Microbiology, Volume 45, Issue 2, pp122 - 127

Kim J.R., Cheng S., Oh S.E. and Logan B.E. (2007), Power generations using different cathode, anode and ultrafiltration membranes in microbial fuel cells, Environmental Science Technology, Volume 41, Issue 3, pp 1004 -1009

Kim S., Chae K.J., Cha M.J. and Verstracte W., (2008), Microbial fuel cells: Recent advances, bacterial communities and application beyond electricity generation, Environmental Engineering Resources, Volume 13, Issue 2, pp 51-65

Kim J.R., Kim J., Han S., Park K., Saratale G.D., and Oh S., (2011), Application of Co-naphthalocyanine (CoNPc) as alternative cathode catalyst and support structure for microbial fuel cells, Bioresource Technology, Volume 102, Issue 1, pp 342-347

Kumar N., and Das D., (2001), Continuous hydrogen production by immobilised *Enterobacter cloacae* IIT-BT 08 using lignocellulosic materials as solid matrices, International Journal of Hydrogen Energy, Volume 26, Issue 11, pp 1153 – 1163

Lee J.Y., Yoo C., Jun S.Y., Ahn C.Y. and Oh H.M., (2010), Comparison of several methods for effective lipid extraction from microalgae, Bioresource Technology, Volume 101, Issue 1, pp S75 – S77

Li F., Lin X.Q. and Cui H., (2002), Comparative studies on the electrogenerated chemiluminescent and amperometric behaviour of the $Ru(bpy)_3^{2+}$ system on a paraffin-impregnated graphite electrode and a glassy carbon electrode, Electroanalytical Chemistry, Volume 534, Issue 1, pp 91 - 98

Li W., Sheng G., Liu X., and Yu H., (2011), Recent advances in the separators for Microbial fuel cells, Bioresource Technology, Volume 102, Issue 1, pp 244 – 252

Liang P., Wang H., Xia X., Huang X., Mo Y., Cao X., and Fan M., (2011), Carbon nanotube powders as electrode modifiers to enhance the activity of anodic biofilm in microbial fuel cells, Biosensors and Bioelectronics, Volume 26, Issue 6, pp 3000-3004

Liu H., Cheng S. and Logan B.E. (2005), Power generation in fed-batch microbial fuel cell as a function of ionic strength, temperature and reactor configuration, Environmental Science Technology, Volume 39, Issue 14, pp 5488 - 5493

Liu X., Sun X., Huang Y., Sheng G., Zhou K., Zeng R.J., Dong F., Wang S., Xu A.,Tong Z., Yu H., (2010), Nano-structured manganese oxide as a cathodic catalyst for enhanced oxygen reduction in a microbial fuel cell fed with a synthetic wastewater, Water Resources, Volume 44, Issue 18, pp 5298-5305

Logan B.E., (2006), electricity producing bacterial communities in microbial fuel cells, trends in microbiology, Volume 14, Issue 12, pp 512-518

Logan B.E., (2008), in Microbial fuel cells, Introduction, in Logan B.E., pp 3-7, Wiley-Interscience, USA

Logan B.E., Hamelers B., Rozendal R., Schroder V., Keller J., Frequiag S., Aelteman P., Verstraete W. and Rabaey K., (2006), Microbial fuel cells: Methodolody and technology, Environmental Science Technology, Volume 40, Issue 17, pp 5181 -5192

Mahon C.R., Lehman D.C. and Manuselis G., (2011), Lab identification of significant isolate, 19 Enterobacteriaceae, Textbook of Diagnostic Microbiology, pp 441-451, Saunders Elsevier, USA

Martin E., Tartakovsky B., and Savadogo O., (2011), cathode materials evaluation in microbial fuel cells: a comparison of carbon, Mn_2O_3, Fe_2O_3 and platinum materials, Electrochemica Acta, Volume 58, pp 58-66

Mshoperi E., Fogel R. and Limson J., (2013), Application of carbon black and iron phthalocyanine composites in bioelectricity production at a brewery wastewater fed microbial fuel cell, Electrochimica Acta, http://dx.doi.org/10.1016/j.electacta.2013.11.016

Neba A. and Rose P.D. (2004), The independent high rate algal pond (I-HRAP) incorporating denitrification in tertiary wastewater treatment, Proceeding of the 2004 water institute of Southern Africa (WISA) Biennial conference, pp 1014-1018

Nimje V.R., Chen C.Y., Chen C.C., Tsai J.Y., Chen H.R., Huang Y.M., Jean J.S., Chang Y.F. and Shih R.C. (2011), Microbial fuel cell of *Enterobacter cloacae*: effect of anodic pH microenvironment on current, power density, internal resistance and electrochemical losses, International journal of Hydrogen Energy, Volume 36, Issue 17, pp 11093 - 11101

Oswald W.J. and Asce F., (1990), Advanced integrated wastewater pond systems, supplying water and saving the environment for 6 billion people, proceeding/session, ASCE convention EE Div/Asce, San Francisco, Ca, pp 73-81

Park J.B.K., Graggs R.J. and Shilton A.N. (2011a), Recycling algae to improve species control and harvest efficiency from a high rate algal pond, Water Research, Volume 45, Issue 20, pp 6637 - 6649

Park J.B.K., Graggs R.J. and Shilton A.N. (2011b), Wastewater treatment high rate algal ponds for biofuel production, Bioresource Technology, Volume 102, issue 1, pp 35 – 42

Pant D., Van B.G., Diels L., and Vanbroekhoven K., (2010), A review of the substrates used in microbial fuel cells (MFCs) for sustainable energy production Bioresource Technology, Volume 101, Issue 6, pp 1533-1543

Peighambardoust S.J., Rowshanzamir S., and Amjadi M., (2010), Review of the proton exchange membranes for fuel cell applications, International Journal of Hydrogen Energy Volume 35, Issue 17, Pages 9349-9384

Penfold J., Staples E., Tucker I., Soubiran L., and Thomas R.K., (2002) Comparison of the Coadsorption of Benzyl Alcohol and Phenyl Ethanol with the Cationic Surfactant, Hexadecyl Trimethyl Ammonium Bromide, at the Air–Water Interface, Journal of Colloid and interface Science, Volume 247, Issue 2, pp 397 – 403

Peng L., You S., and Wang J., (2010), carbon nanotubes as electrode modifier promoting direct electron transfer from *Shewanella oneidensis*, Biosensors and bioelectronics, Volume 25, Issue 5, pp 1248 -1251

Pittman J.K., Dean A.P. and Osundeko O. (2011), The potential of sustainable algal biofuel production using wastewater resources, Bioresource technology, Volume 102, Issue 1, pp 17 25

Powell E.E., and Hill G.A., (2009), Economic assessment of an integrated bioethanol–biodiesel–microbial fuel cell facility utilizing yeast and photosynthetic algae, Chemical Engineering Research and Design, Volume 87, Issue 9, pp 1340-1348

Powell E.E., Maoiour M.L., Evitts R.W. and Hill G.A. (2009), Growth kinetics of *Chlorella vulgaris* and its use as a cathodic half-cell, Bioresource technology, Volume 100, Issue 1, pp 269-274

Qiao Y., Bao S.J. and Li C.M. (2010), Electrocatalysis in microbial fuel cells from electrode material to direct electrochemistry, Energy Environmental Science, Volume 3, pp 544 - 553

Rabaey K., Lissens G. and Verstraete W., (2005), in Biofuels for fuel cells: renewable energy from biomass fermentation, Integrated environmental technology series, Microbial fuel cells: performances and perspectives, Lens P., Westerman P., Haberbauer M. and Moreno A., pp 377, IWA Publishing, Great Britain

Rajesekhar P., Fan L., Nguyen T. and Roddick F.A., (2012), A review of the use of sonication to control cyanobacterial blooms, Water Research, Volume 46, Issue 14, pp 4319 – 4329

Rashid N., Cui Y.F., Rehman M.S.U. and Han J.I. (2013), Enhanced electricity generation by using algae biomass and activated sludge in microbial fuel cells, Science of Total Environment, Volume 456-457, pp 91-94

Rodrigo M.A., Camzares P., Labato J., Paz R., Saez C., and Linares J.J., (2007), Production of electricity from the treatment of urban waste water using a microbial fuel cell, Journal of Power Sources, Volume 169, Issue 1, pp 198-204

Rozendal R.A., Hamelers H.V., Rabaey K., Keller J., and Buisman C.J., (2008), Towards practical implementation of bioelectrochemical wastewater treatment, Trends in biotechnology, volume 26 issue 8, pp 450-459

Russel L.B., Siegel J.E., Daniels N., Gold M.R., Luce B.R. and Mandelblatt J.S. (1996), Cost effective analysis as a guide to reverse allocation on health: Roles and limitaions, in Cost effectiveness in health and medicine, Gold M.R. (ed.), pp 3 – 24, Oxford University Press, New York, USA

Sadasivam S., and Manickam A., (1996), in Phenol sulphuric acid method for total carbohydrate, Biochemical methods, Carbohydrates, in Sadasivam S., and Manickam A., pp 10, New age international ,New Delhi, India

Sambamurty A.V.S.S, (2005), in A textbook of Algae,Classification of algae, in Sambamurty A.V.S.S, pp 1-4, I. K. International Pvt Ltd, Mumbai, India

Sanchez-Luna L.D., Bezerra R.P., Matsudo S.S., Converti A. and de Carvalho J.C.M. (2006), Influence of pH, Temperature, and Urea Molar Flowrate on Arthrospira platensis Fed-Batch Cultivation: A Kinetic and Thermodynamic Approach, Biotechnology and Bioengineering, Volume 96, Issue 4, pp 702-711

Selembo P.A., Merill M.D., and Logan B.E., (2009), the use of stainless steel and nickel alloys as low-cost cathodes in microbial electrolysis cells, Journal of power sources, Volume 190, Issue2, pp 271-278

Sheng J., Yu F., Xin Z., Zhao L., Zhu X., and Hu Q., (2007), Preparation, identification and their antitumor activities in vitro of polysaccharides from Chlorella pyrenoidosa, Food chemistry, Volume 105, Issue 2, pp 533 – 539

Shi Y., Sheng J., Yang F., and Hu Q., (2007), Purification and identification of polysaccharide derived from *Chlorella pyrenoidosa,* Food Chemistry, Volume 103, Issue 1, pp 101-105

Silveira S., (2005), in Bioenergy: realizing the potential, How to realise bioenergy prospects, Silveira S., Chemical, Petrochemical & Process, pp 4-8, Elsevier, USA

Sun M., Sheng G., Mu Z., Liu X., Chen Y., Wang H., and Yu H., (2009), manipulating the hydrogen production from acetate in a microbial electrolysis cell – microbial fuel cell coupled system, Journal of Power sources, Volume 191, Issue 2, pp 338-343

Tadesse I., Green F.B. and Puhakka J.A., (2004), Seasonal and diurnal variations of temperature, oH and dissolved oxygen in advanced integrated wastewater pond system® treating tannery effluent, Water Research, Volume 38, Issue 3, pp 645 – 654

Talwalkar A. and Kailasapathy K. (2004), The role of oxygen in the viability of probiotic bacteria with reference to *L. acidophilus* and *Bifidobacterium spp*., Current Issues Intest Microbiology, Volume 5, pp 1-8

Tomaseli L., (2008), in Microalgal cell, Handbook of Microalgal Culture: Biotechnology and Applied Phycology, The microalgal cell, Richmond A., pp 3-16, John Wiley & Sons, UK

Tsai H., Wu C., Lee C., and Shih E.P., (2009), microbial fuel cell performance of multiwalled carbon nanotubes on carbon cloth as electrodes, Journal of Power Sources, Volume 194, Issue 1, pp 199 - 205

Uria N., Sanchez D., Mas R., Sanchez O., Munoz F.X., and Mas J., (2011), Effect of the cathode/anode ratio and the choice of cathode catalyst on the microbial activity, Sensors and Actuators B: chemical, pp 1-7

Valkiainen M., Tuurala S., Smolander M. and Kaukoniemi O.V. (2010), in Innovations in Fuel Cell Technologies, Printed Enzymatic Current Sources, Steinberger-Wilckens R.,and Werner L., Volume 1 of RSC Energy and Environment Series, pp 3-26, Royal Society of Chemistry, USA

Velasquez-Orta S.B, Curtis T.P., and Logan B.E., (2009), Energy from algae using microbial fuel cells, Biotechnology and Bioengineering, Volume 103, Issue. 6, pp 1068 – 1076

Velasquez-Orta S.B., Head I.M., Curtis T.P. and Scott K., (2011), Factors affecting current production in MFCs using different industrial wastewater, Bioresource Technology, Volume 102, Issue 88, pp 5105-5112

Wang H., Liu D., Lu L., Zhao Z., Xu Y. and Cui F. (2012), Degradation of algal organic matter using microbial fuel cells and its association with trihalomethane precursor removal, Bioresource Technology, Volume 116, pp 80 -85

Wang H., Wu Z., Plaseied A., Jenkins P., Simpson L., Engtrakul C., and Ren Z., (2011), carbon nanotubes modified air-cathodes for electricity production in microbial fuel cells, Journal of Power Sources, Volume 196, Issue 18, pp 7465-7469

Wei L., Yuan Z., Cui M., Han H., and Shen J., (2012), Study on electricity-generation characteristic of 2-chambered microbial fuel cell in continuous flow mode, International Journal of Hydrogen Energy, Volume 37, Issue 1, pp 1067 – 1073.

Wise D.L. (1980), Fuel and organic chemicals via anaerobic fermentation of residues and biomass, in Biochemical and photosynthetic aspects of energy production, Pietro A.S., pp 81 -117, Academic press, New York, USA

Wu X., Joyce E.H. and Mason T.J., (2011), The effects of ultrasound on cyanobacteria, Harmful Alga, Volume 10, Issue 6, pp 738-745

Wu Y.C., Wang Z.J., Zheng Y., Xiao Y, Yang Z.H. and Zhao F, (2014), Light intensity affects the performance of a photo-Microbial fuel cell with Desmodesmus sp. A8 as cathodic microorganism, Applied Energy, Volume 116, Issue 1, pp 86-90.

Xu J., Sheng G.P., Luo H.W., Li W.W., Wang L.F. and Yu H.Q. (2012), Fouling of proton exchange membrane (PEM) deteriorates the performance of microbial fuel cell, Water Research, Volume 46, Issue 6, pp 1817 – 1824

Yuan Y., Zhao B., Jeon Y., Zhong S., Zhou S. and Kim S., (2011), Iron phthalocyanine supported on amino-functionalised multi-walled carbon nanotubes as an alternative cathodic oxygen catalyst in microbial fuel cells, Bioresource Technology, Volume 102, Issue 10, pp 5849 – 5855

Zawadzinski T.A., Deroin C., Radzinski S., Sherman R.J., Smith V.T., Springer T.E. and Gottesfeld S. (1993), Water uptake by and transport through Nafion® 117 membranes, Electrochemical Society, Volume 140, Issue 4, pp 1041 – 1047

Zhao F., Harnisch F., Schroder U., ScholzF., Bagdanoff P. and Herman I. (2005), Application of pyrolised iron (II) phthalocyanice and CoTMPP based oxygen reduction catalysts as cathode materials in microbial fuel cells, Electrochem Communications, Volume 7, Issue 12, pp 1405 - 1410

Zheng H., Yin J., Huang H., Ji X. and Dou C. (2011), Disruption of *Chlorella vulgaris* cells for the release of biodiesel-producing lipids: a comparison of grinding, ultrasonication, bead

milling, enzymatic lysis, and microwaves, Applied Biochemistry and Biotechnology, Volume 164, Issue 7, pp 1215 - 1224

Zhu N., Chen X., Zhang T., Wu P., Li P. and Wu J. (2011), Improved performance of membrane free single-chamber air cathode microbial fuel cell with nitric acid and ethylenediamine surface modified activated carbon fibre felt anodes, Bioresource technology, Volume 102, Issue 1, pp 422 - 426

Zhuang L., Zhou S., Yuan Y., Liu T., Wu Z., and Cheng J., (2011), Development of *Enterobacter aerogenes* fuel cells: from in situ biohydrogen oxidization to direct electroactive biofilm, Bioresource Technology, Volume 102, Issue 1, pp 284-289

Zou Y., Xiang C., Yang L., Sun L., Xu F., and Cao Z., (2008), A mediatorless microbial fuel cell using polypyrrole coated carbon nanotubes composite as anode material, International Journal of Hydrogen Energy, Volume 33, Issue 18, pp 4856-4862

Q-sense, (2002), methods and protocols, appendix C, C6

Internet references

Internet reference 1 http://www.instituteforenergyresearch.org/2013/06/27/statistical-review-of-world-energy-2013-viva-la-shale-revolucion/ (19/12/2013)

Internet reference 2, biotechproduct.blogspot.com (17/7/2012)